

Title: Nodal Quasiparticles and Spin and Charge Order in the Cuprate Superconductors

Date: Apr 24, 2008 09:00 AM

URL: <http://pirsa.org/08040031>

Abstract: I will discuss the interplay between the fermionic nodal quasiparticles of a d-wave superconductor and the various spin and charge orders that have been observed in the cuprate superconductors. Fluctuations of a composite '\nematic' order are identified as the dominant source of inelastic scattering which broadens the quasiparticle spectral function.



# Electronic quasiparticles and competing orders in the cuprate superconductors

Andrea Pelissetto, Rome

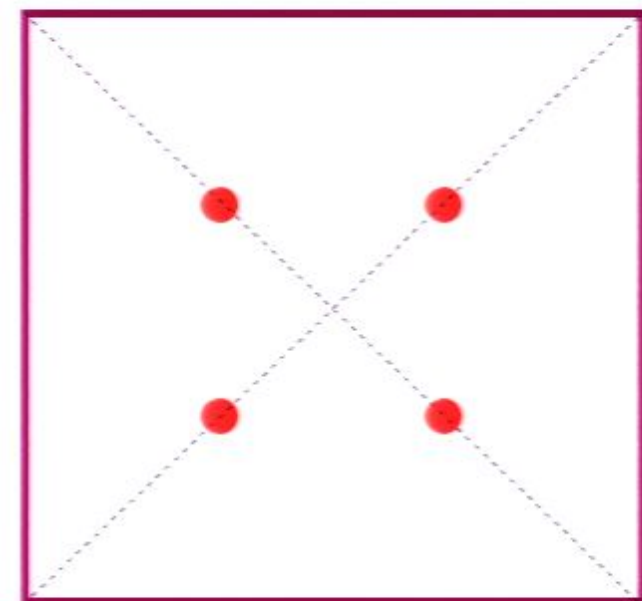
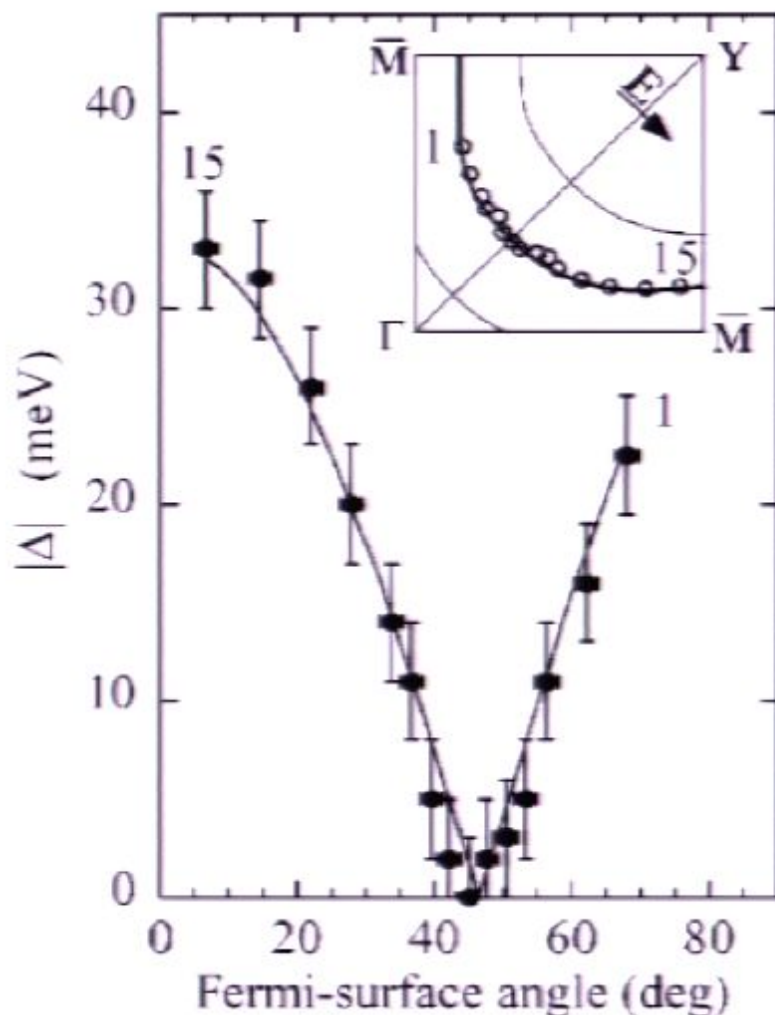
Ettore Vicari, Pisa



Yejin Huh  
Subir Sachdev



# Gapless nodal quasiparticles in $d$ -wave superconductors



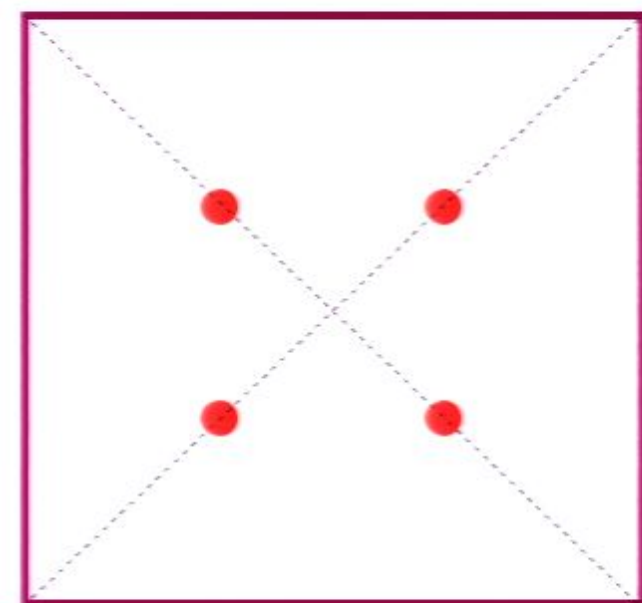
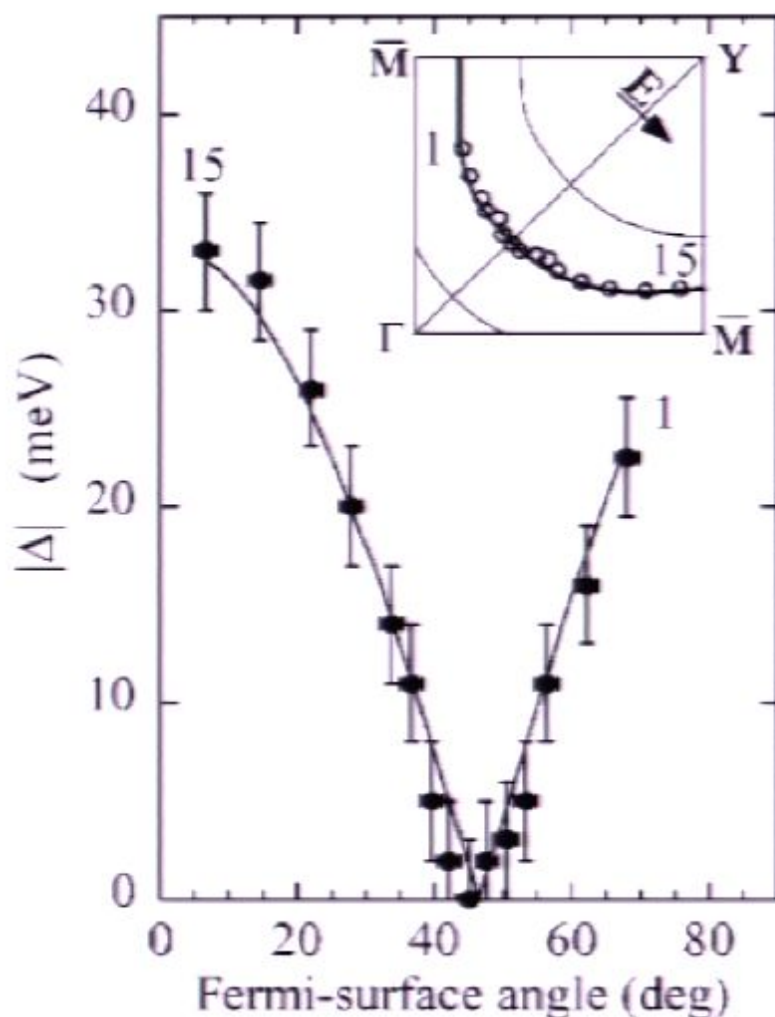
Brillouin zone

FIG. 46. Superconducting gap measured at 13 K on Bi2212 ( $T_c=87$  K) plotted vs the angle along the normal-state Fermi surface (see sketch of the Brillouin zone), together with a  $d$ -wave fit. From Ding, Norman, *et al.*, 1996.

$$E_k = \sqrt{(\varepsilon_k - \mu)^2 + \Delta_k^2}$$



# Gapless nodal quasiparticles in $d$ -wave superconductors



Brillouin zone

FIG. 46. Superconducting gap measured at 13 K on Bi2212 ( $T_c=87$  K) plotted vs the angle along the normal-state Fermi surface (see sketch of the Brillouin zone), together with a  $d$ -wave fit. From Ding, Norman, *et al.*, 1996.

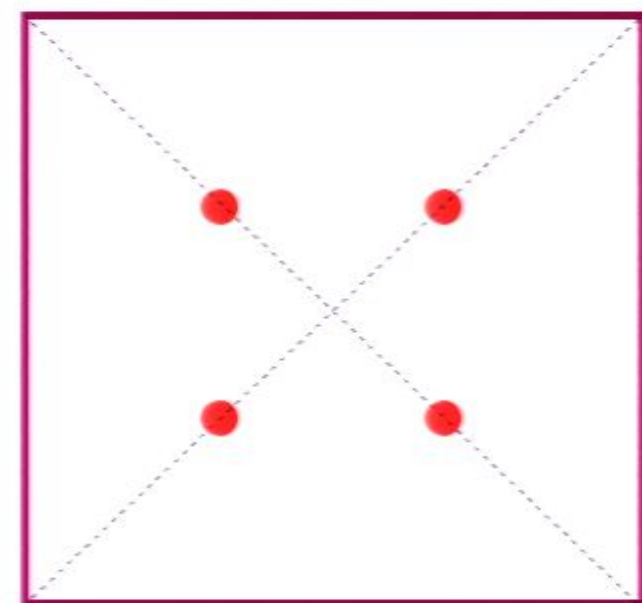
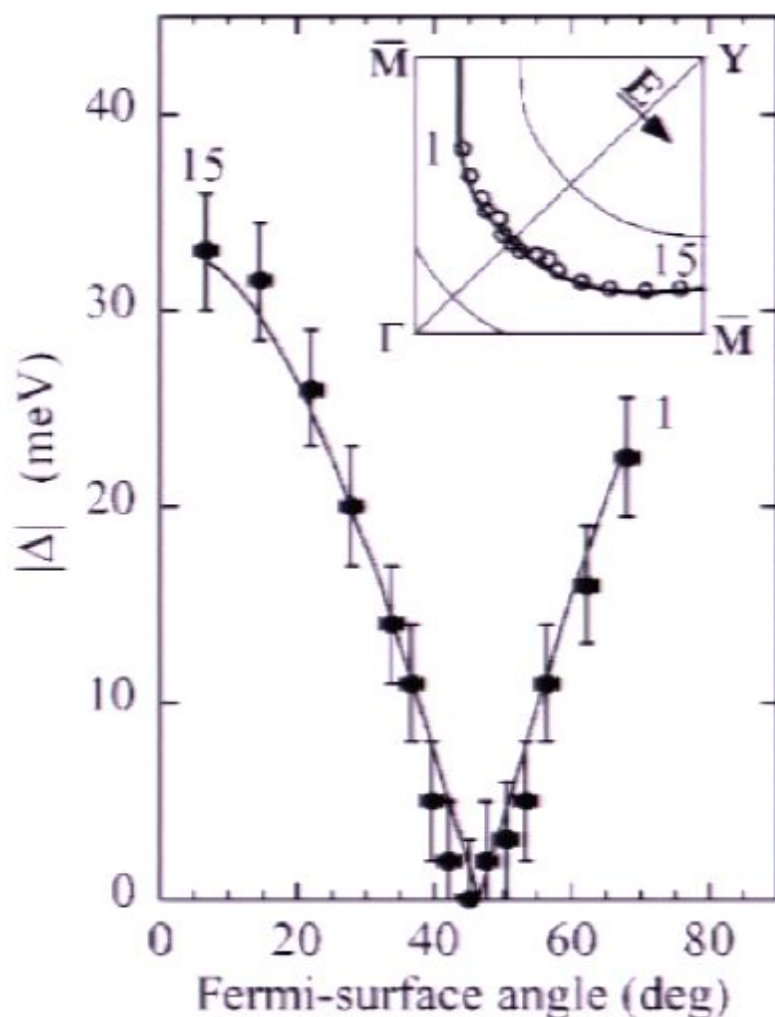
$$E_k = \sqrt{(\varepsilon_k - \mu)^2 + \Delta_k^2}$$

$$\Delta_k \sim \cos k_x - \cos k_y$$



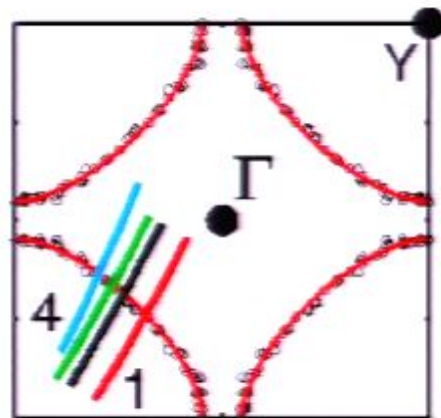


# Gapless nodal quasiparticles in $d$ -wave superconductors



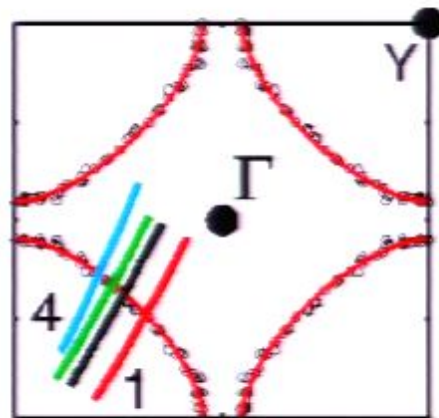
Brillouin zone

FIG. 46. Superconducting gap measured at 13 K on Bi2212 ( $T_c=87$  K) plotted vs the angle along the normal-state Fermi surface (see sketch of the Brillouin zone), together with a  $d$ -wave fit. From Ding, Norman, *et al.*, 1996.



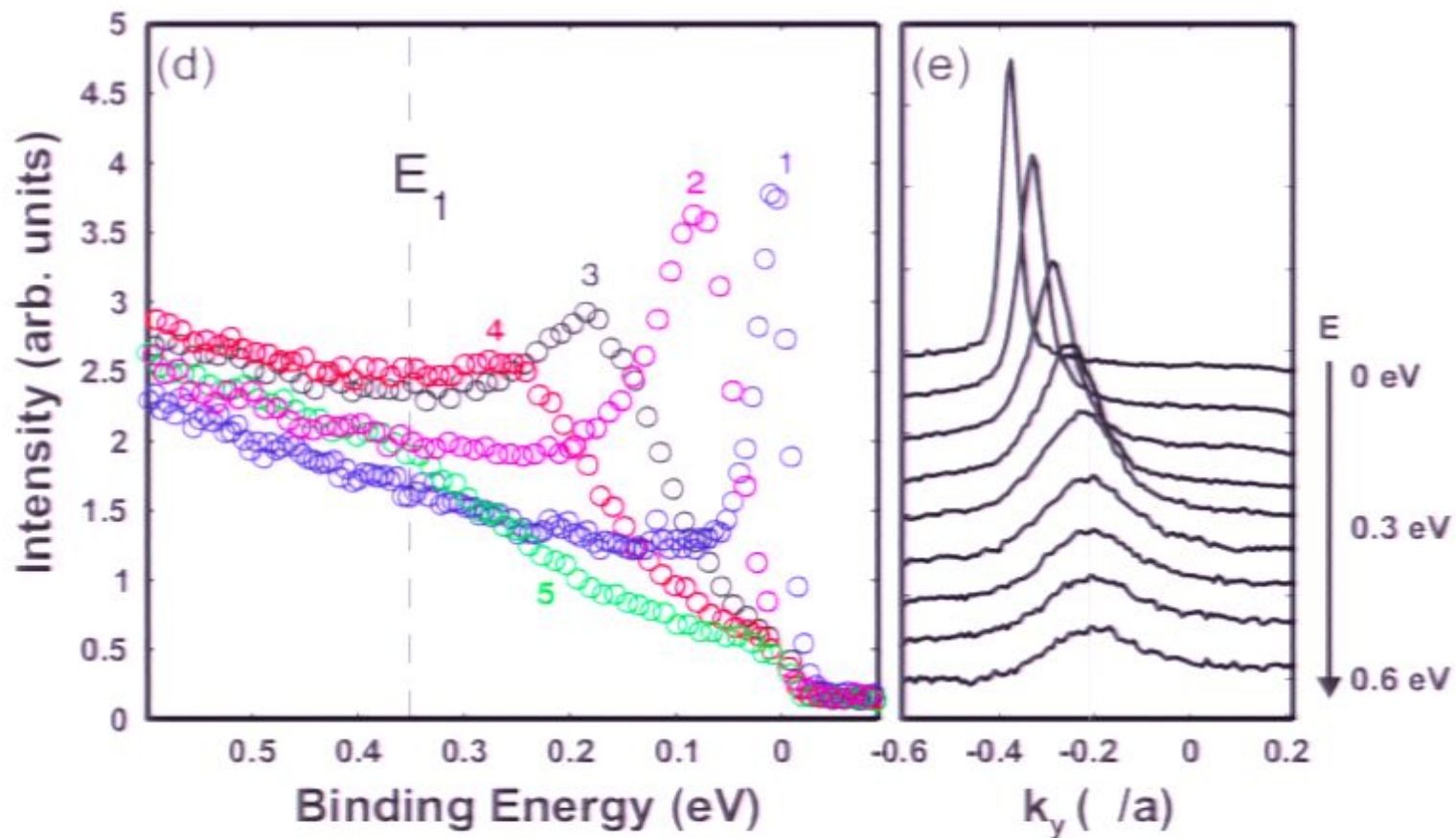
## Photoemission spectra of $\text{La}_{2-x}\text{Sr}_x\text{CuO}_4$

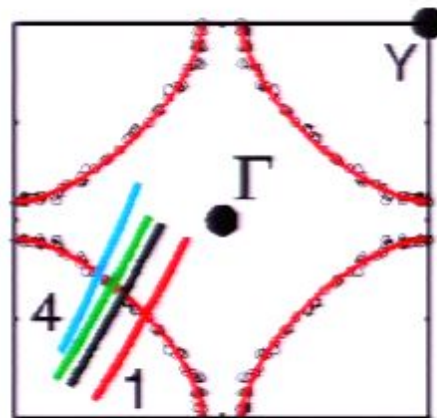
$x=0.145$



## Photoemission spectra of $\text{La}_{2-x}\text{Sr}_x\text{CuO}_4$

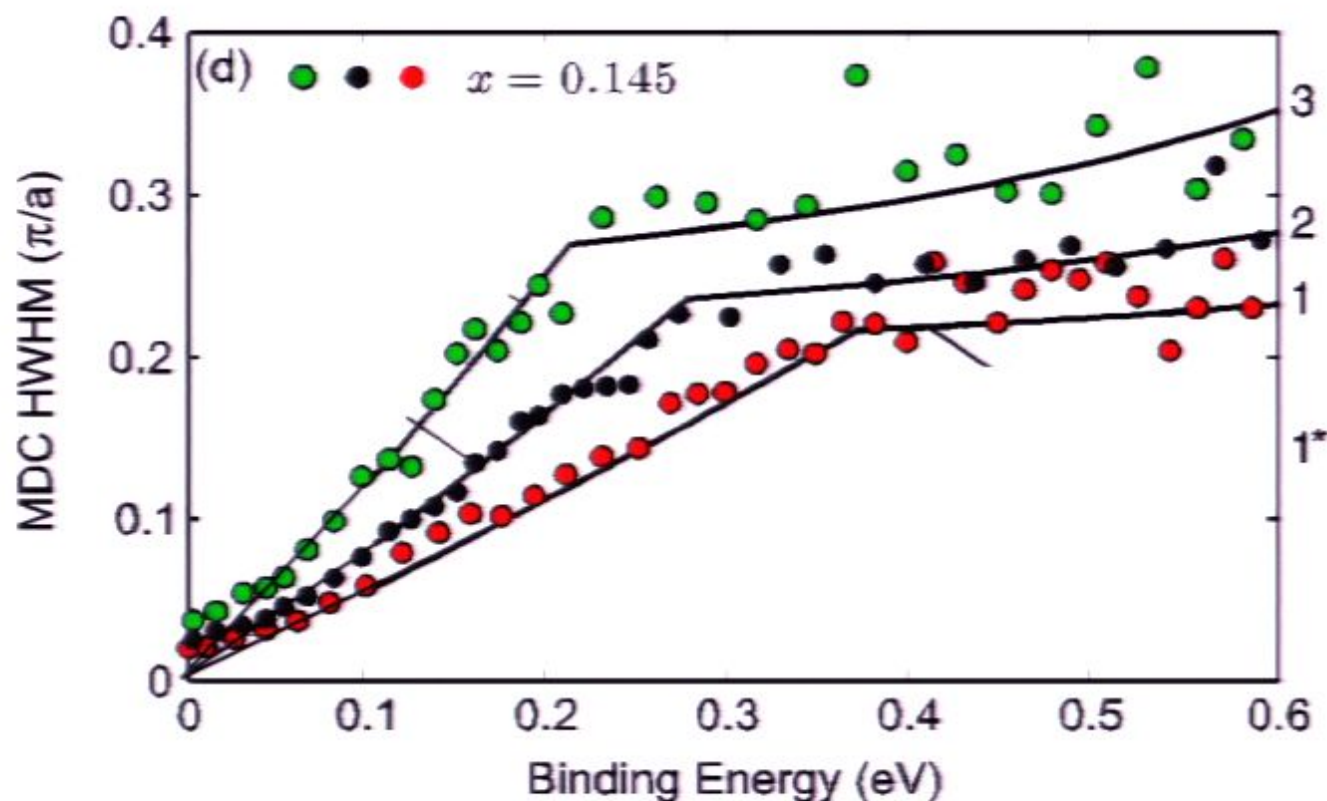
$x=0.145$





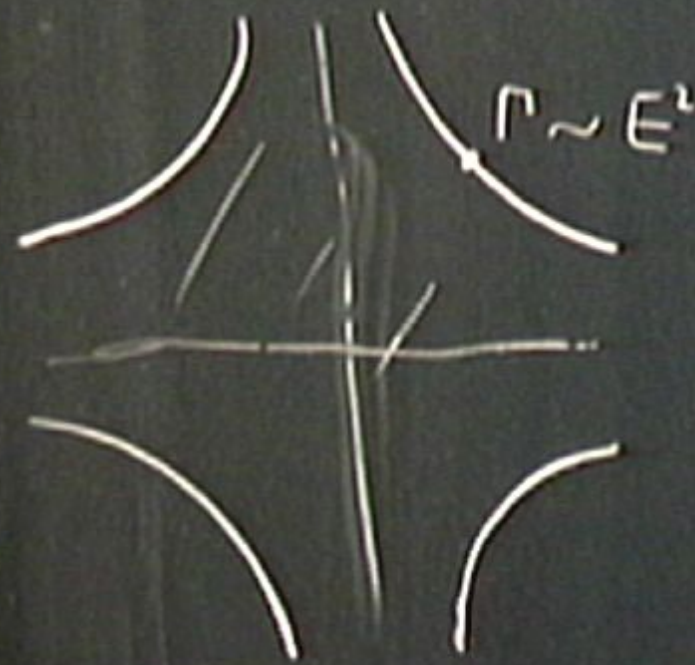
## Photoemission spectra of $\text{La}_{2-x}\text{Sr}_x\text{CuO}_4$

$x=0.145$

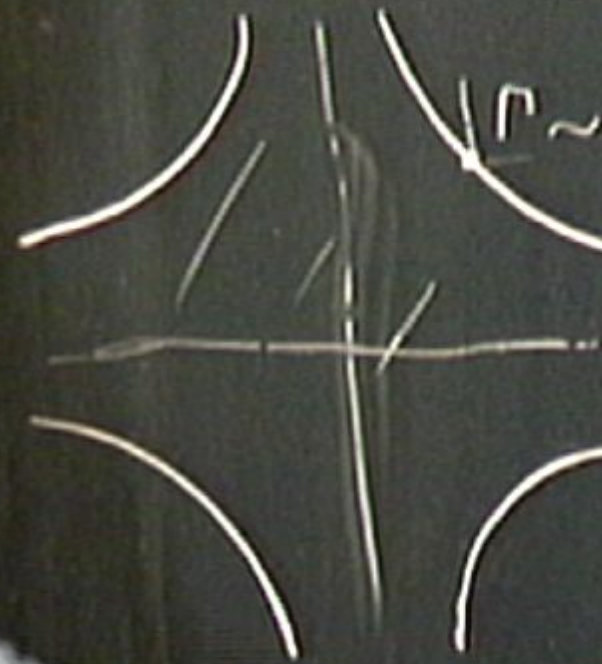


$$E_k = \sqrt{(\varepsilon_k - \mu)}$$

$$\Delta_k \sim$$



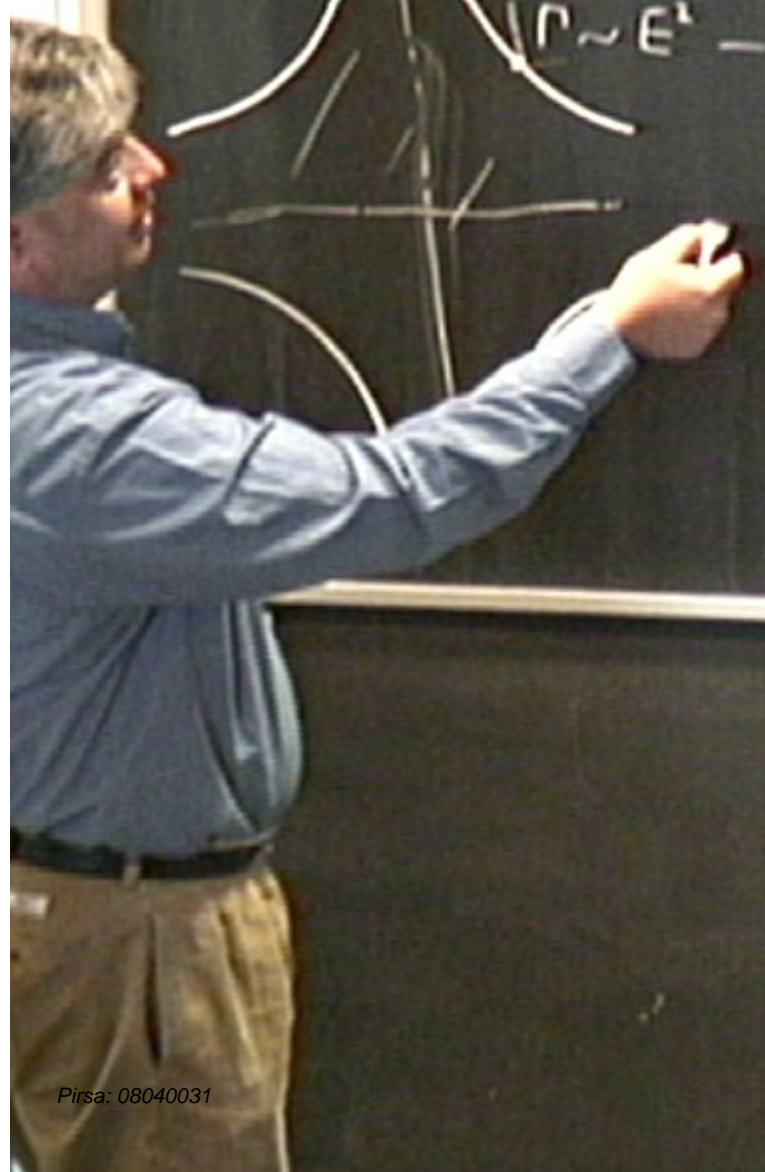
$$E_k = \sqrt{(\epsilon_k - \mu)}$$

$$n \sim E^2 - FL \quad \Delta_k \sim$$


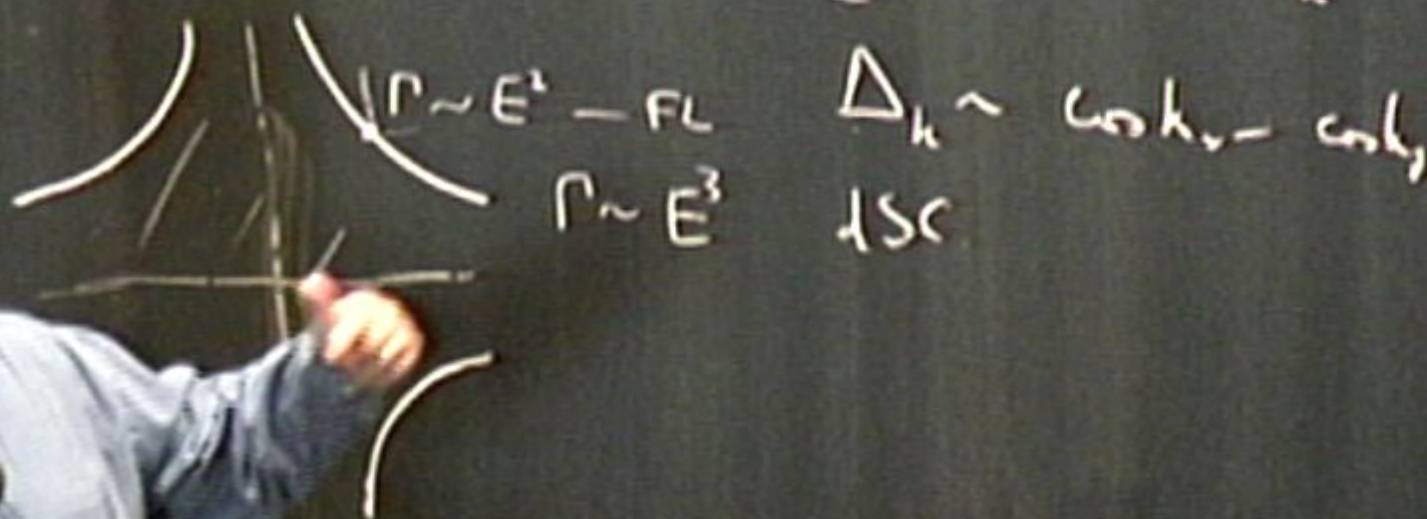


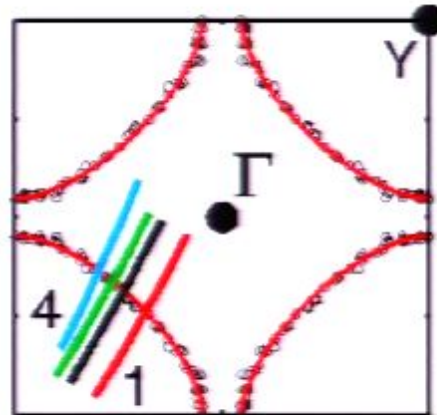
$$E_k = \sqrt{(\epsilon_k - \mu)^2 + \Delta_k^2} \sim \sqrt{k_x^2 + k_y^2}$$

$$\langle P \sim E^2 - FL \rangle \quad \Delta_k \sim \cos k_x - \cos k_y$$



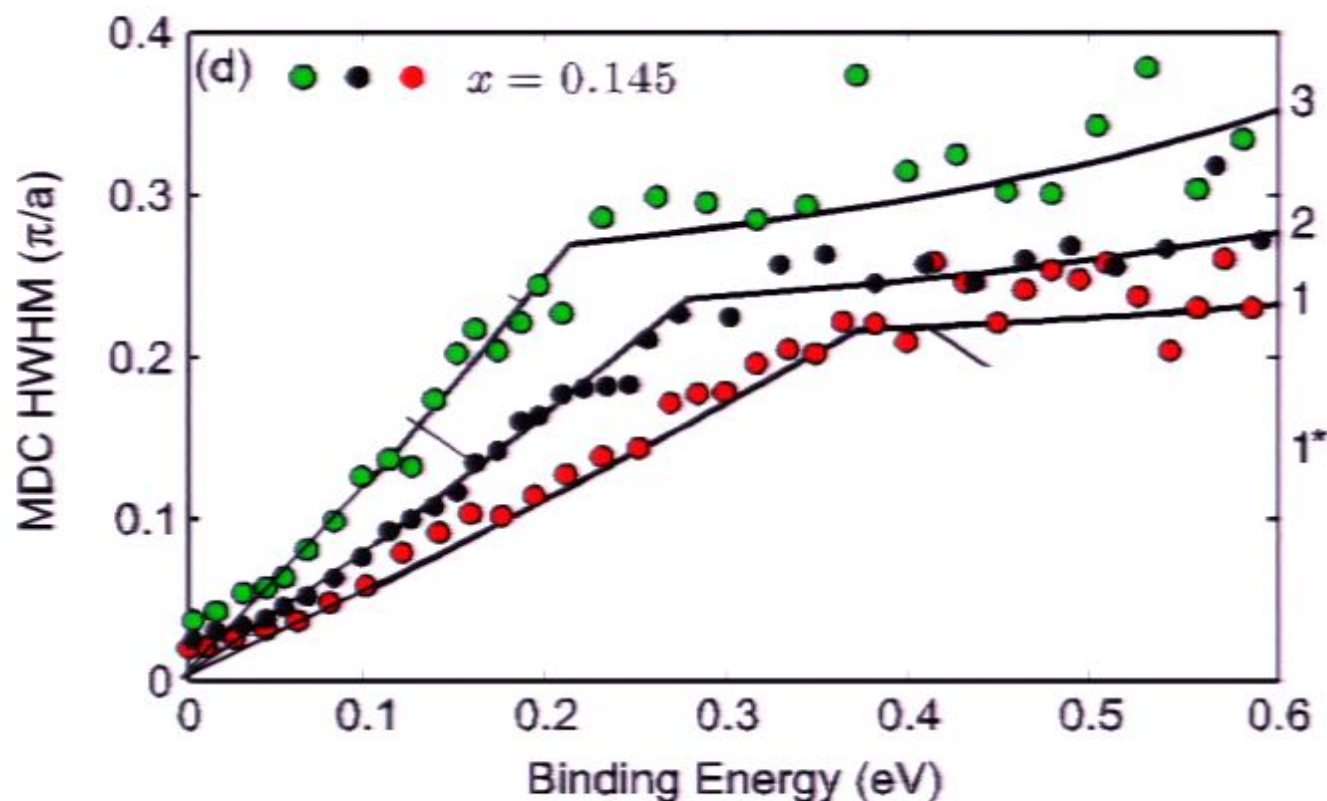
$$E_k = \sqrt{(\varepsilon_k - \mu)^2 + \Delta_k^2} \sim \sqrt{k_x^2 + k_y^2}$$


$$\begin{array}{ccc} P \sim E^1 - FL & & \Delta_k \sim \cos k_x - \sin k_y \\ P \sim E^3 & LSC & \end{array}$$



## Photoemission spectra of $\text{La}_{2-x}\text{Sr}_x\text{CuO}_4$

$x=0.145$

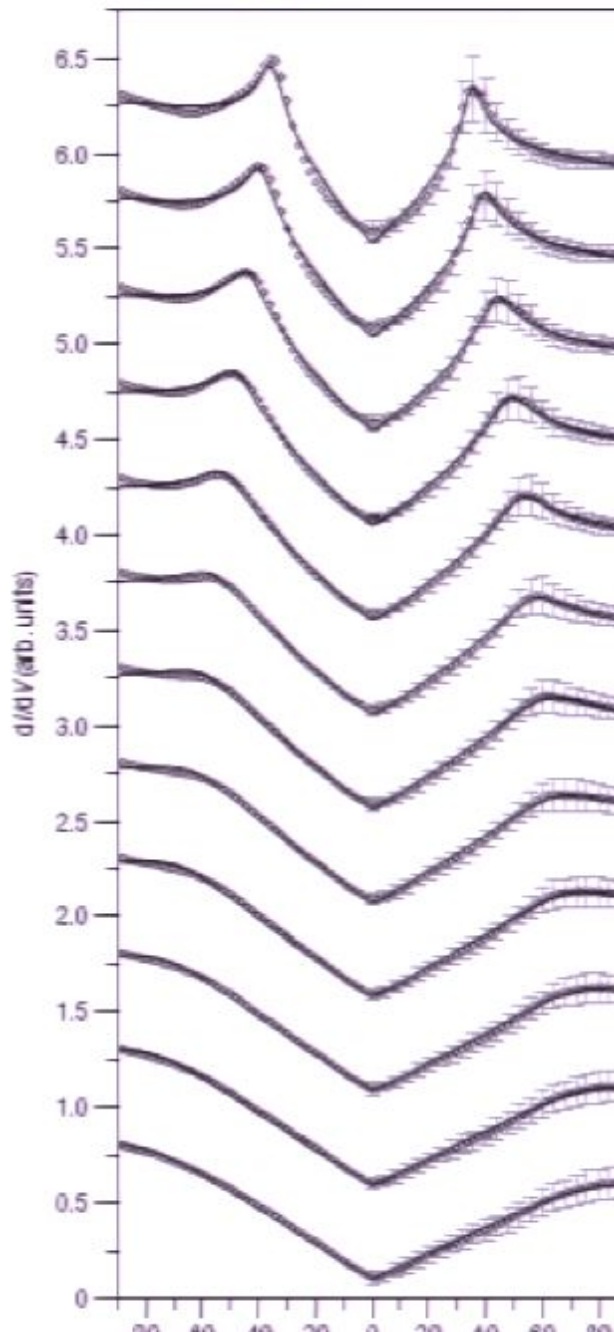


# Scanning tunneling microscopy of BSCCO

$$N(E, \Gamma_2) = A \times \text{Re} \left( \left\langle \frac{E + i\Gamma_2(E)}{\sqrt{(E + i\Gamma_2(E))^2 - \Delta(k)^2}} \right\rangle_{f_z} \right) + I$$

Good fit with  
 $\Gamma_2(E) = \alpha E$

J. W. Alldredge, Jinho Lee,  
K. McElroy, M. Wang, K.  
Fujita, Y. Kohsaka, C. Taylor,  
H. Eisaki, S. Uchida,  
P. J. Hirschfeld, J. C. Davis



Needed:  
Quantum critical  
point with nodal  
quasiparticles part of  
the critical theory



$$(E_k - \mu) + \Delta_k \sim \sqrt{h_x +}$$

$$\Delta_k \sim \omega_{k_x} - \omega_{k_y}$$

ISC

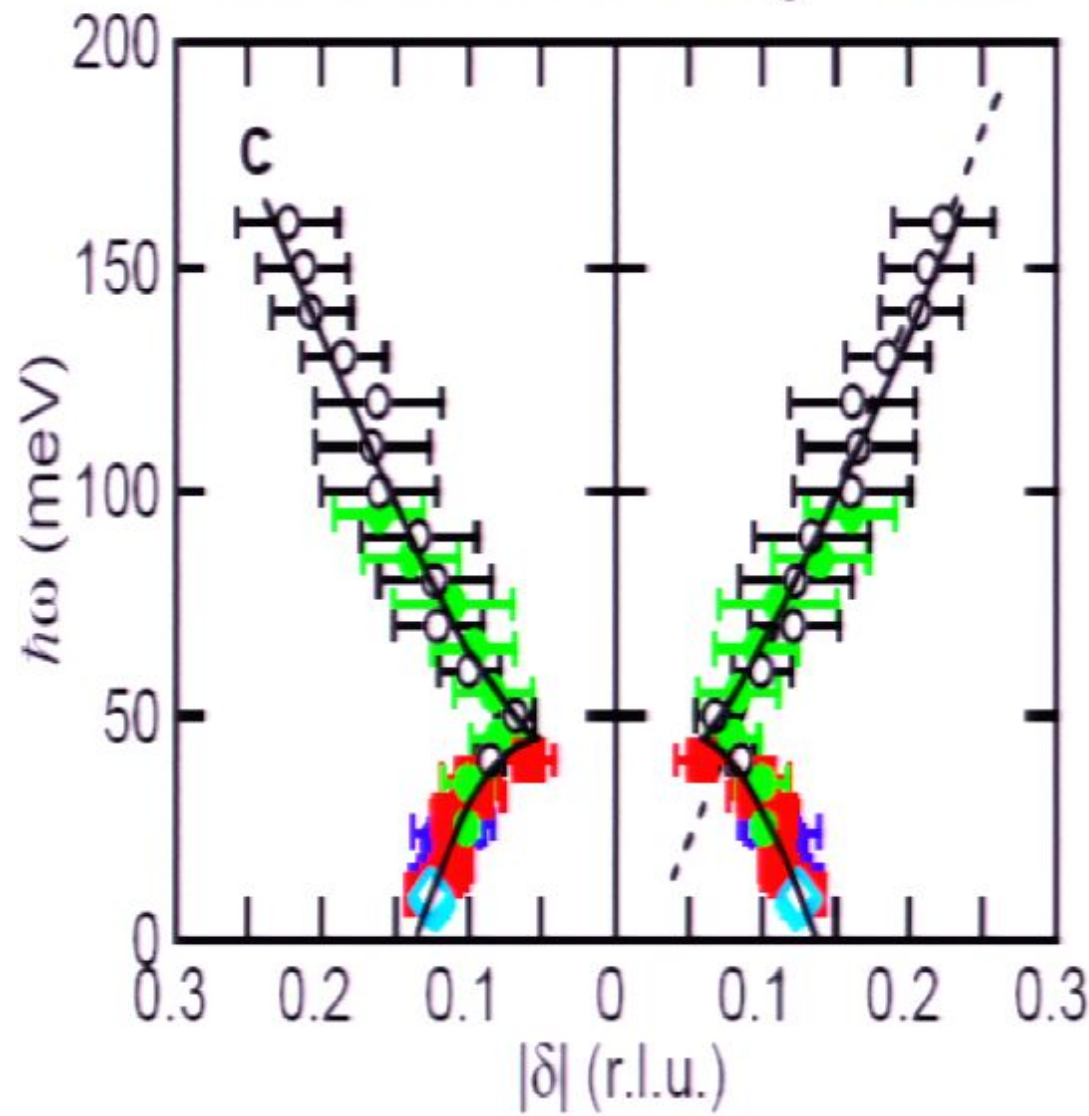
$$\Gamma(E) \sim E$$

Quantum cut off

Needed:  
Quantum critical  
point with nodal  
quasiparticles part of  
the critical theory

Needed:  
Quantum critical  
point with nodal  
quasiparticles part of  
the critical theory

## Neutron Scattering-LSCO

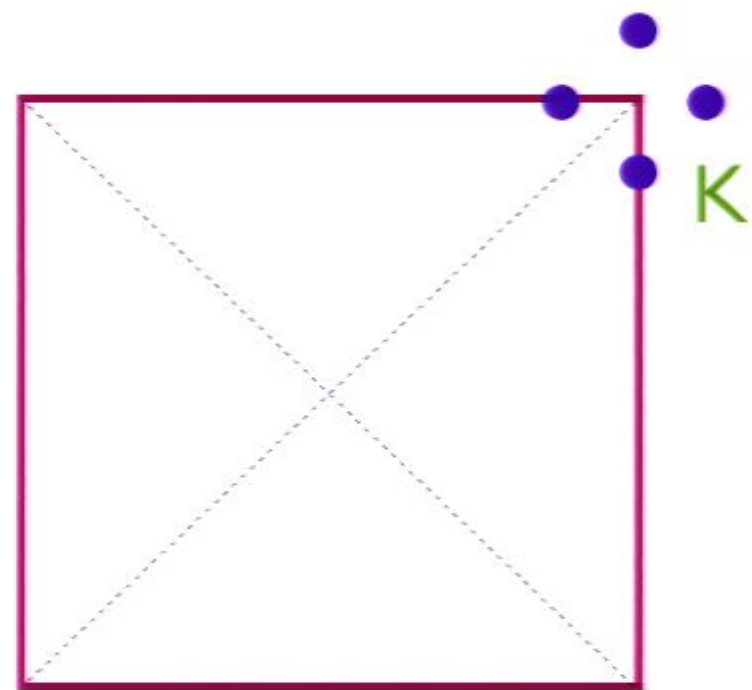


Vignolle *et al.*, Nature Phys. 07

Christensen *et al.*, PRL 04

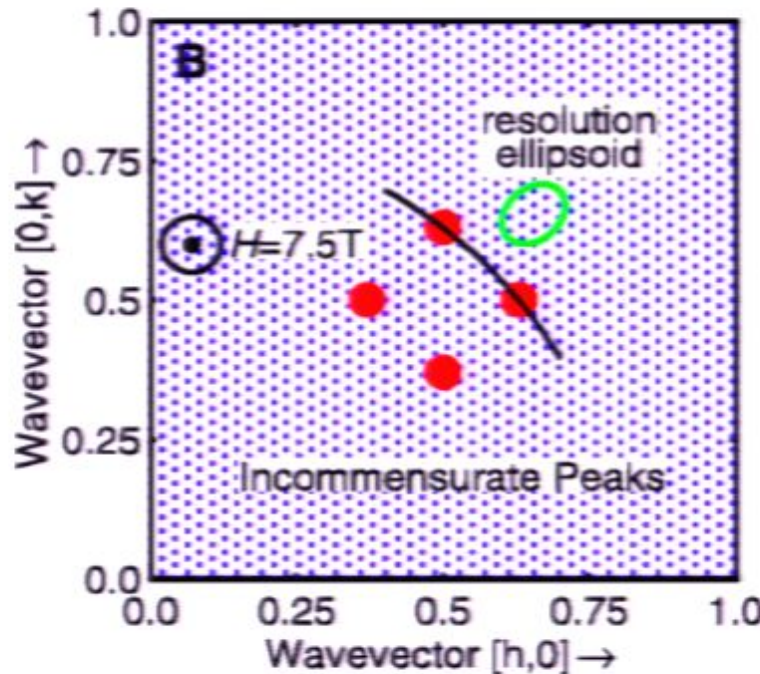
Hayden *et al.*, Nature 04

Tranquada *et al.*, Nature 04



# Neutron scattering measurements of dynamic spin correlations of the superconductor (SC) in a magnetic field

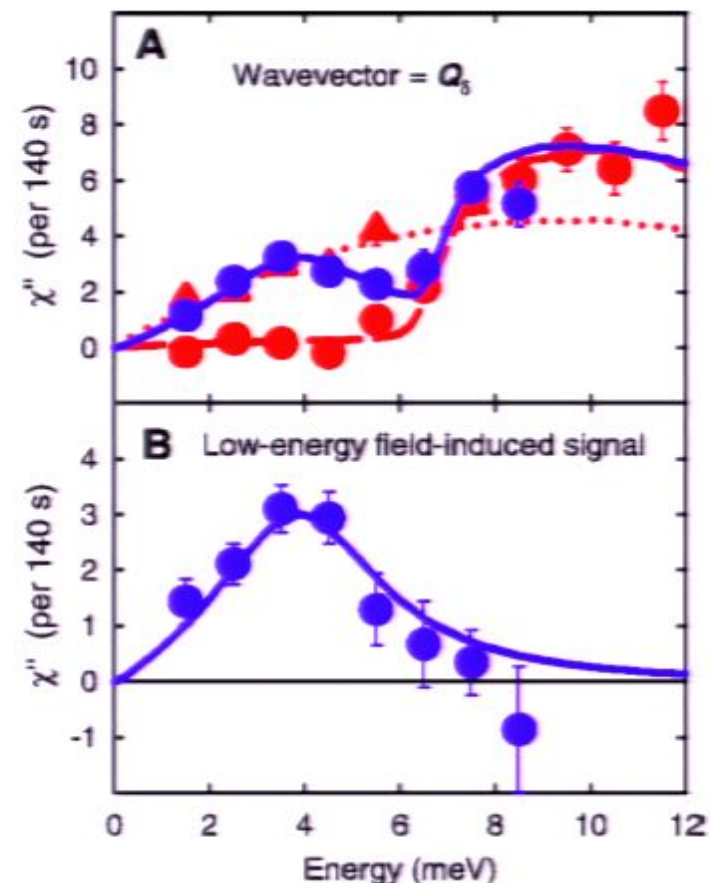
B. Lake, G. Aeppli, K. N. Clausen, D. F. McMorrow,  
K. Lefmann, N. E. Hussey, N. Mangkorntong,  
M. Nohara, H. Takagi, T. E. Mason, and A. Schröder,  
*Science* **291**, 1759 (2001).



Peaks at  $(0.5, 0.5) \pm (0.125, 0)$

and  $(0.5, 0.5) \pm (0, 0.125)$

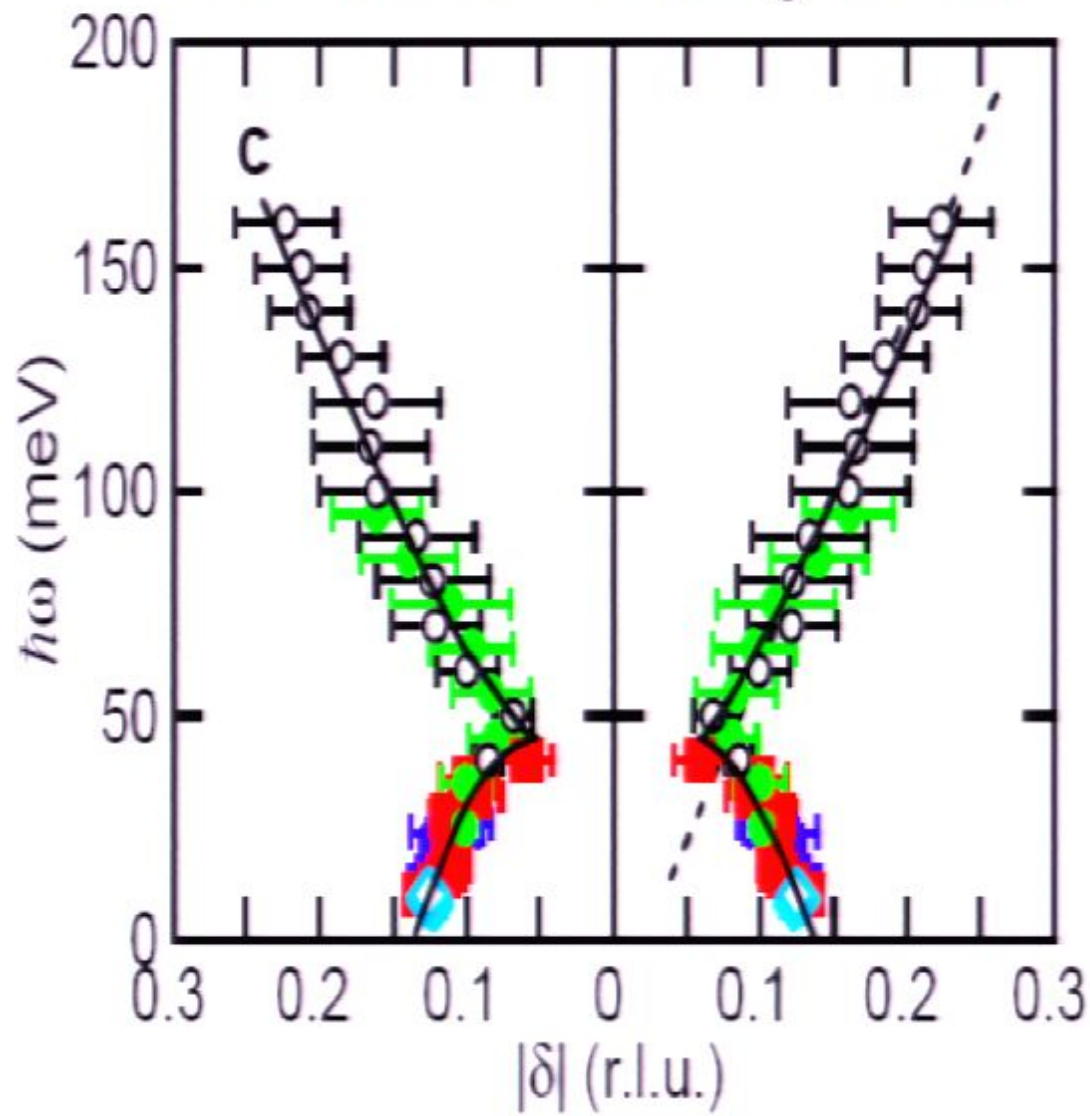
⇒ dynamic SDW of period 8



Neutron scattering off  $\text{La}_{2-\delta}\text{Sr}_\delta\text{CuO}_4$  ( $\delta = 0.163$ , *SC phase*)

at low temperatures in  $H=0$  (red dots) and  $H=7.5\text{T}$  (blue dots)

## Neutron Scattering-LSCO

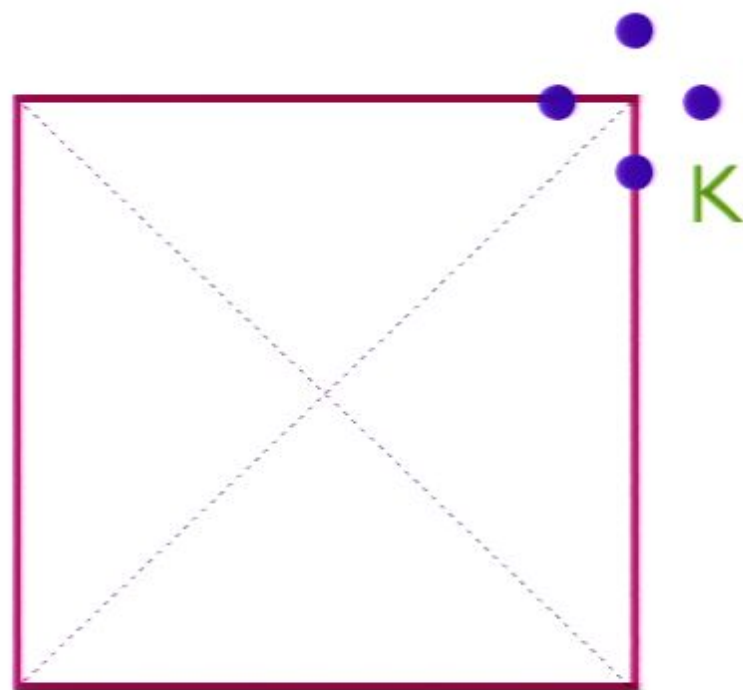


Vignolle *et al.*, Nature Phys. 07

Christensen *et al.*, PRL 04

Hayden *et al.*, Nature 04

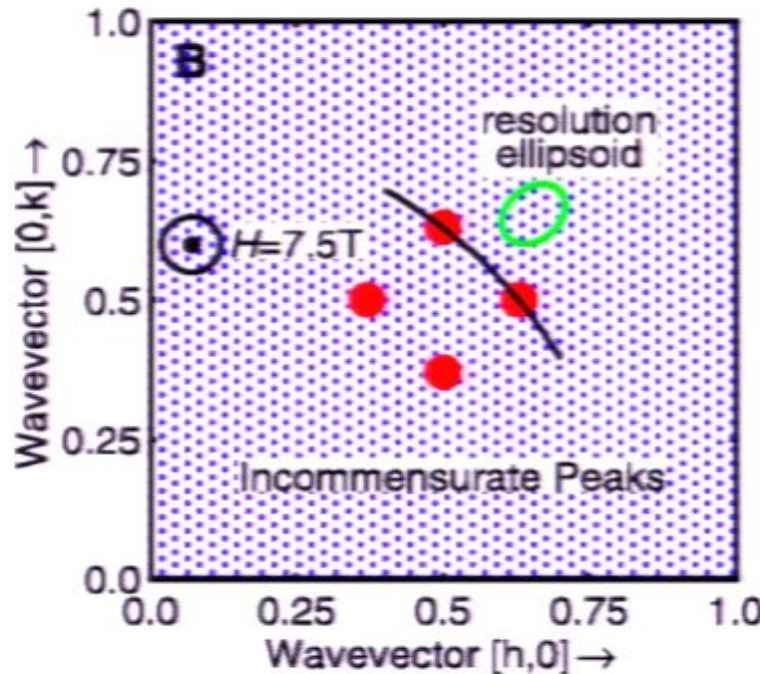
Tranquada *et al.*, Nature 04



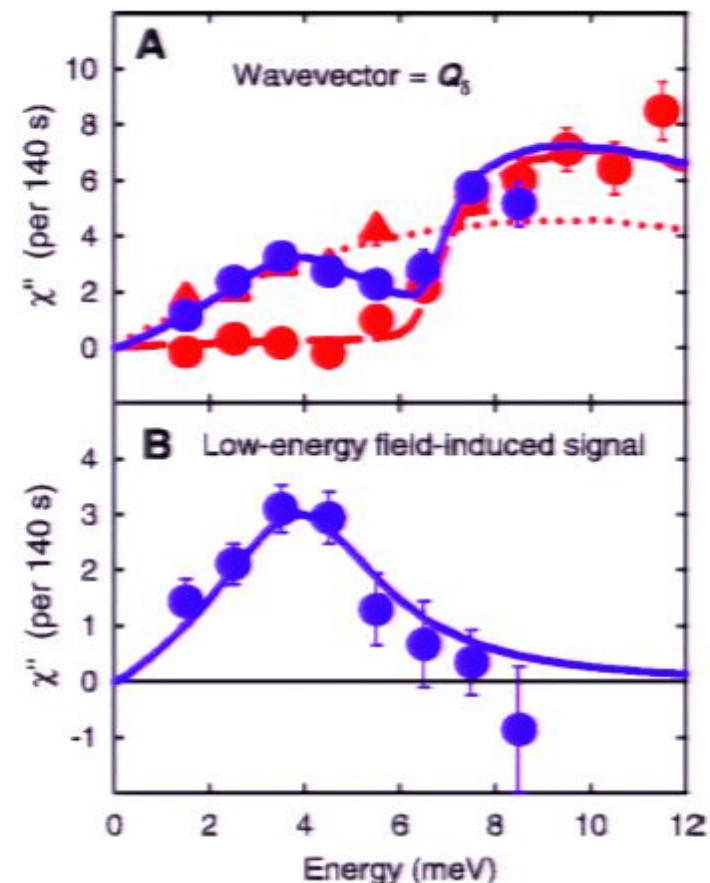
Brillouin zone

# Neutron scattering measurements of dynamic spin correlations of the superconductor (SC) in a magnetic field

B. Lake, G. Aeppli, K. N. Clausen, D. F. McMorrow,  
K. Lefmann, N. E. Hussey, N. Mangkorntong,  
M. Nohara, H. Takagi, T. E. Mason, and A. Schröder,  
*Science* **291**, 1759 (2001).



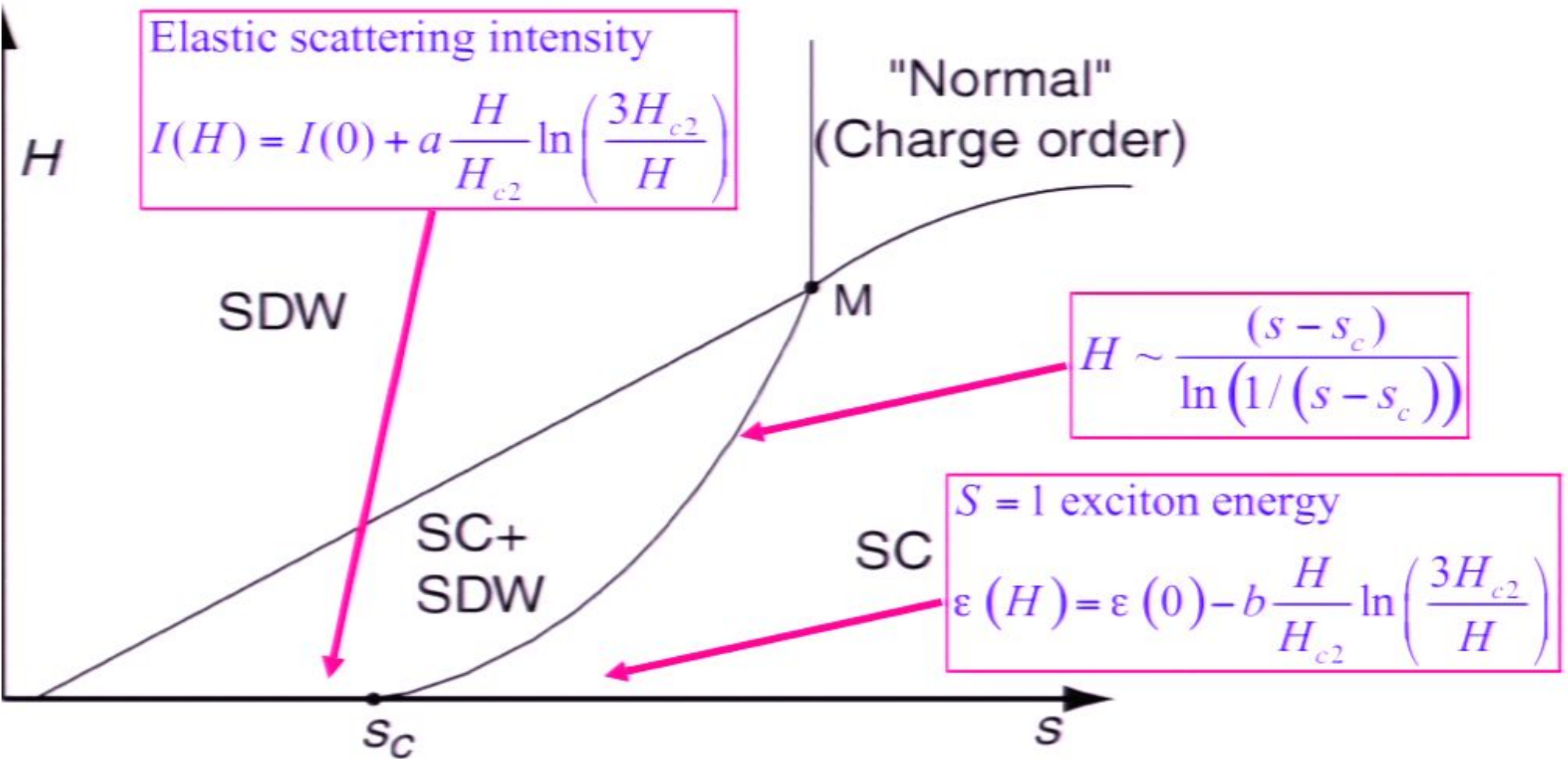
Peaks at  $(0.5, 0.5) \pm (0.125, 0)$   
and  $(0.5, 0.5) \pm (0, 0.125)$   
 $\Rightarrow$  dynamic SDW of period 8



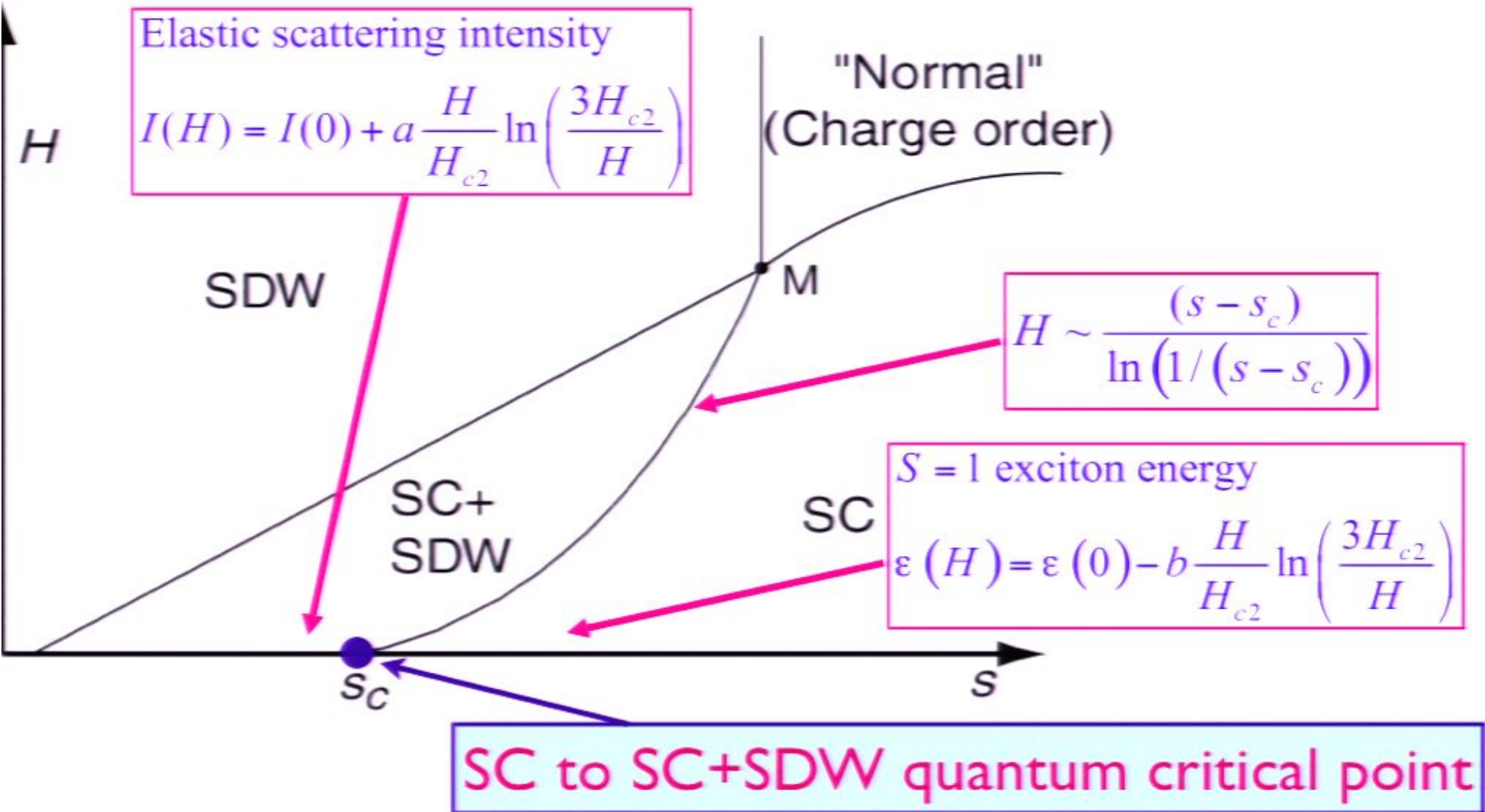
Neutron scattering off  $\text{La}_{2-\delta}\text{Sr}_\delta\text{CuO}_4$  ( $\delta = 0.163$ , *SC phase*)

at low temperatures in  $H=0$  (red dots) and  $H=7.5\text{ T}$  (blue dots)

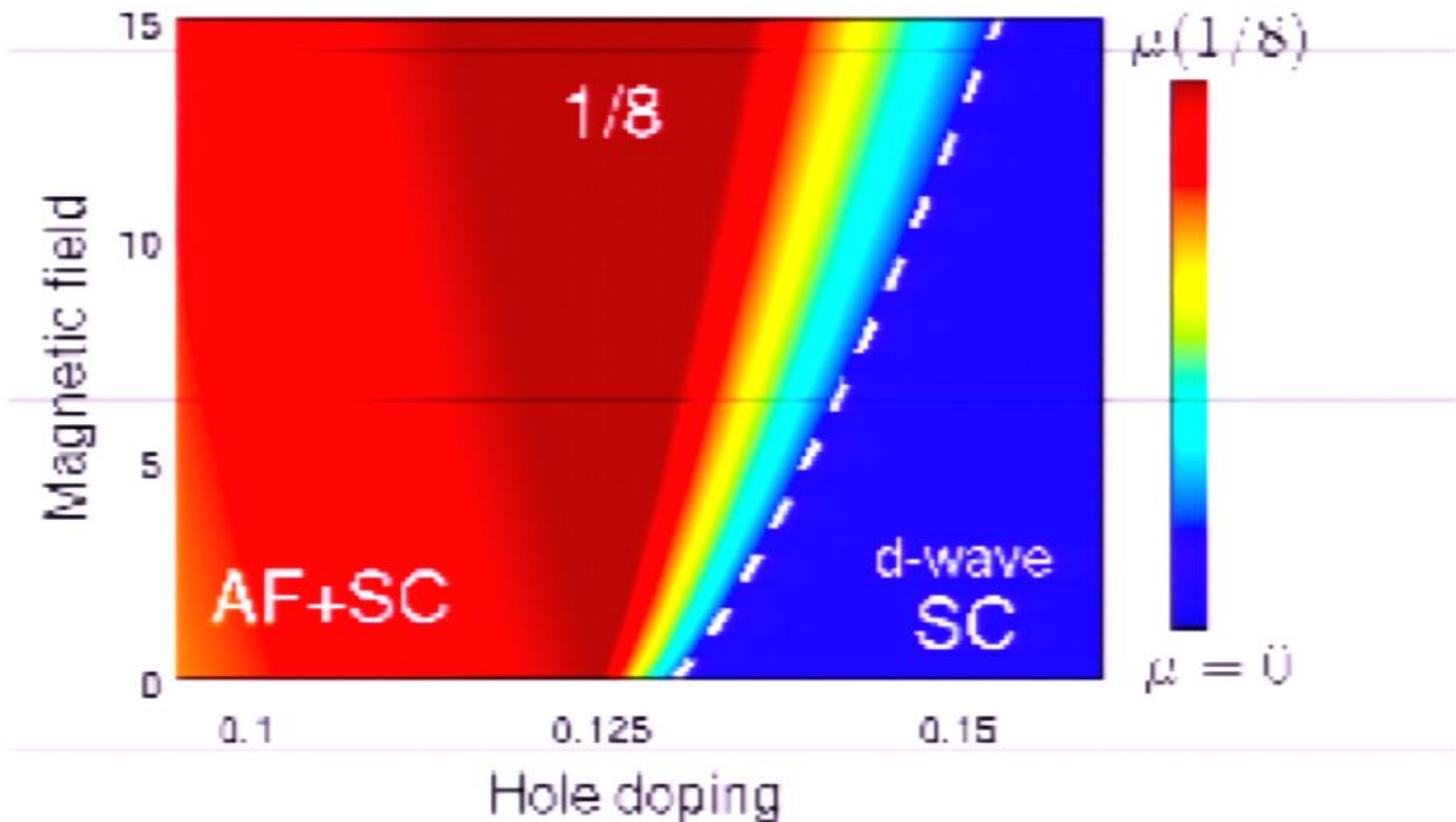
$T=0$



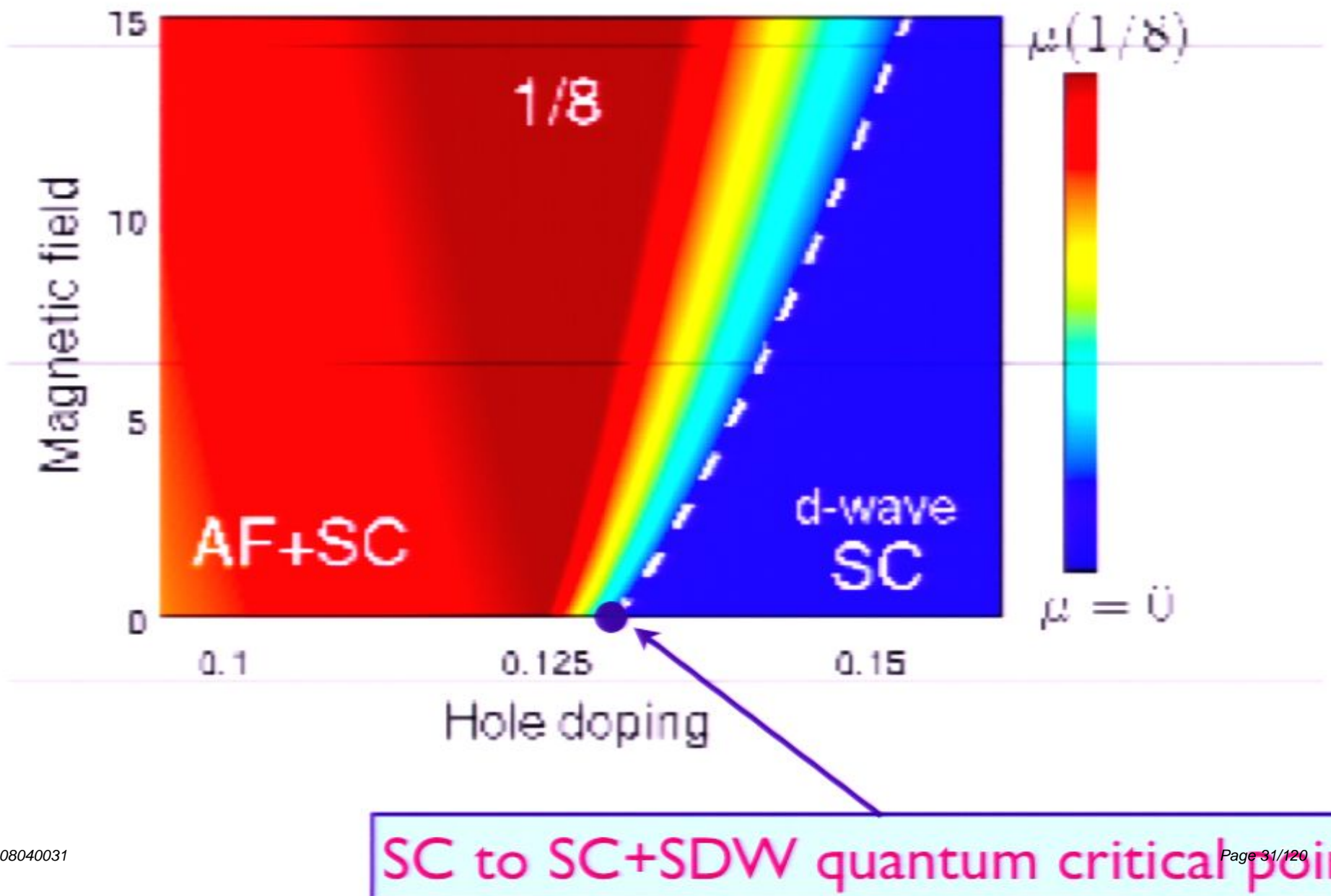
$T=0$



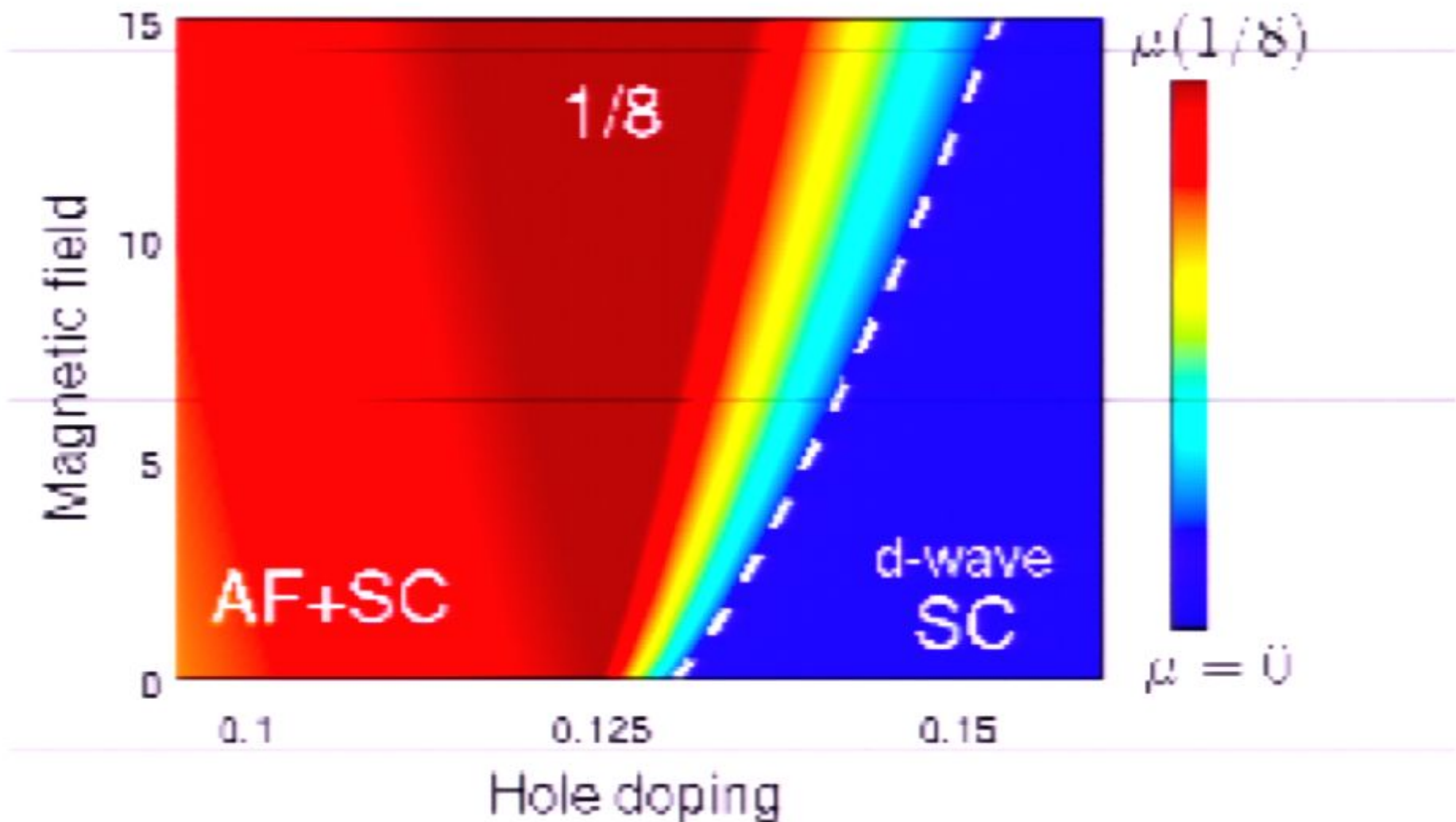
J. Chang et al. (PSI Mesot group), arXiv:0712.2181



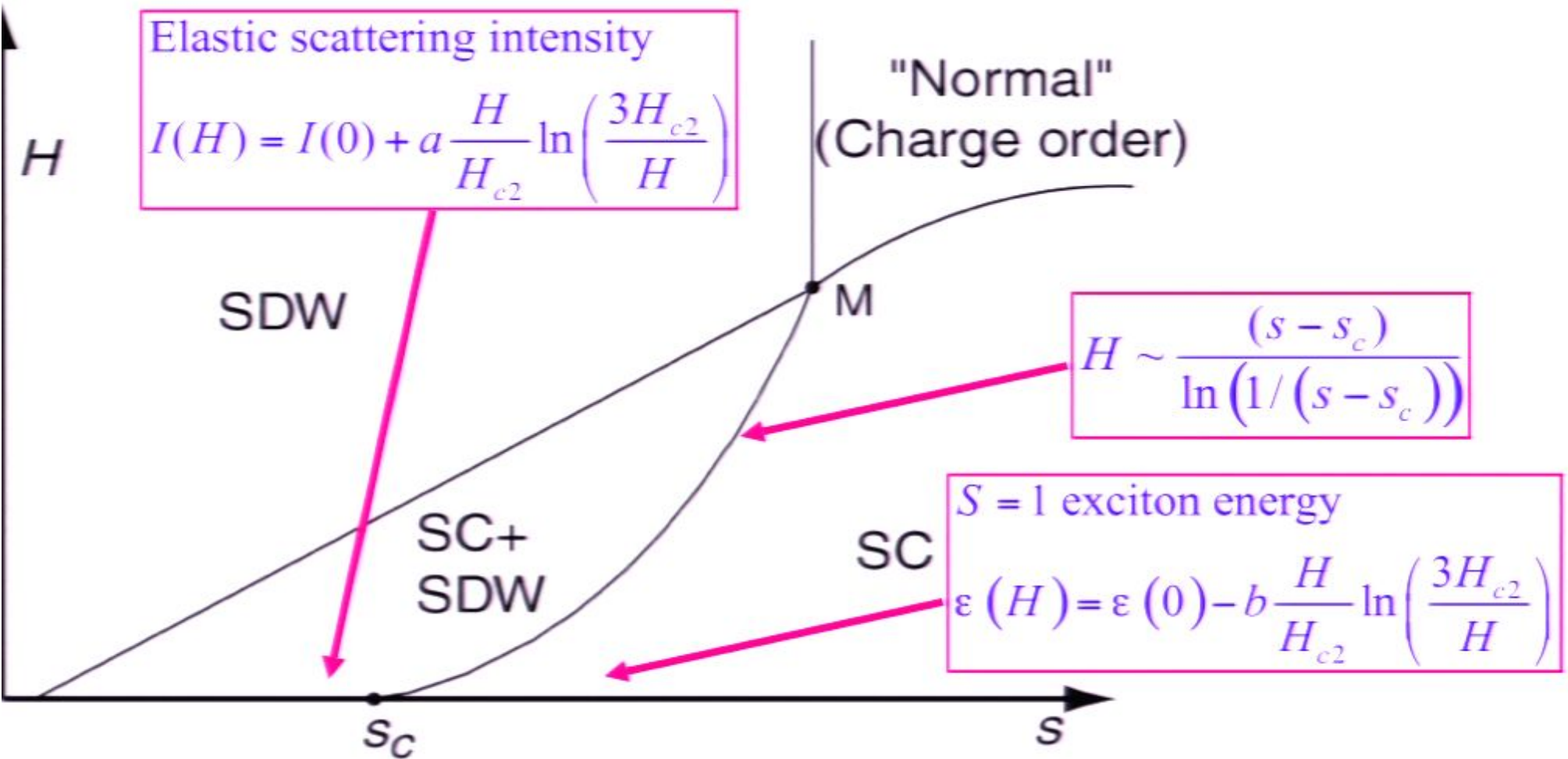
J. Chang et al. (PSI Mesot group), arXiv:0712.2181



J. Chang et al. (PSI Mesot group), arXiv:0712.2181

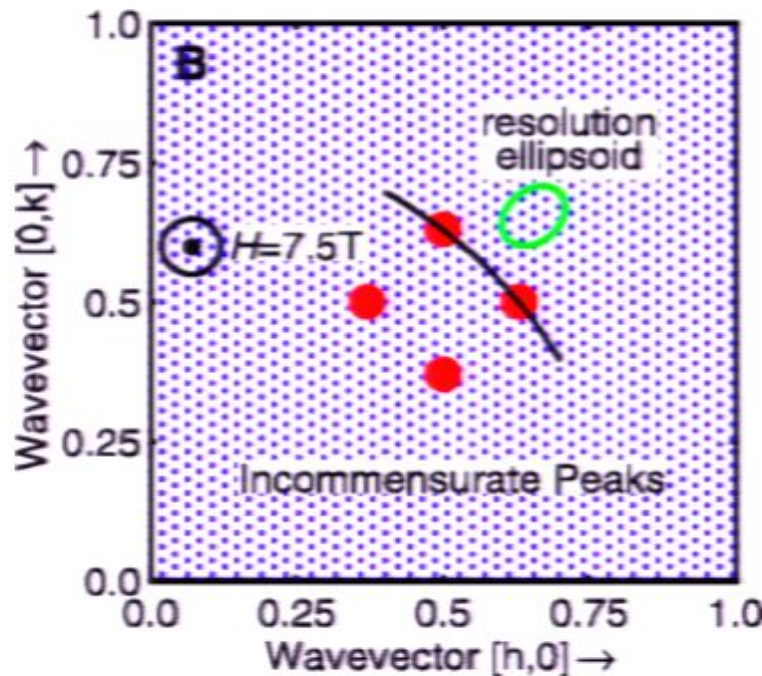


$T=0$



# Neutron scattering measurements of dynamic spin correlations of the superconductor (SC) in a magnetic field

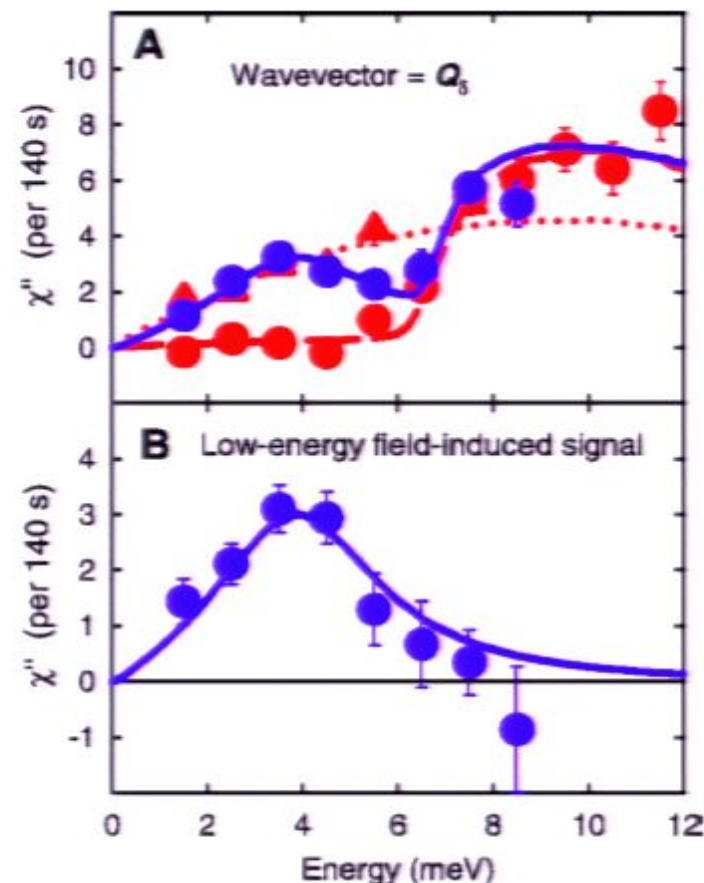
B. Lake, G. Aeppli, K. N. Clausen, D. F. McMorrow,  
K. Lefmann, N. E. Hussey, N. Mangkorntong,  
M. Nohara, H. Takagi, T. E. Mason, and A. Schröder,  
*Science* **291**, 1759 (2001).



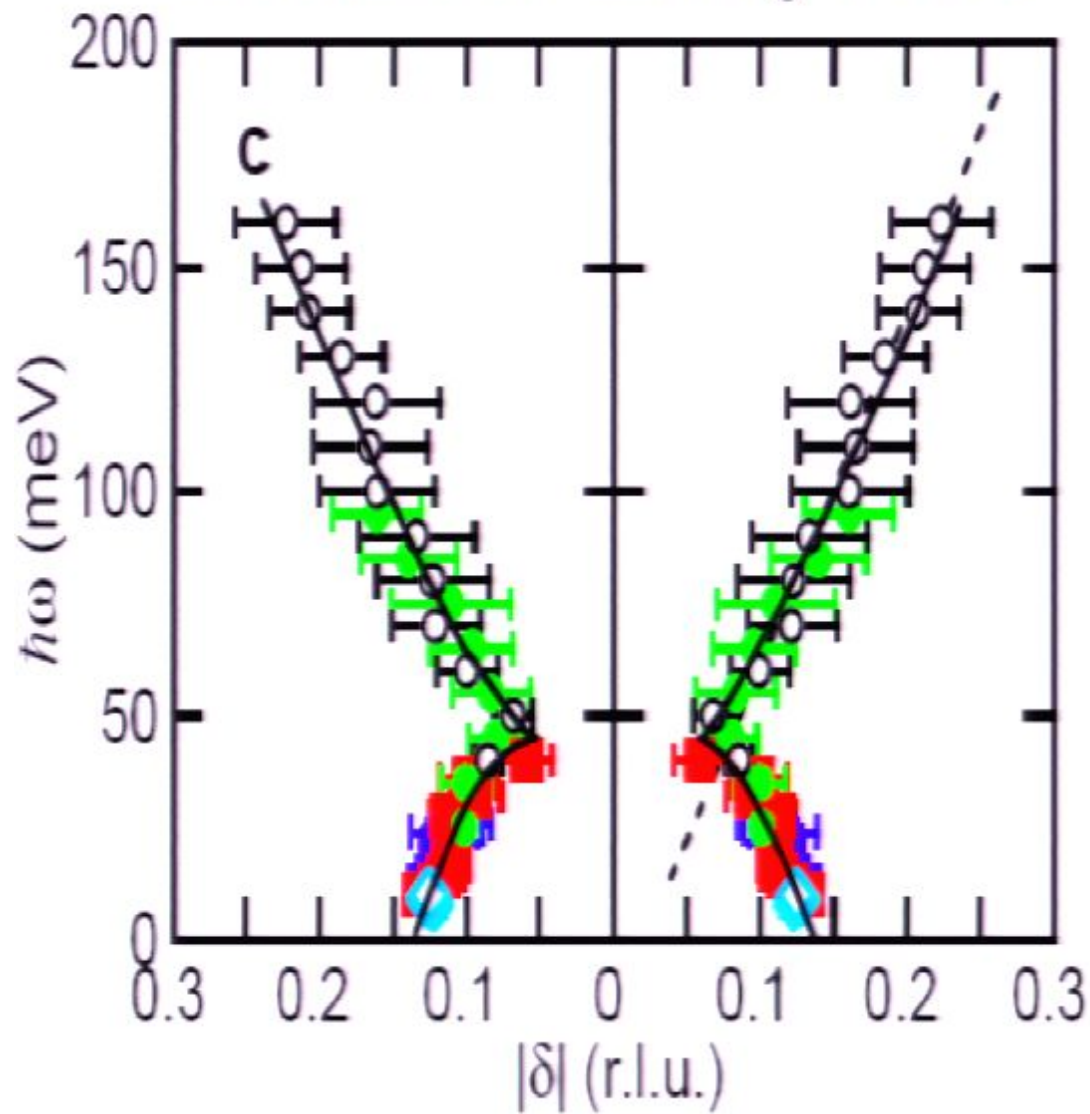
Peaks at  $(0.5, 0.5) \pm (0.125, 0)$

and  $(0.5, 0.5) \pm (0, 0.125)$

⇒ dynamic SDW of period 8



## Neutron Scattering-LSCO

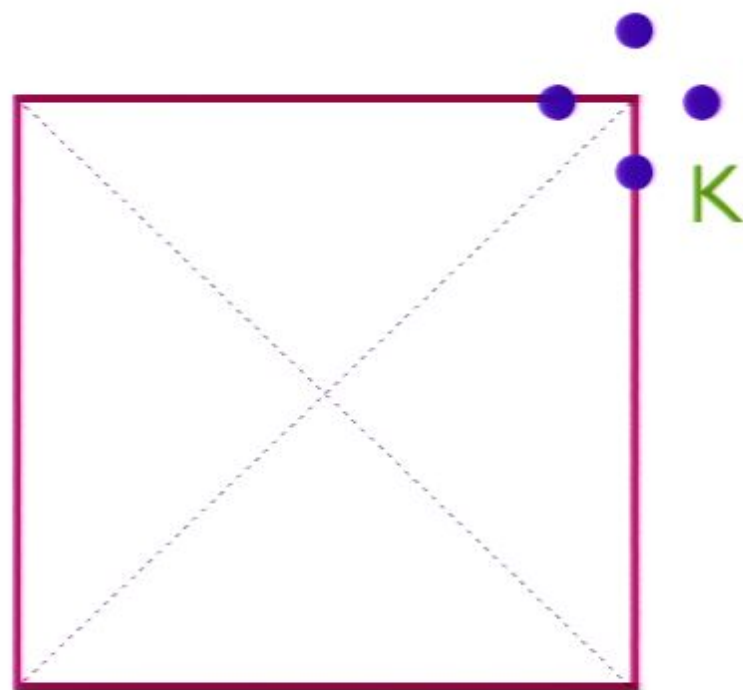


Vignolle *et al.*, Nature Phys. 07

Christensen *et al.*, PRL 04

Hayden *et al.*, Nature 04

Tranquada *et al.*, Nature 04



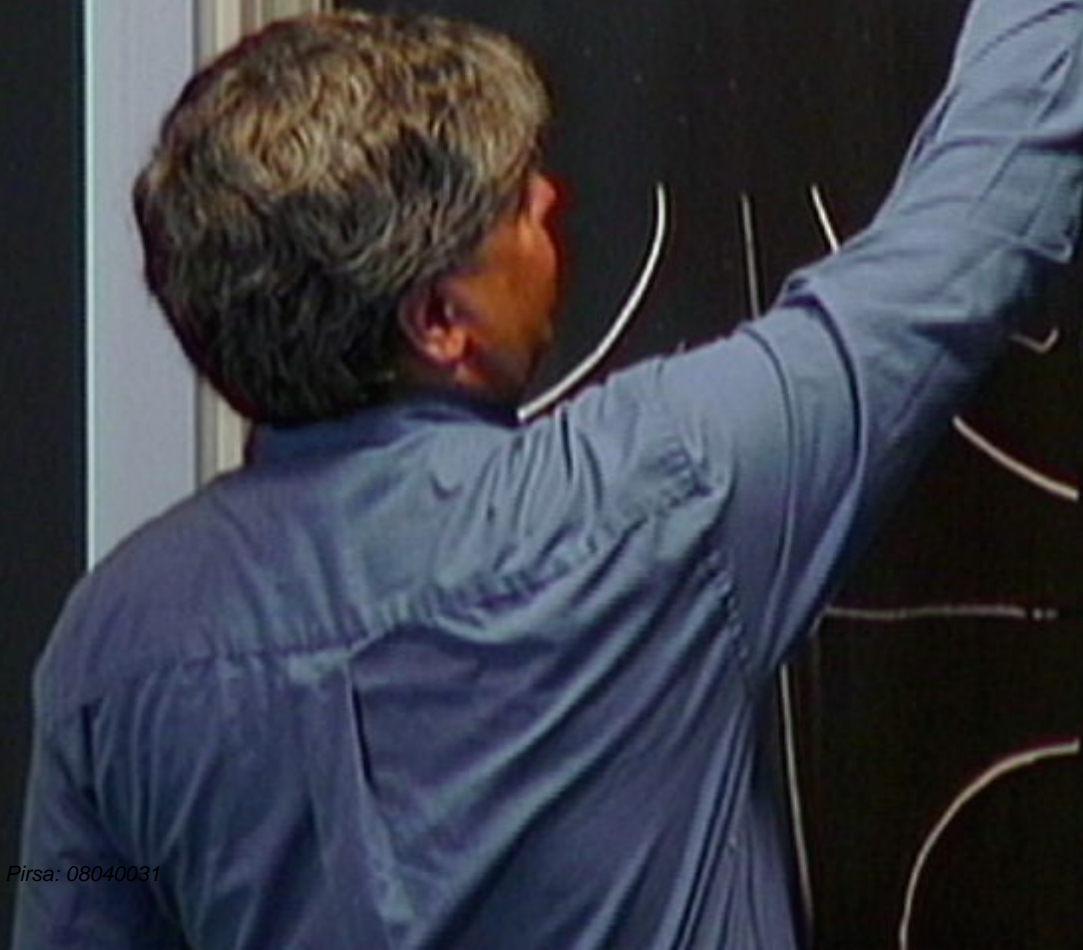
Brillouin zone

$$E_k = \sqrt{(\epsilon_k - \mu)^2}$$

$$\sim E^2 - FL$$

$$F \sim E^3$$

$$\Delta_h \sim \zeta_{dSC}$$





$$E_k = \sqrt{(\epsilon_k - \mu)^2 + \Delta_k^2} \sim$$

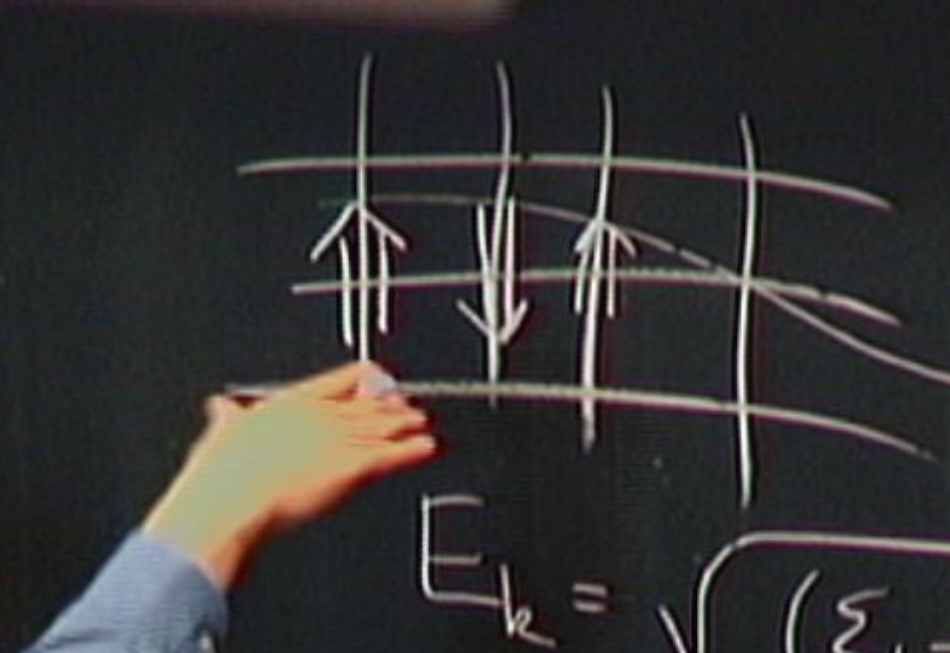
$\Gamma \sim E^2 - FL$

$\Gamma \sim E^3$

$\Delta_k \sim \cos k_x - \cos k_y$

dSC

$$\Gamma(E) \sim E$$


$$E_k = \sqrt{(\varepsilon_k - \mu)^2 + \Delta_k^2}$$

$$\Gamma \sim E^2 - FL$$

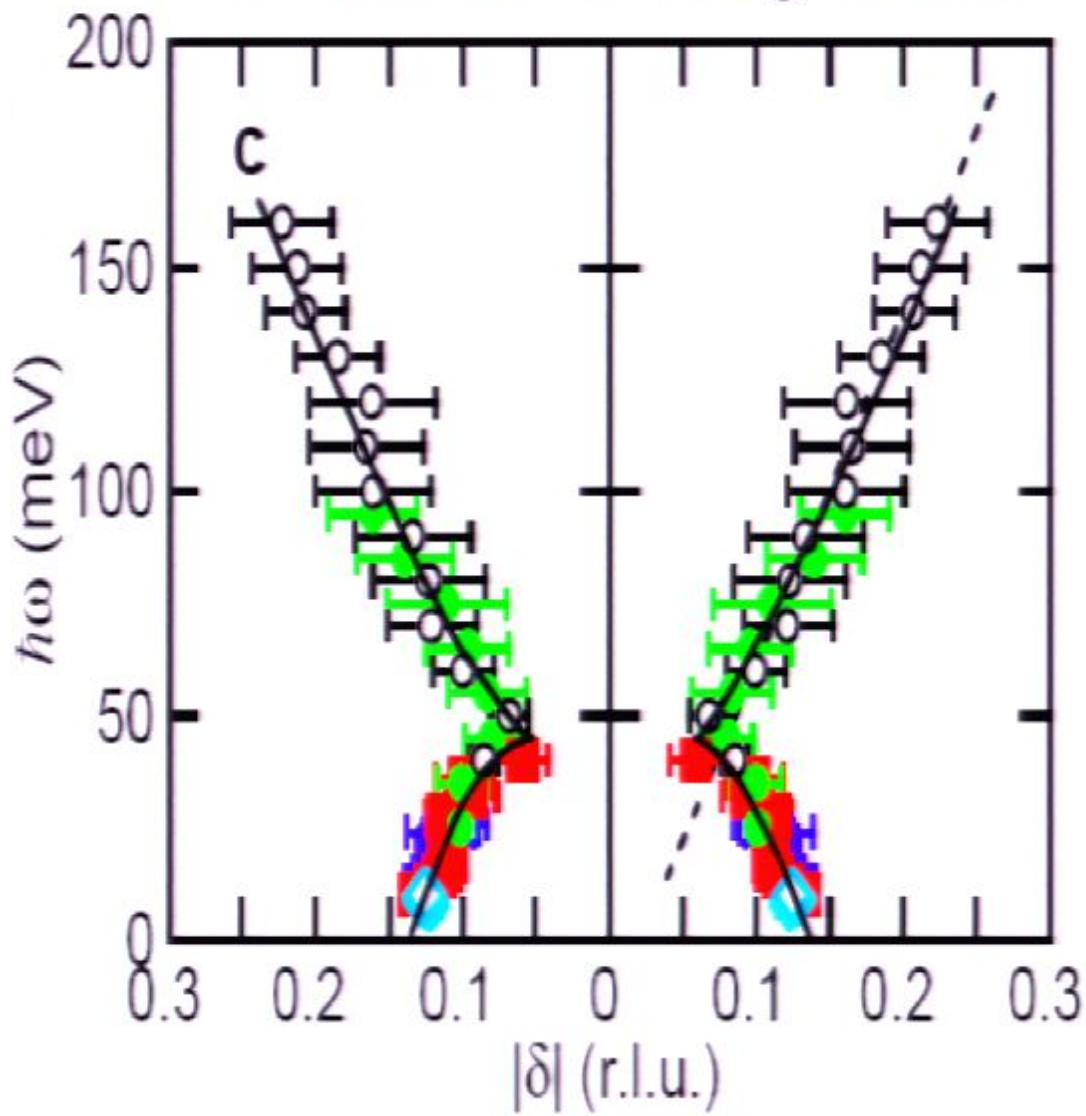
$$\Gamma \sim E^3$$

$$\Delta_k \sim \cos k_x - \cos k_y$$

dSC

$$\Gamma(E) \sim E$$

## Neutron Scattering-LSCO

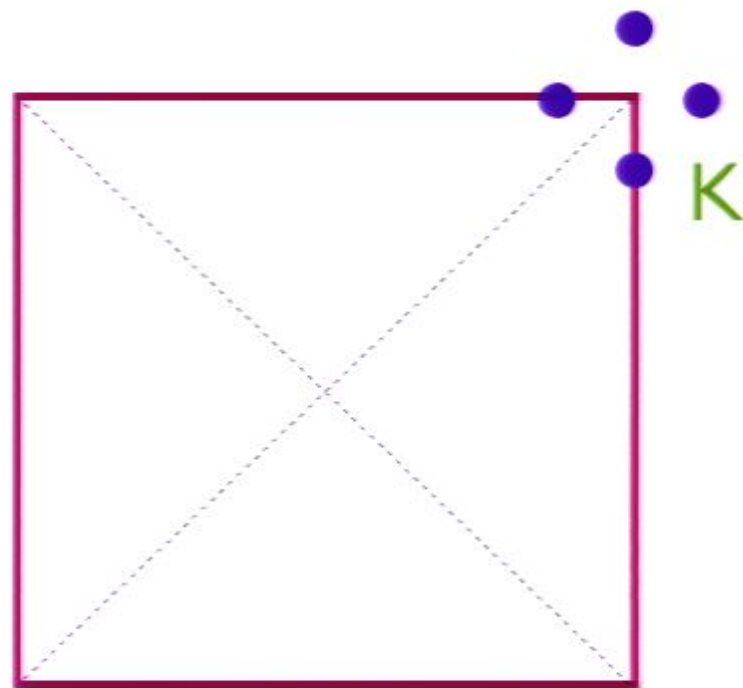


Vignolle *et al.*, Nature Phys. 07

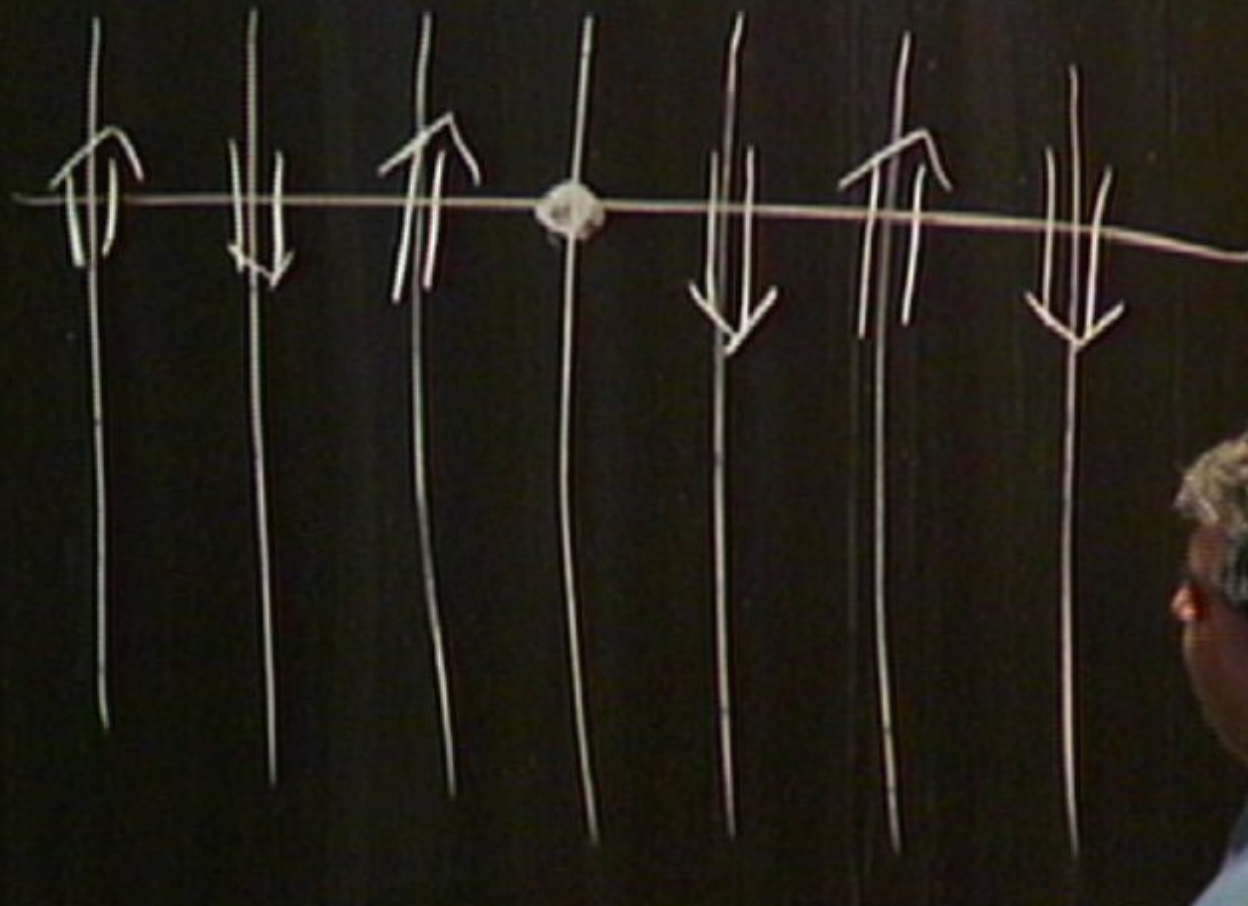
Christensen *et al.*, PRL 04

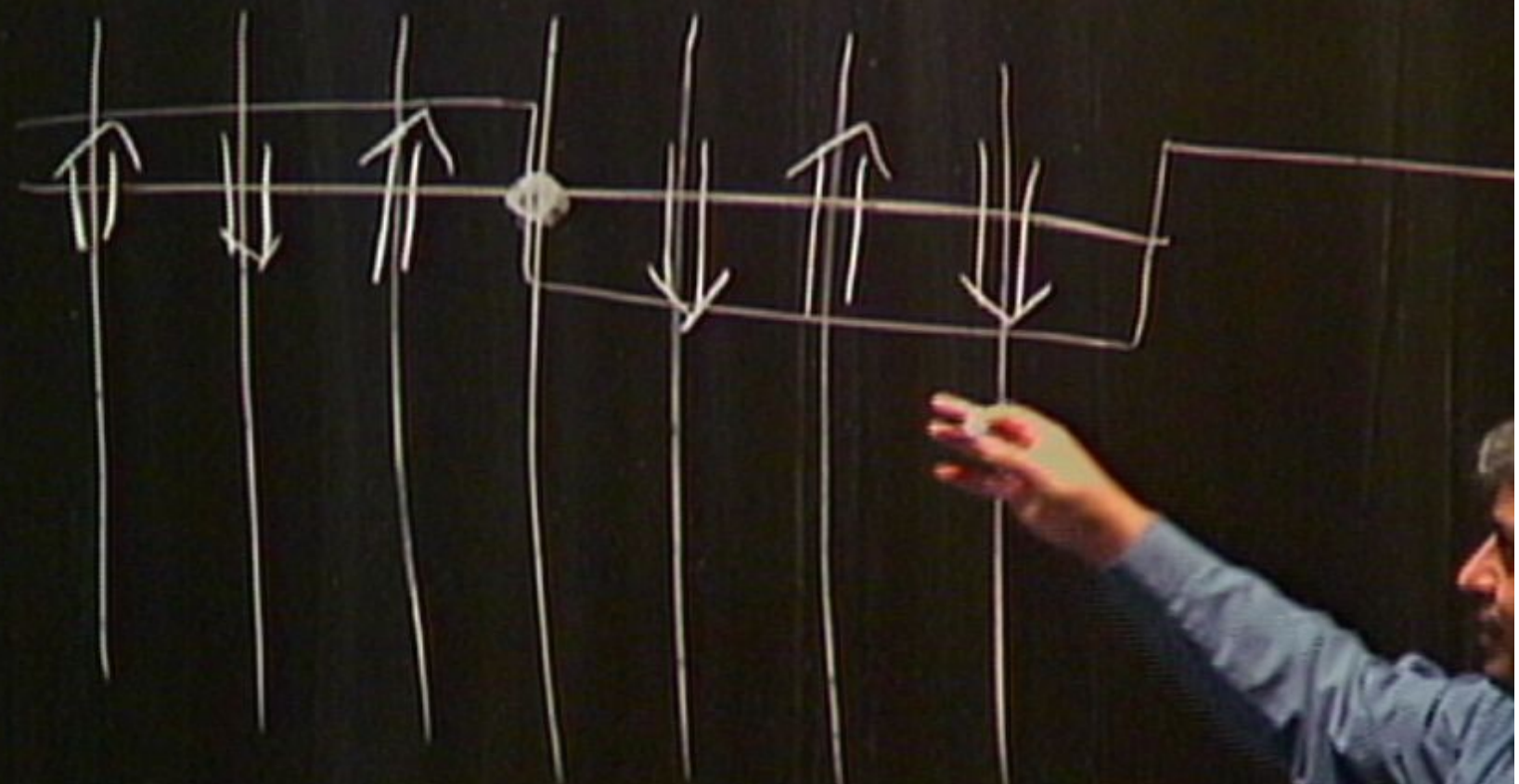
Hayden *et al.*, Nature 04

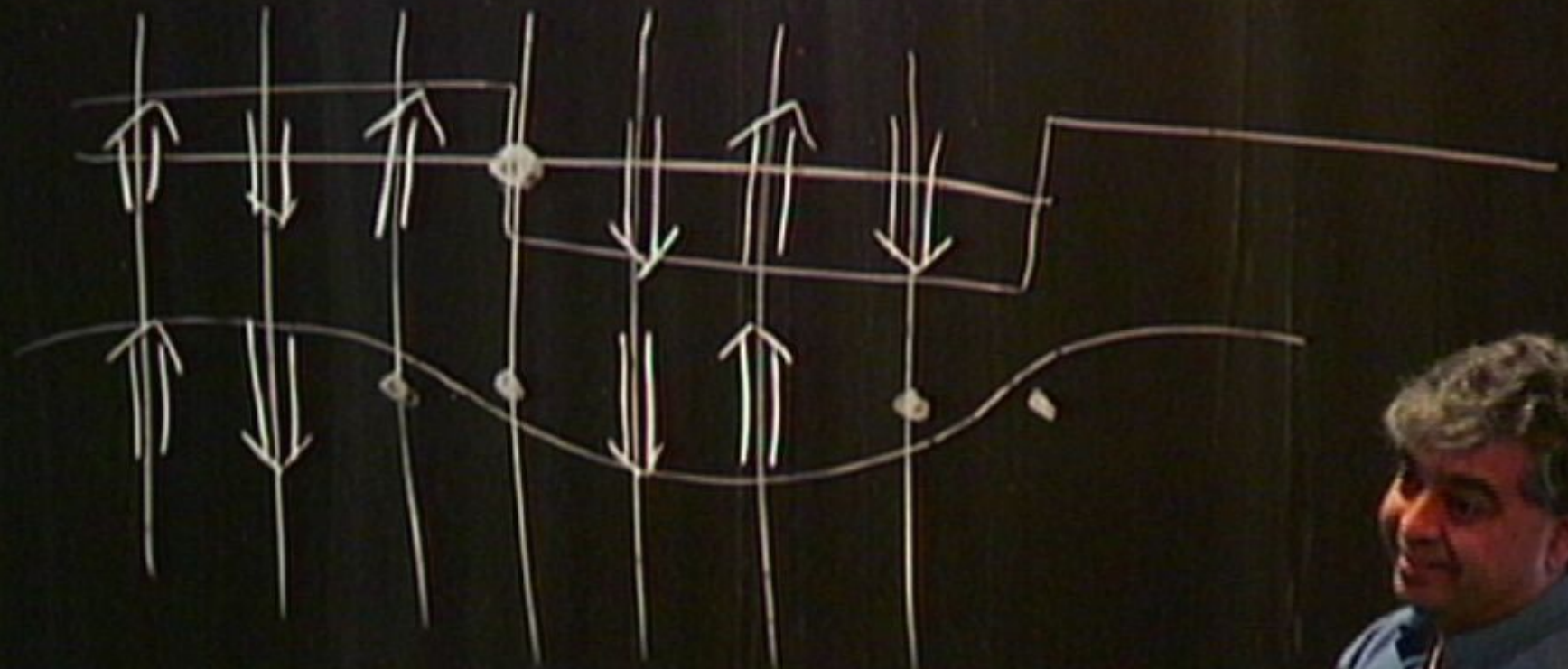
Tranquada *et al.*, Nature 04

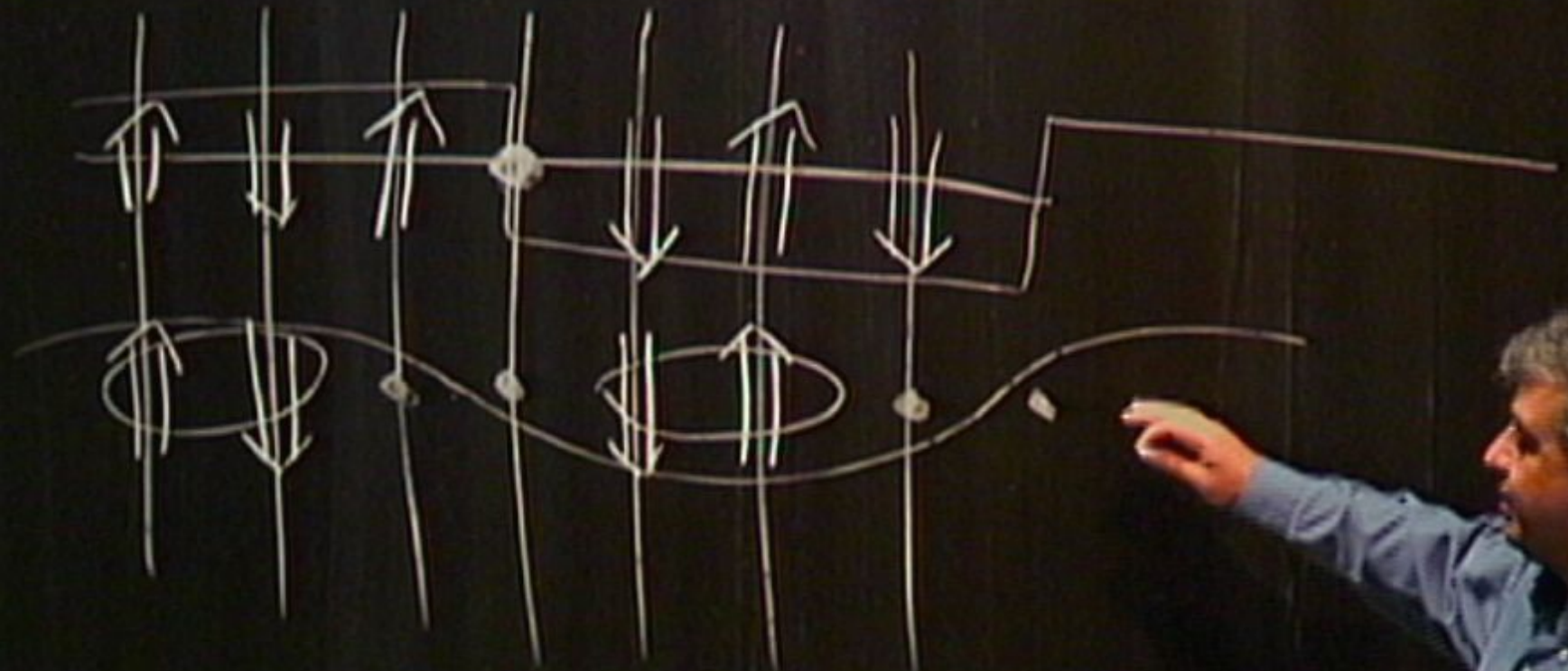


Brillouin zone

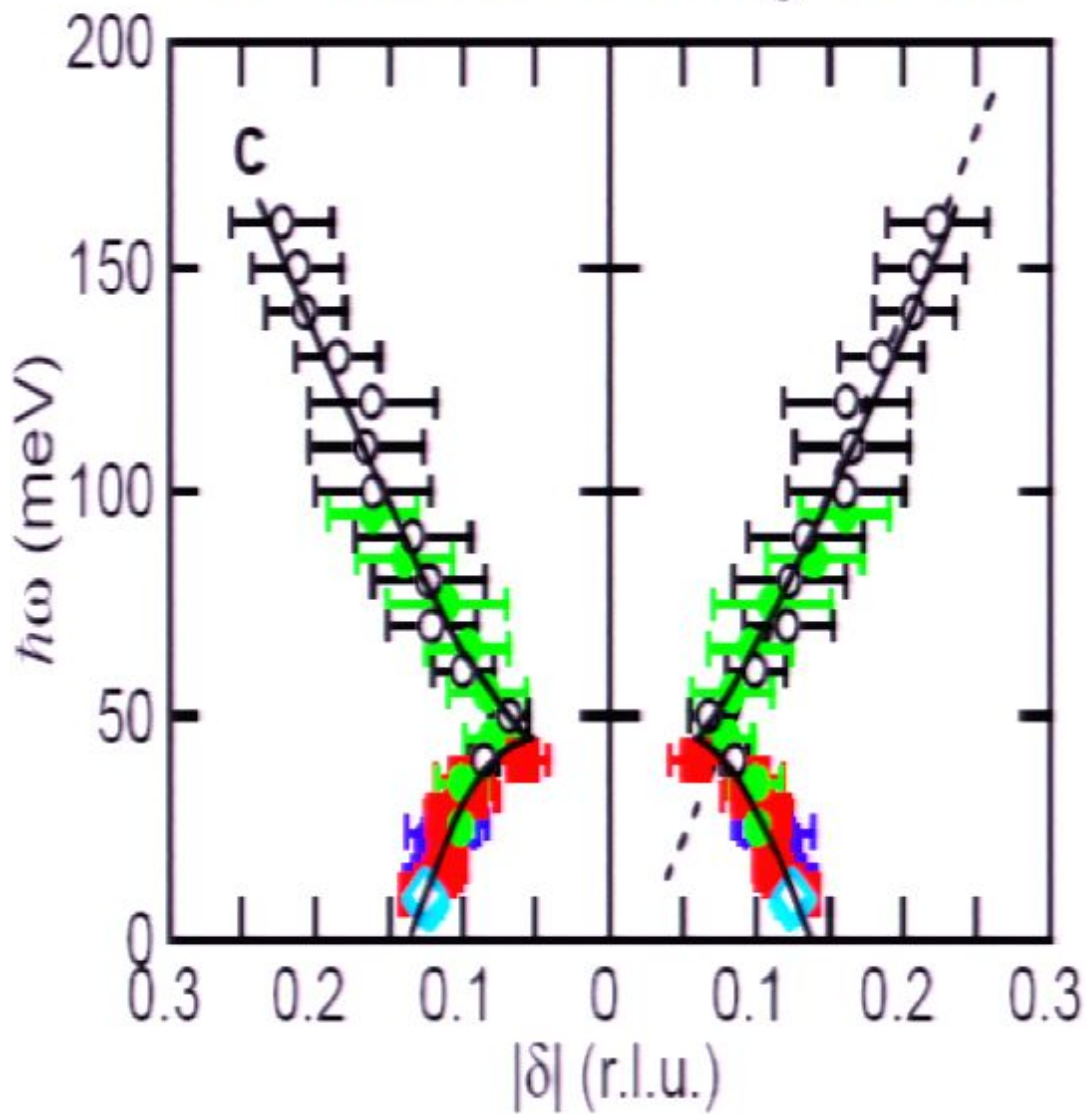








## Neutron Scattering-LSCO

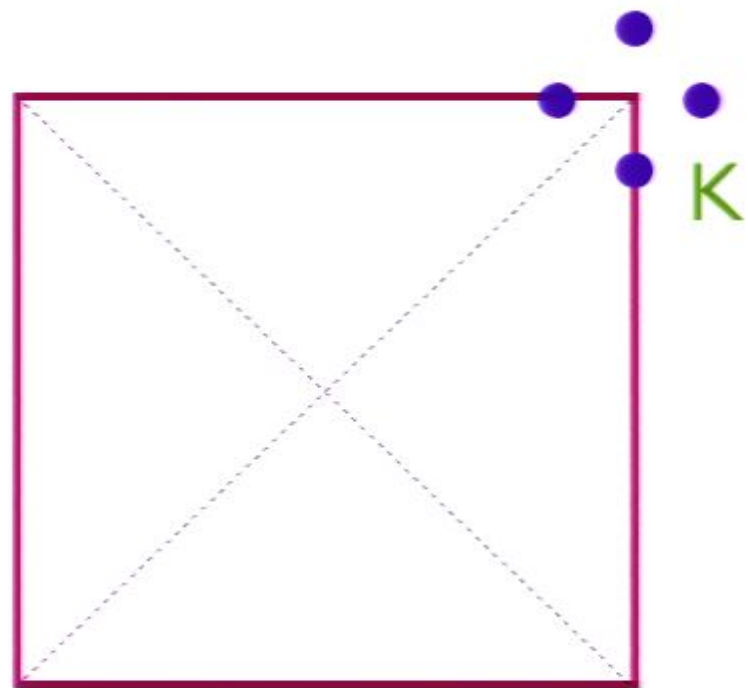


Vignolle *et al.*, Nature Phys. 07

Christensen *et al.*, PRL 04

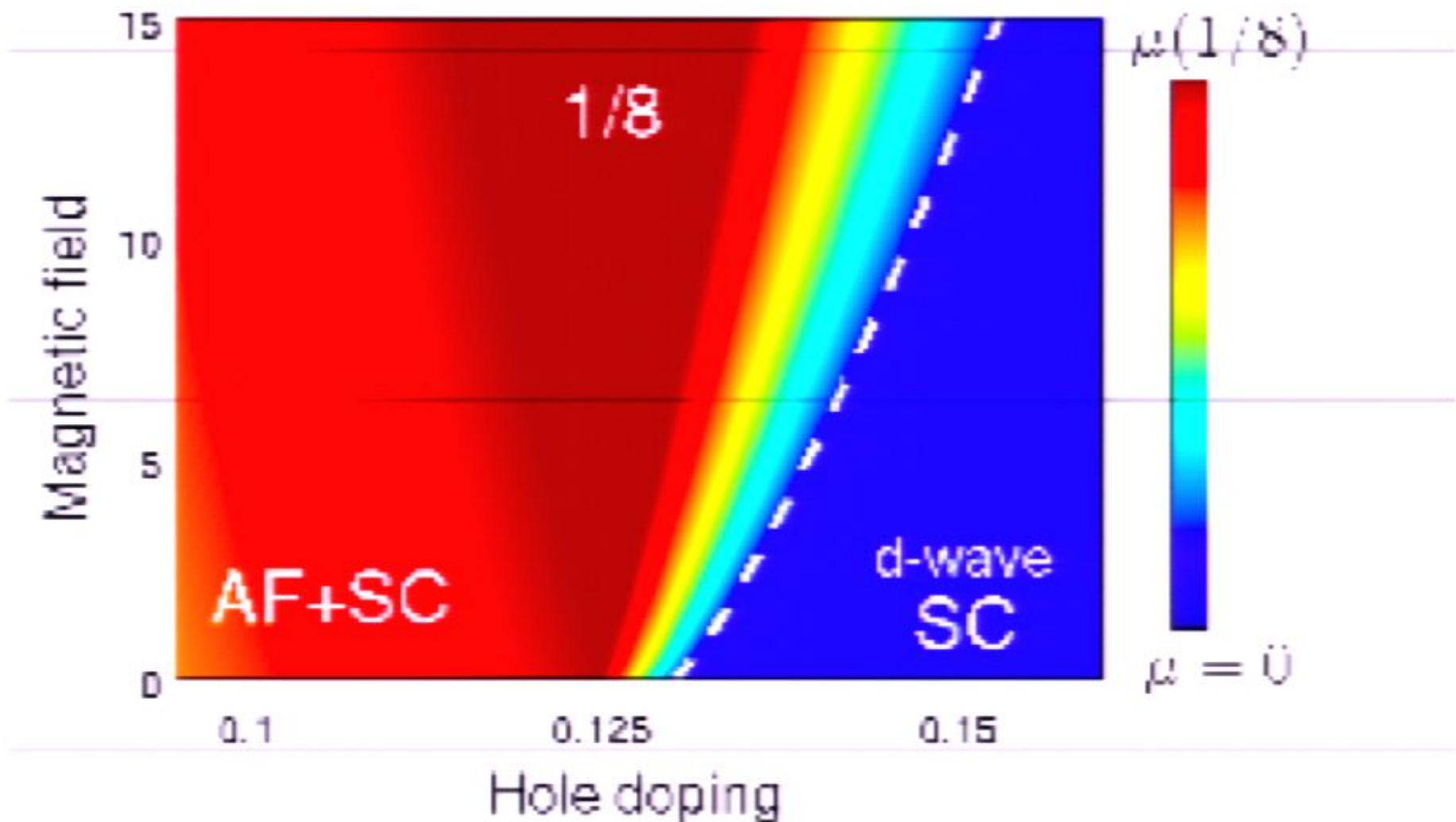
Hayden *et al.*, Nature 04

Tranquada *et al.*, Nature 04

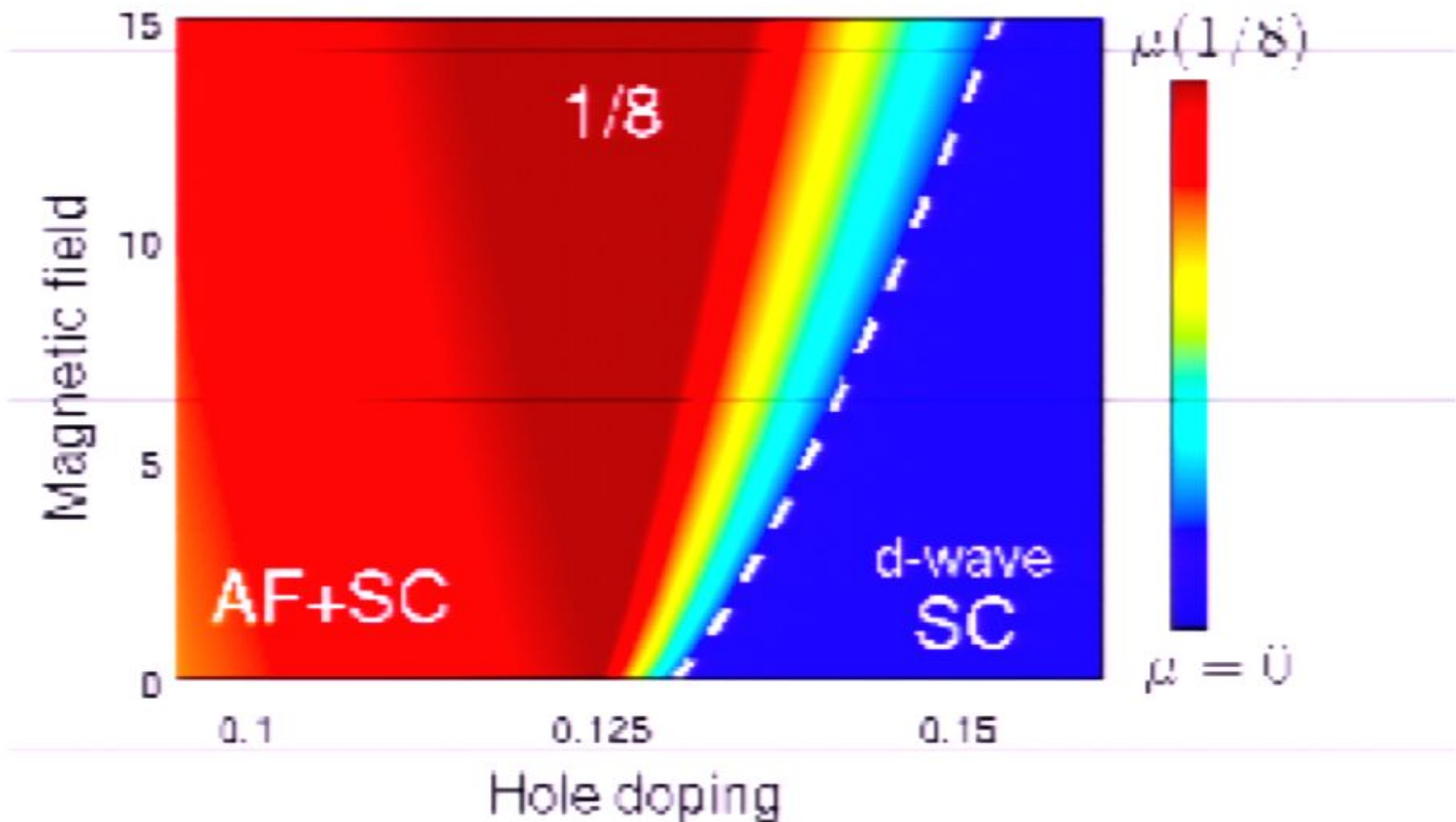


Brillouin zone

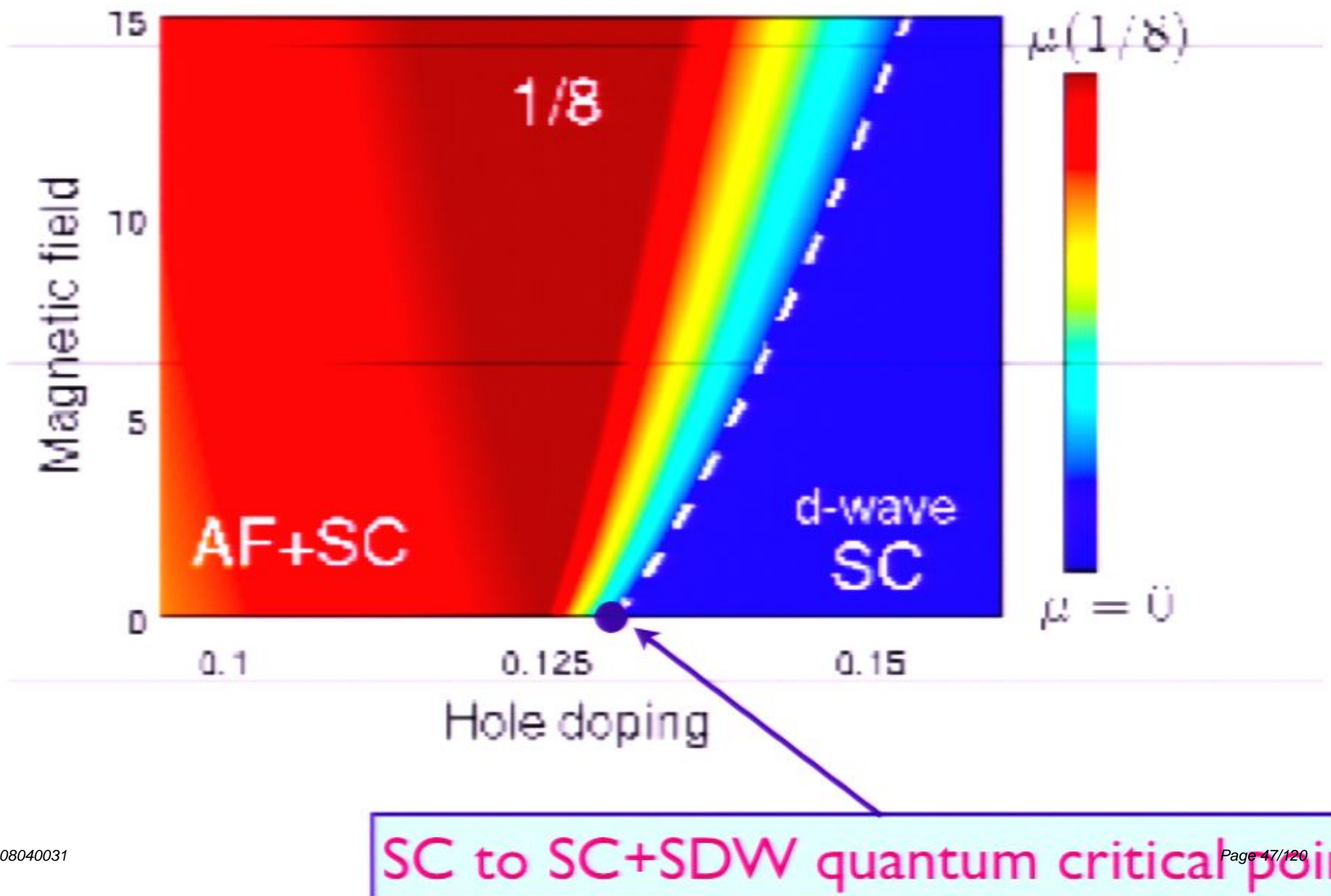
J. Chang et al. (PSI Mesot group), arXiv:0712.2181



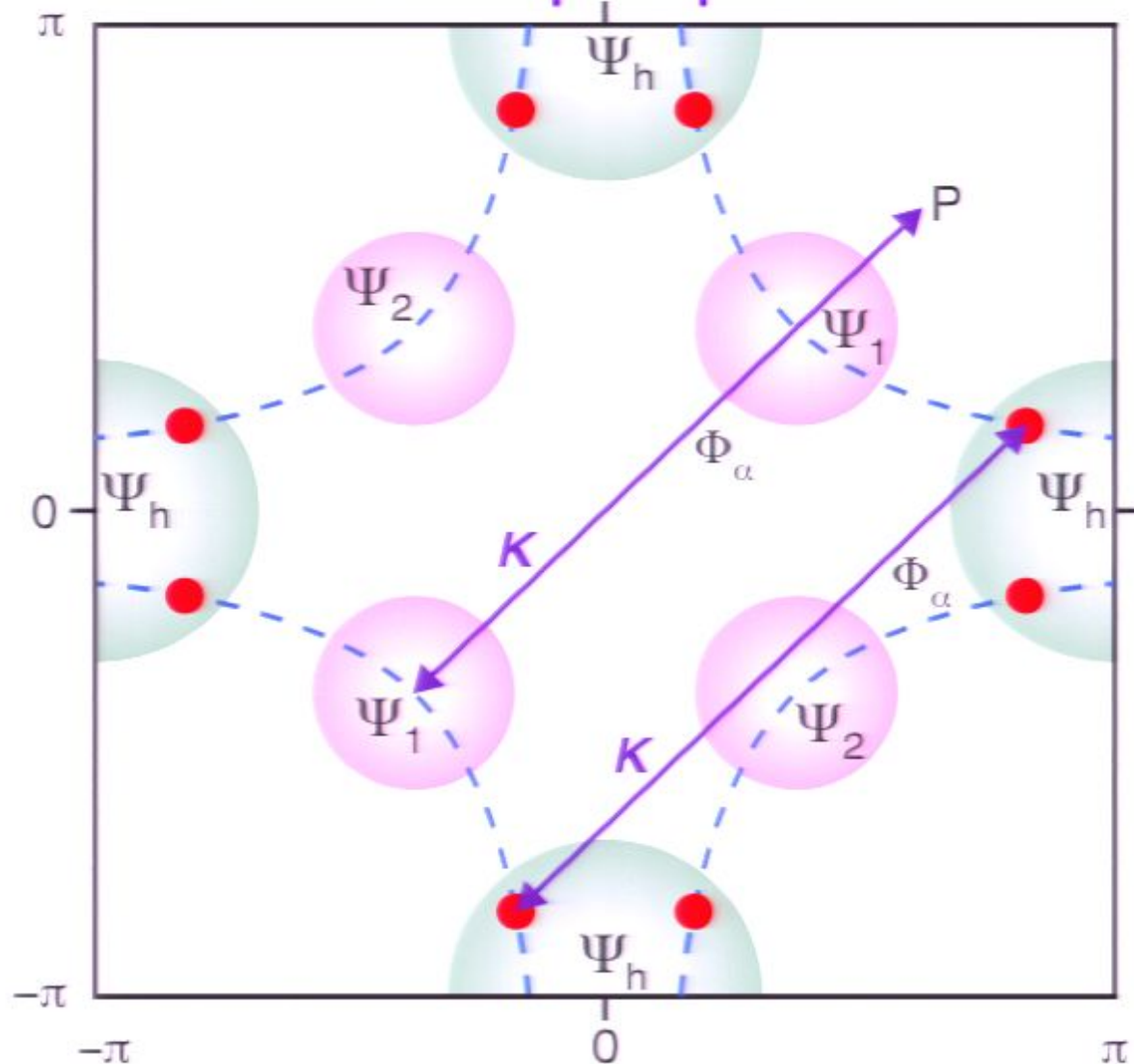
J. Chang et al. (PSI Mesot group), arXiv:0712.2181



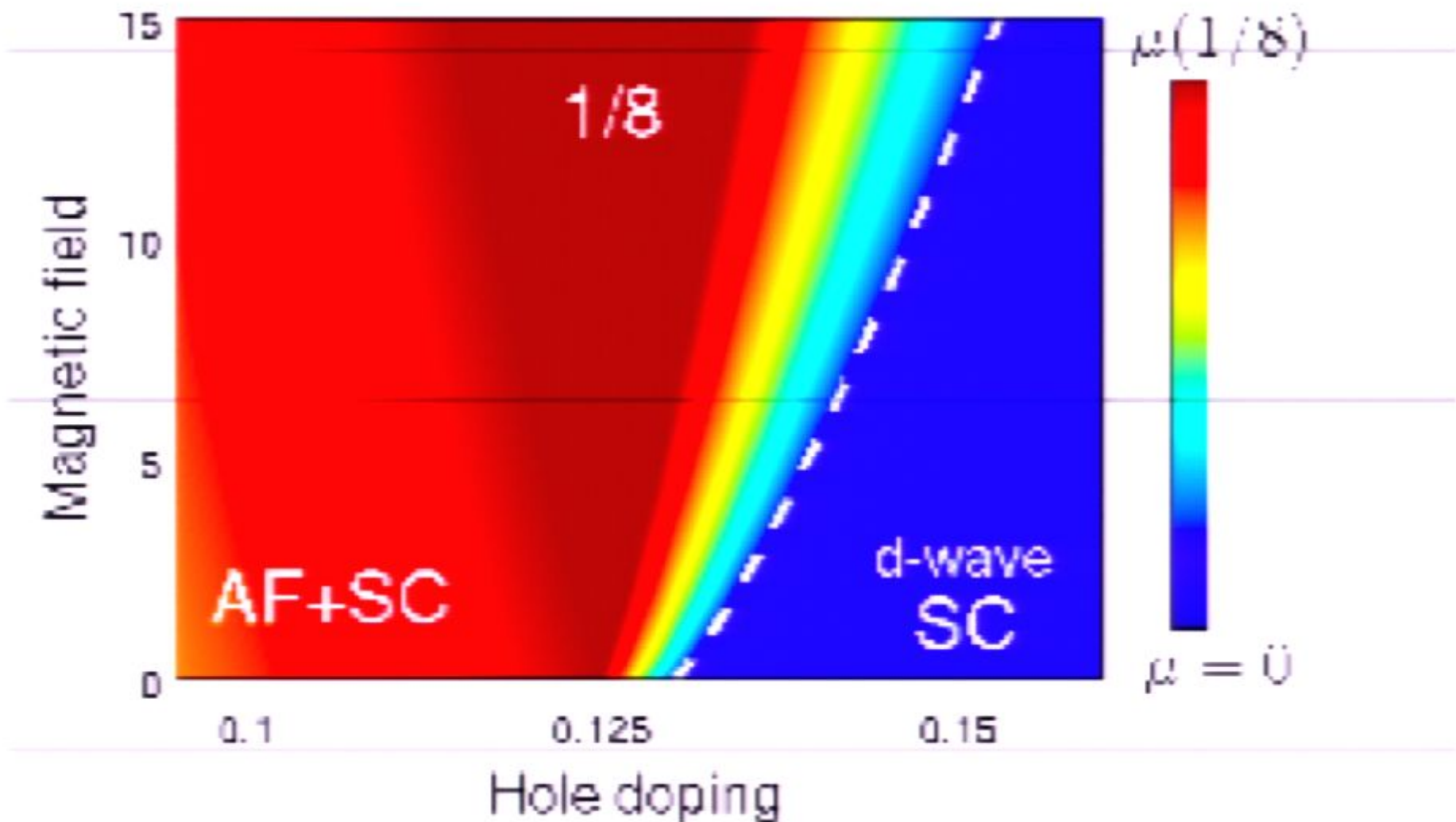
J. Chang et al. (PSI Mesot group), arXiv:0712.2181



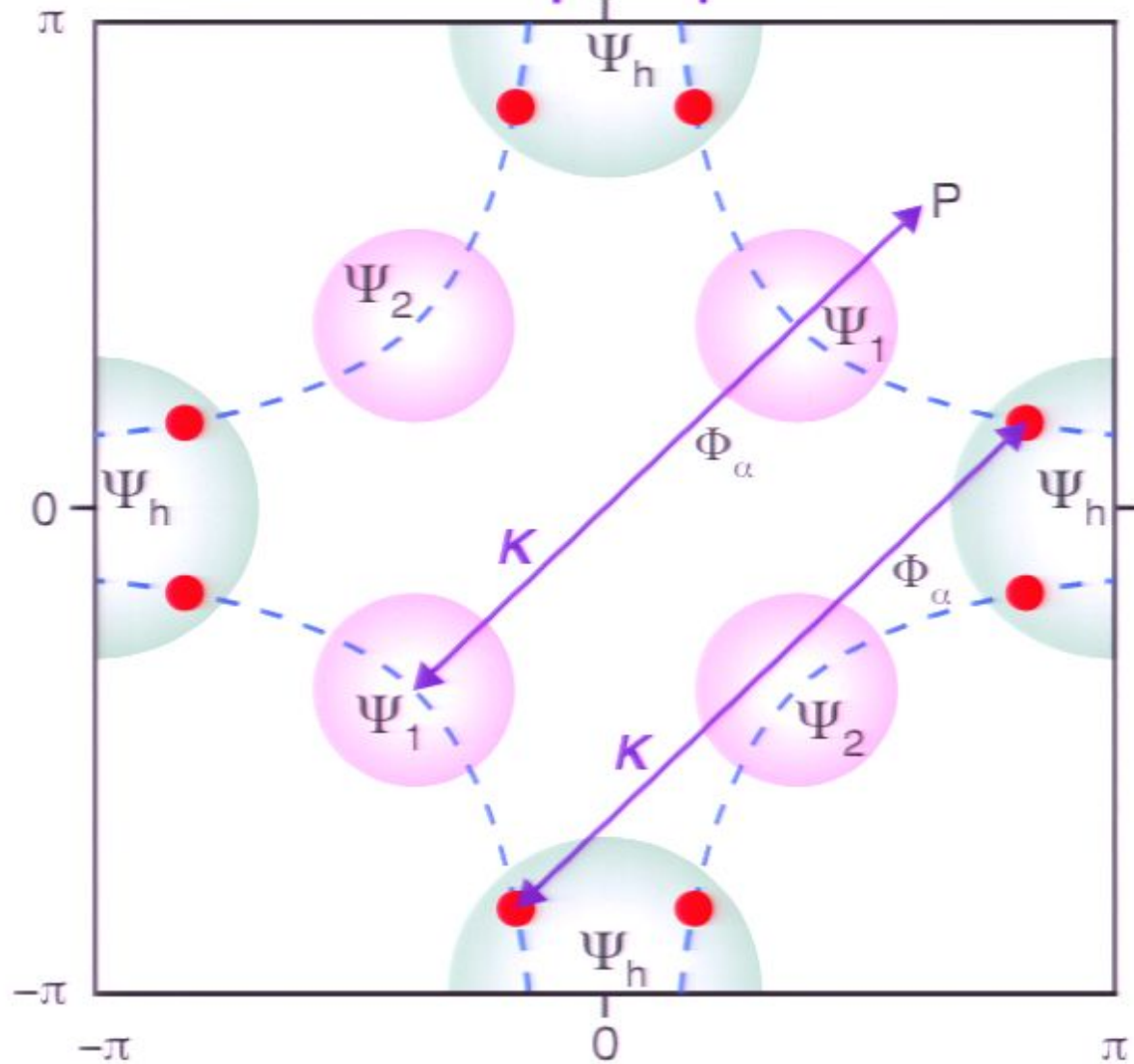
# Coupling between SDW order and nodal quasiparticles



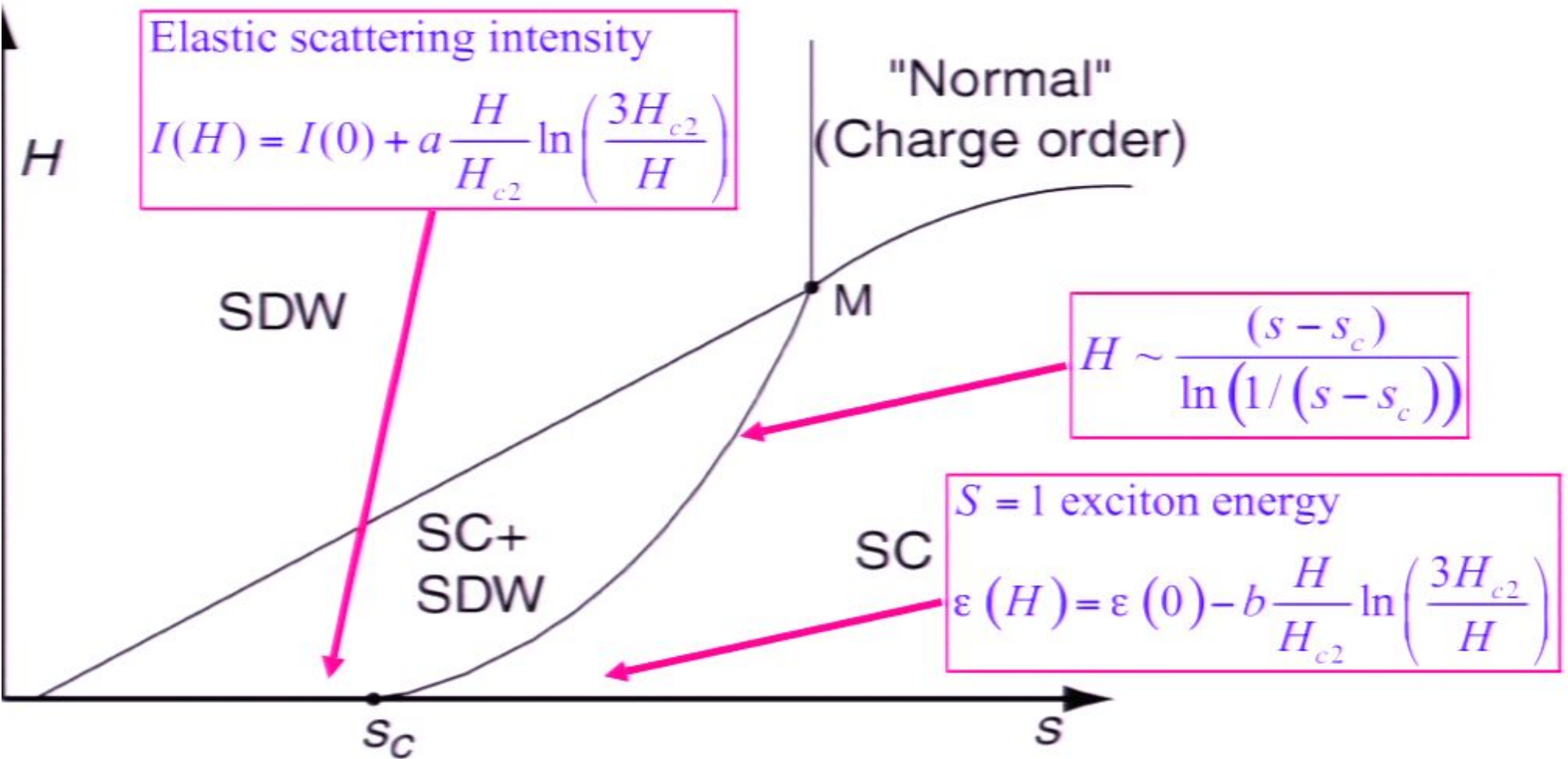
J. Chang et al. (PSI Mesot group), arXiv:0712.2181



# Coupling between SDW order and nodal quasiparticles

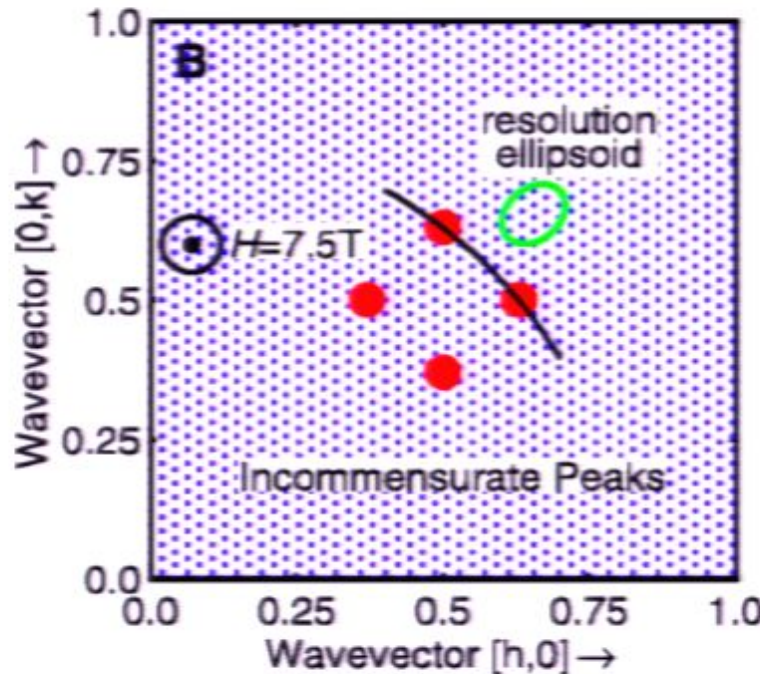


$T=0$



# Neutron scattering measurements of dynamic spin correlations of the superconductor (SC) in a magnetic field

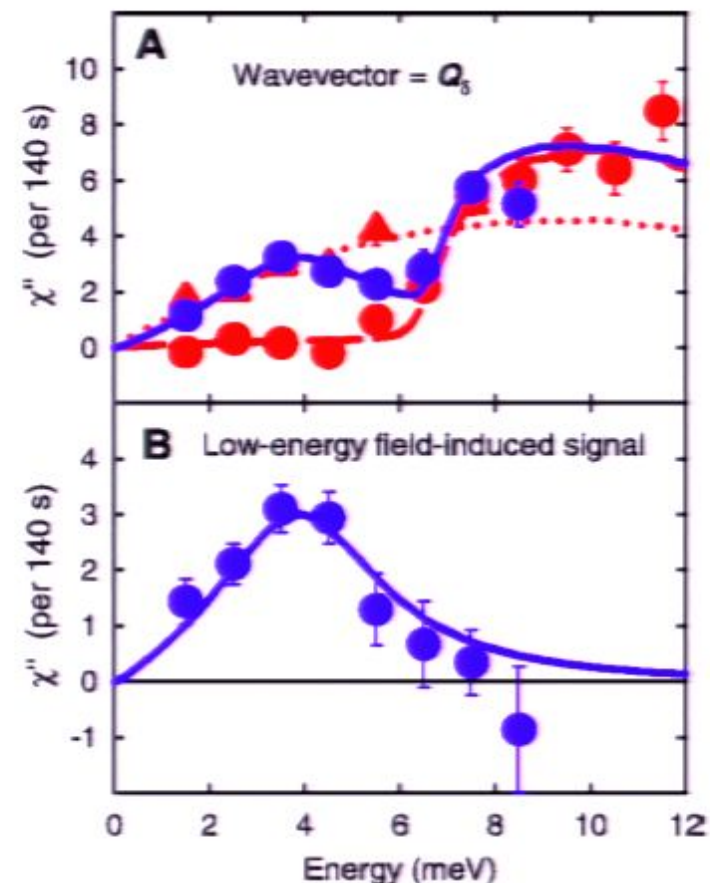
B. Lake, G. Aeppli, K. N. Clausen, D. F. McMorrow,  
K. Lefmann, N. E. Hussey, N. Mangkorntong,  
M. Nohara, H. Takagi, T. E. Mason, and A. Schröder,  
*Science* **291**, 1759 (2001).



Peaks at  $(0.5, 0.5) \pm (0.125, 0)$

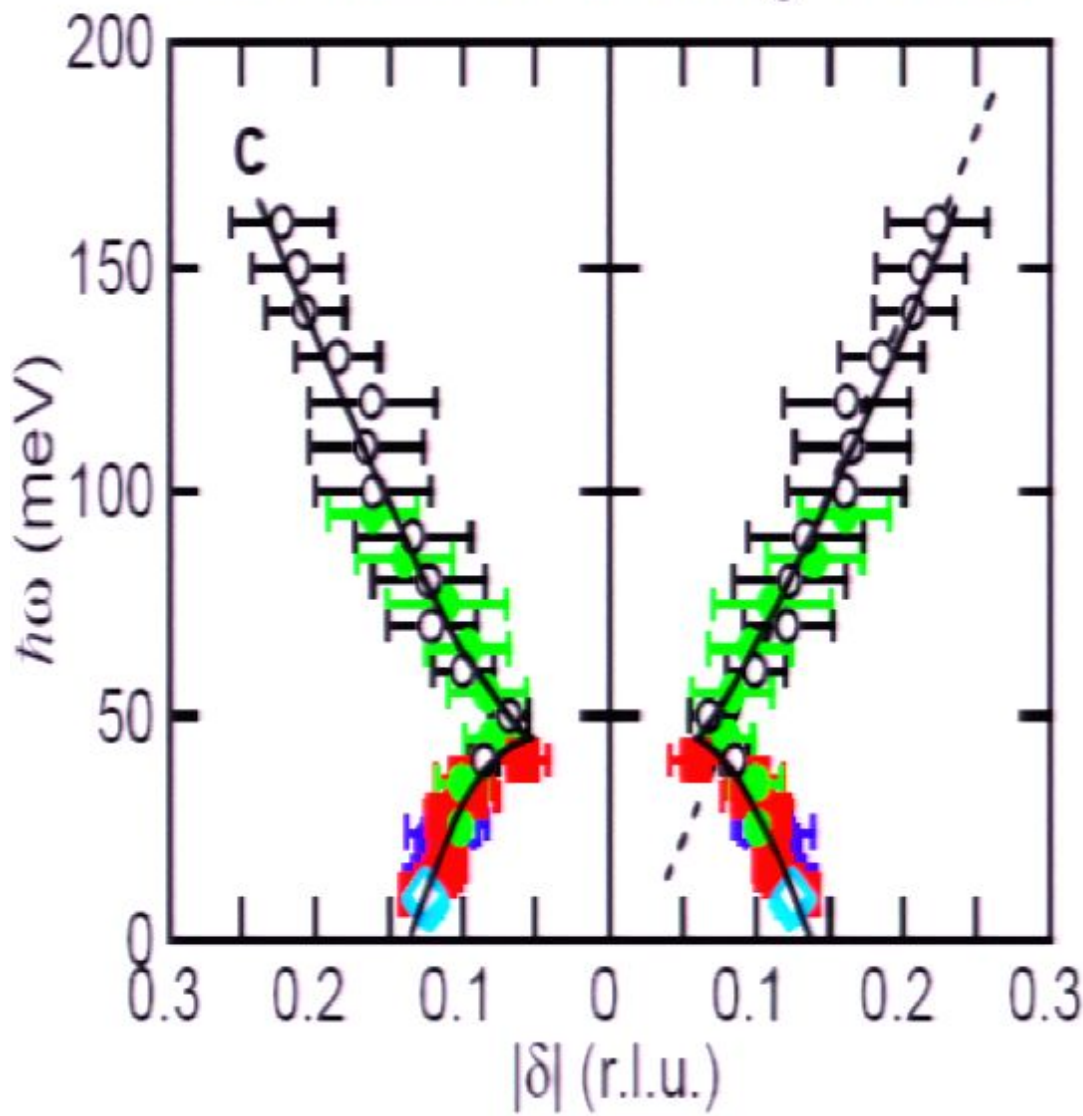
and  $(0.5, 0.5) \pm (0, 0.125)$

$\Rightarrow$  dynamic SDW of period 8



Neutron scattering off  $\text{La}_{2-\delta}\text{Sr}_\delta\text{CuO}_4$  ( $\delta = 0.163$ , *SC phase*)  
at low temperatures in  $H=0$  (red dots) and  $H=7.5\text{T}$  (blue dots)

## Neutron Scattering-LSCO

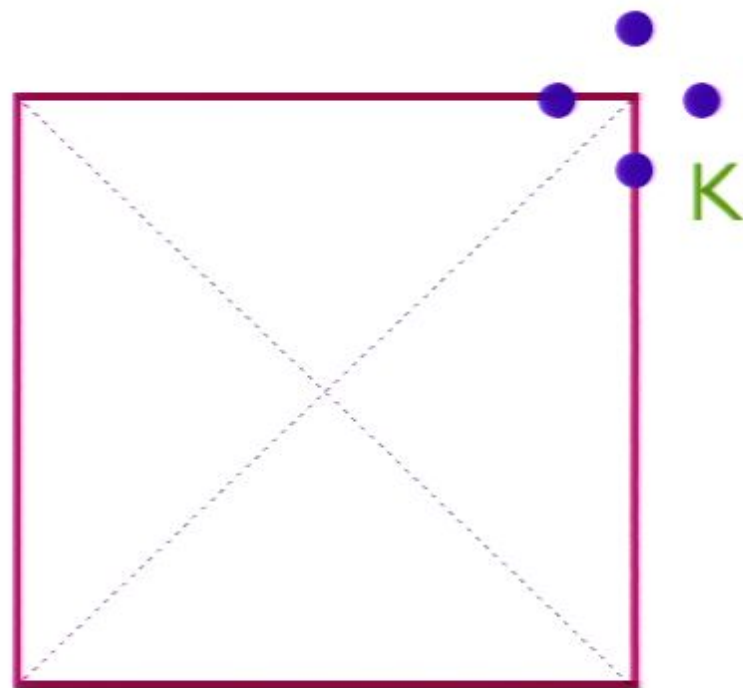


Vignolle *et al.*, Nature Phys. 07

Christensen *et al.*, PRL 04

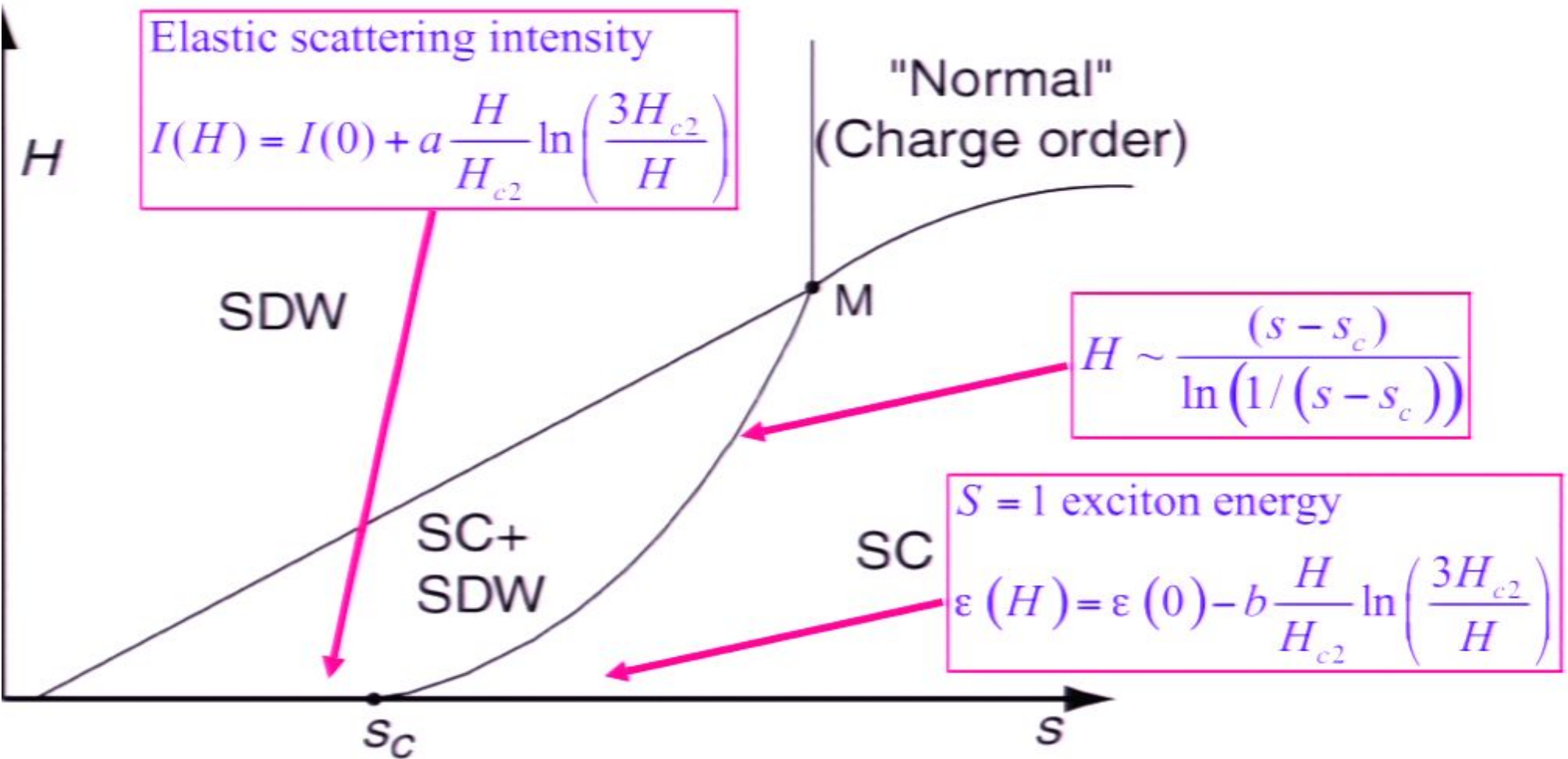
Hayden *et al.*, Nature 04

Tranquada *et al.*, Nature 04

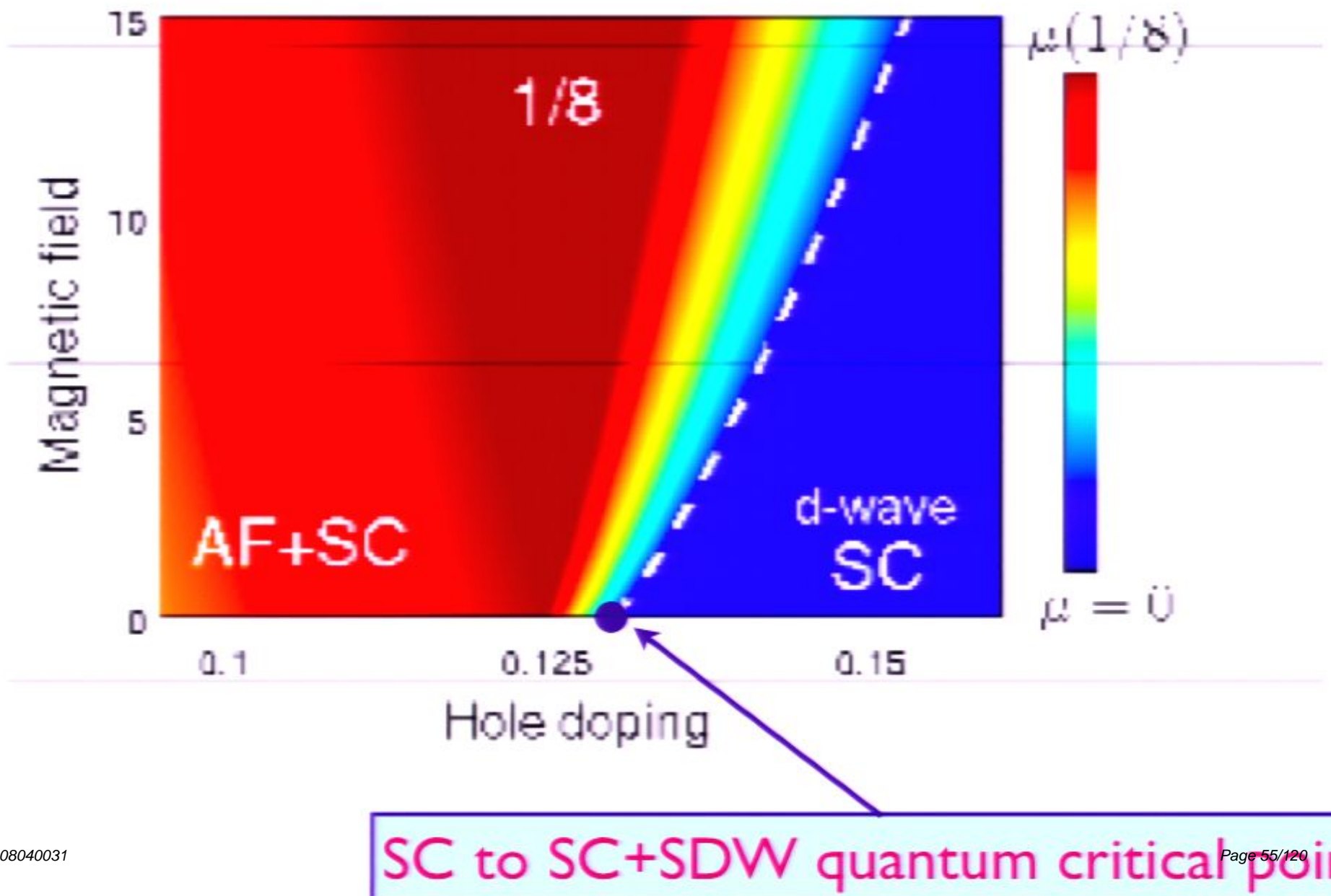


Brillouin zone

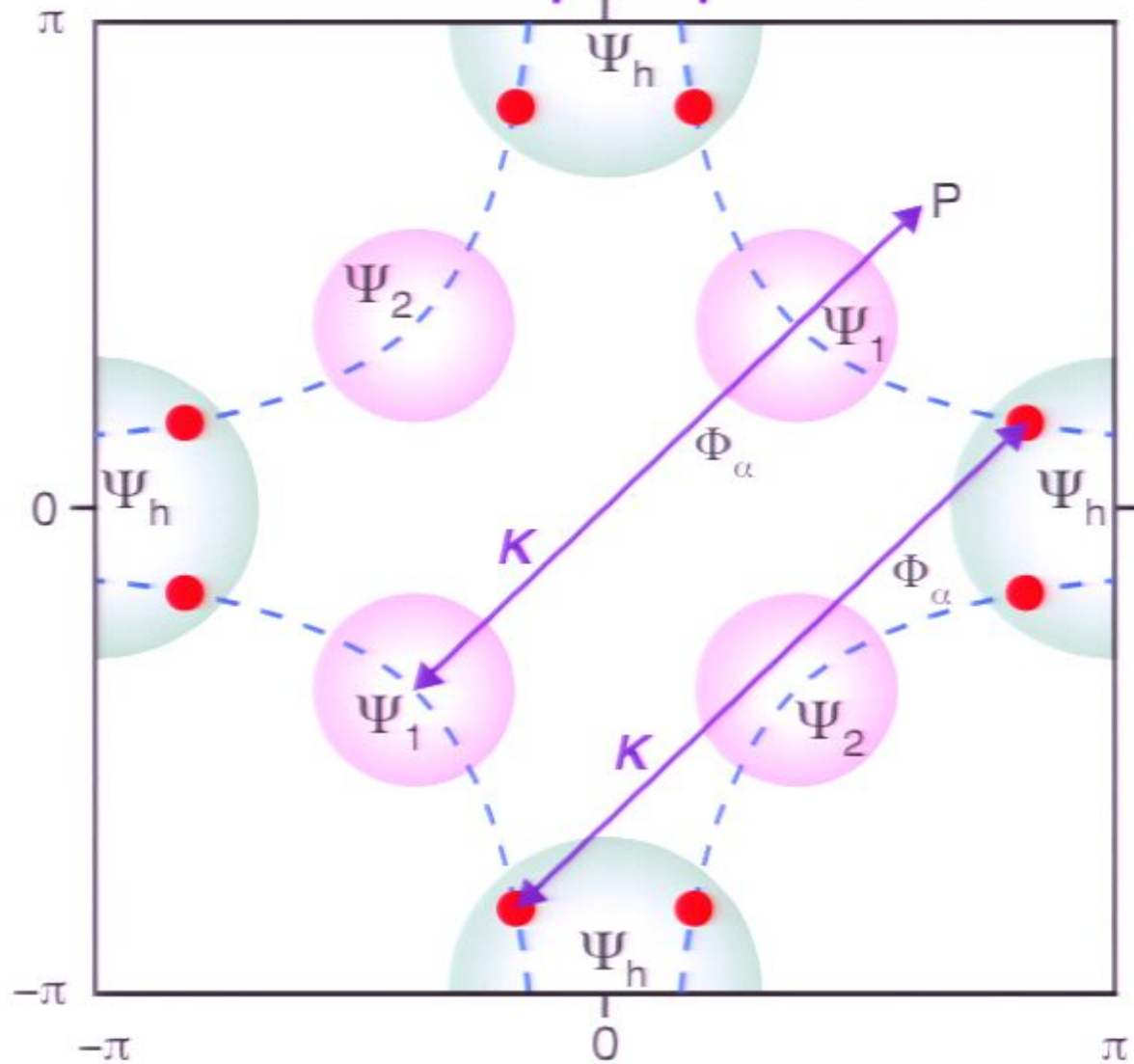
$T=0$



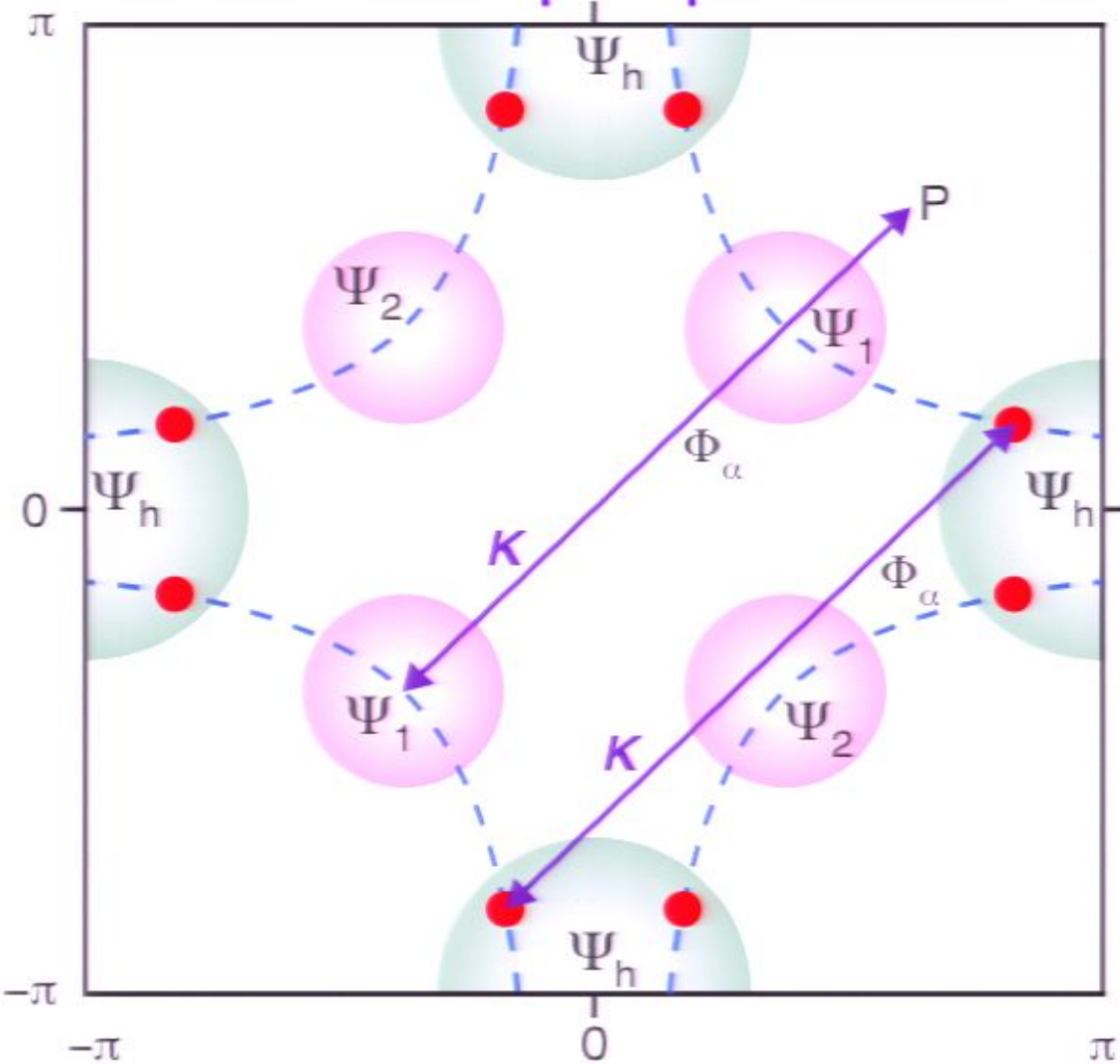
J. Chang et al. (PSI Mesot group), arXiv:0712.2181



# Coupling between SDW order and nodal quasiparticles

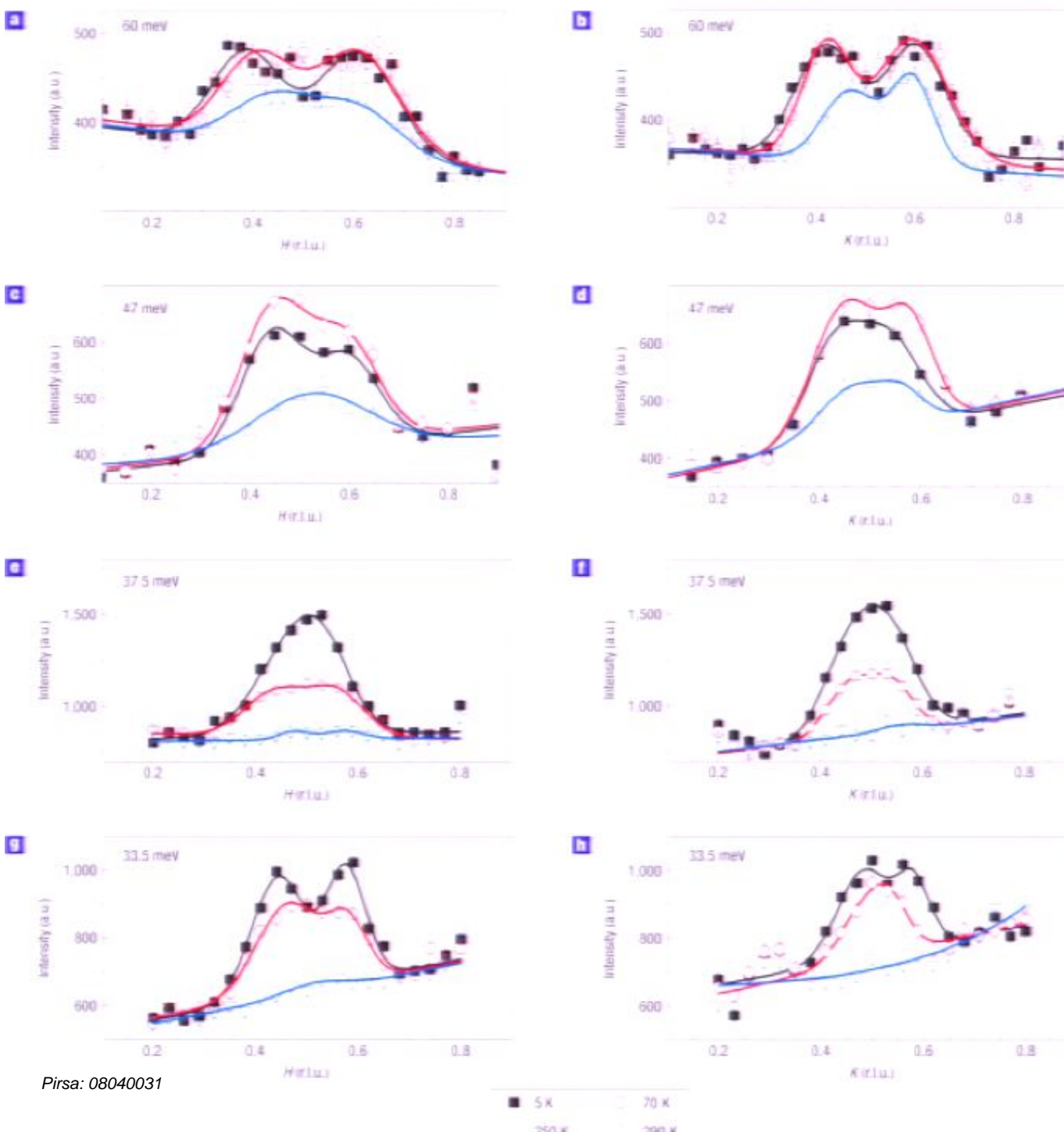


# Coupling between SDW order and nodal quasiparticles



Wavevector mismatch suggests SDW order  
and nodal quasiparticles are decoupled

# Nematic order in YBCO

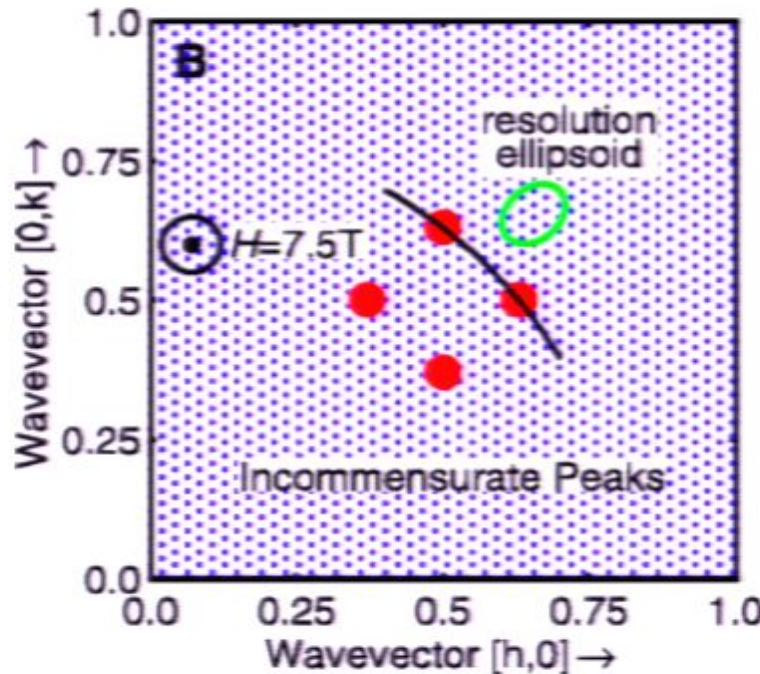


V. Hinkov, P. Bourges,  
S. Pailhès, Y. Sidis, A. Ivanov,  
C. D. Frost, T. G. Perring,  
C. T. Lin, D. P. Chen &  
B. Keimer *Nature Physics* **3**,  
780 - 785 (2007)

**a-h**, The energy transfer was fixed to 60 meV (a,b), 47 meV (c,d), 37.5 meV (e,f) and 33.5 meV (g,h). Panels a,c,e and g show scans along the *a* axis and panels b,d,f and h scans along the *b* axis. The lines are the results of fits to gaussian profiles. We show the raw triple-axis data; the only data processing applied is a subtraction of a constant at 250 and 290 K to account for the increased background from multiphonon scattering. Corrections for the Bose factor are small and were not applied to the data. The final wavevector was fixed to  $2.66 \text{ \AA}^{-1}$  for E37.5 meV and to  $4.5 \text{ \AA}^{-1}$  a Page 58/120e error bars indicate the statistical error.

# Neutron scattering measurements of dynamic spin correlations of the superconductor (SC) in a magnetic field

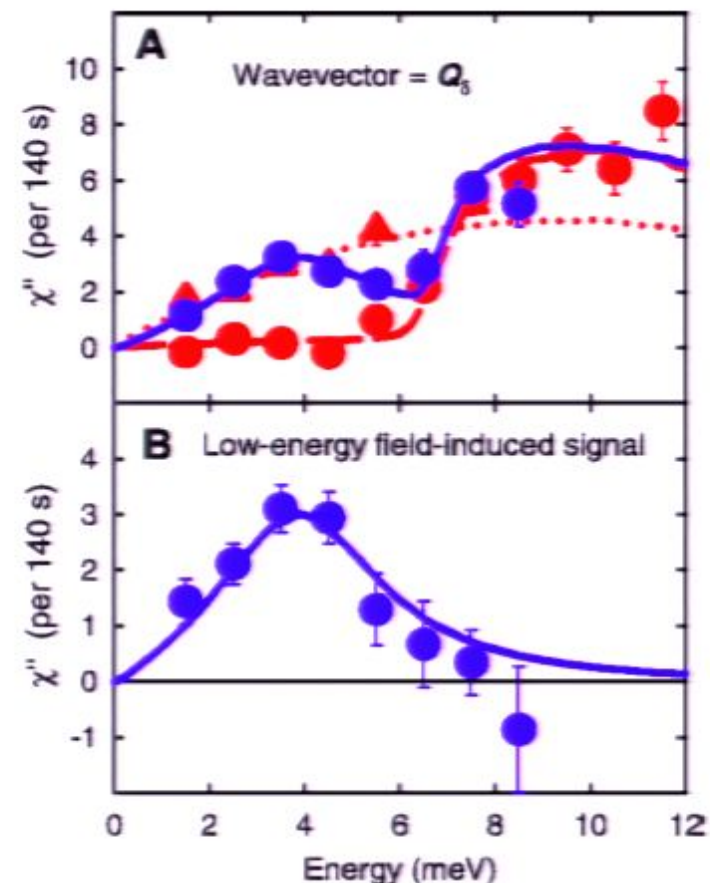
B. Lake, G. Aeppli, K. N. Clausen, D. F. McMorrow,  
K. Lefmann, N. E. Hussey, N. Mangkorntong,  
M. Nohara, H. Takagi, T. E. Mason, and A. Schröder,  
*Science* **291**, 1759 (2001).



Peaks at  $(0.5, 0.5) \pm (0.125, 0)$

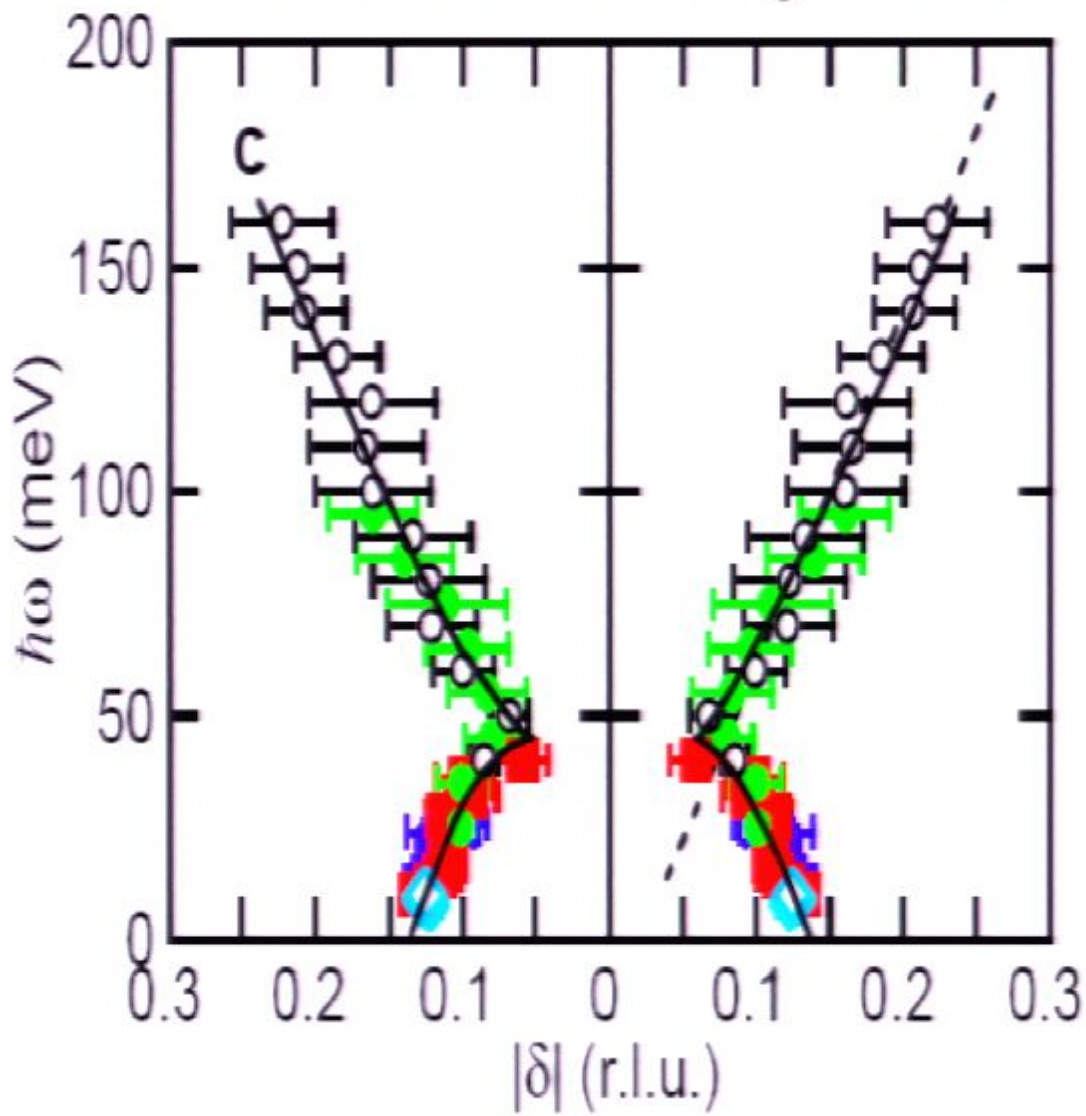
and  $(0.5, 0.5) \pm (0, 0.125)$

⇒ dynamic SDW of period 8



Neutron scattering off  $\text{La}_{2-\delta}\text{Sr}_\delta\text{CuO}_4$  ( $\delta = 0.163$ , *SC phase*)  
at low temperatures in  $H=0$  (red dots) and  $H=7.5\text{T}$  (blue dots)

## Neutron Scattering-LSCO

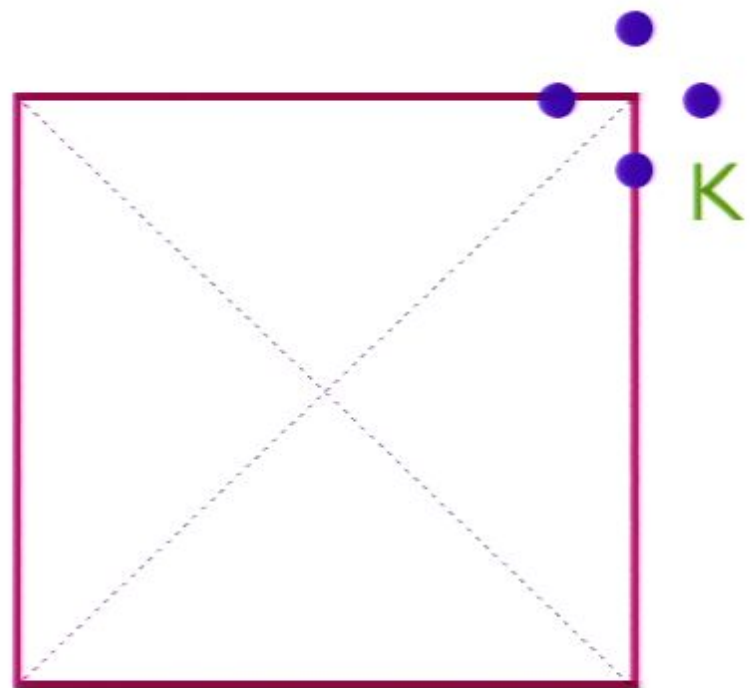


Vignolle *et al.*, Nature Phys. 07

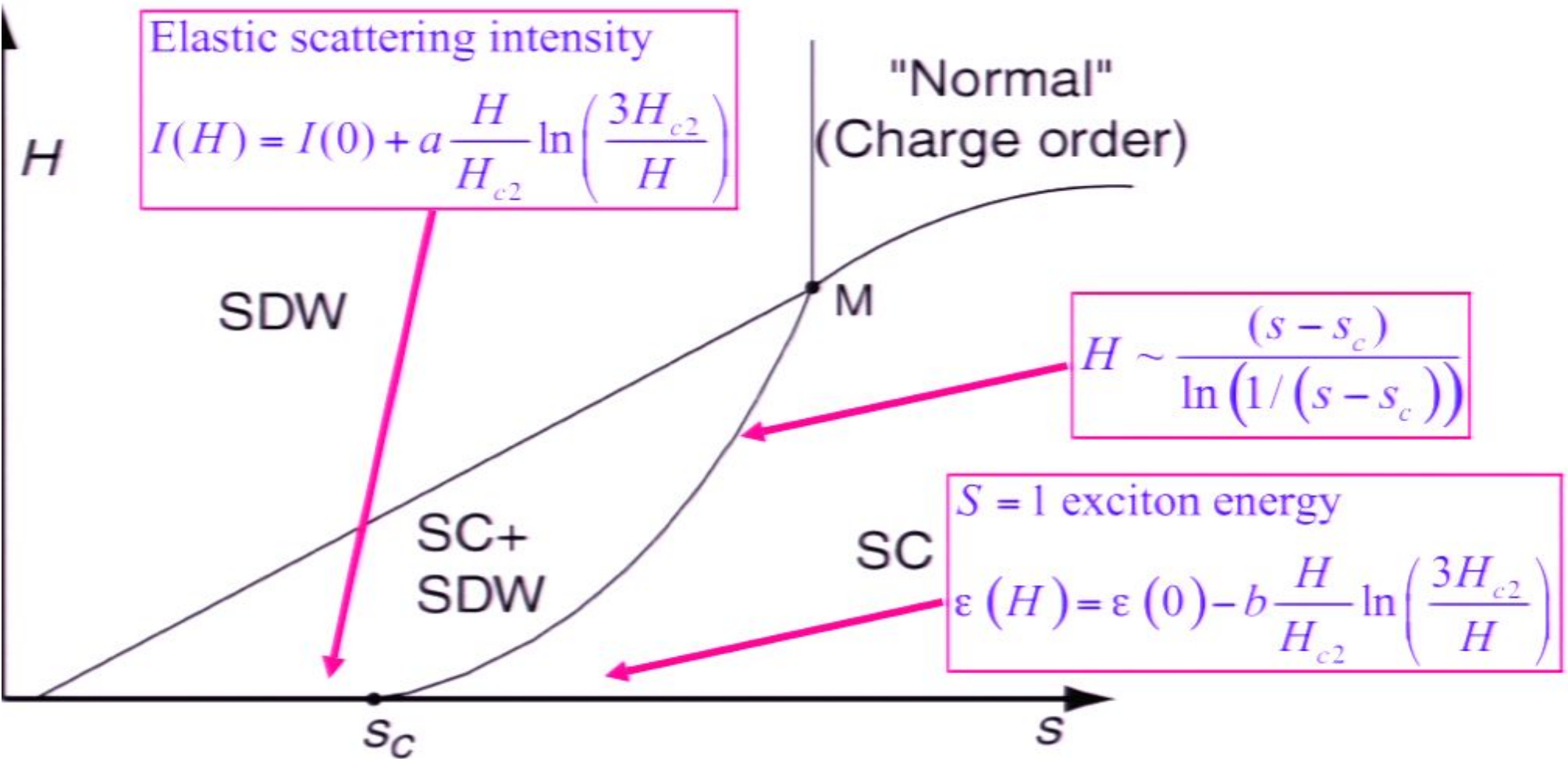
Christensen *et al.*, PRL 04

Hayden *et al.*, Nature 04

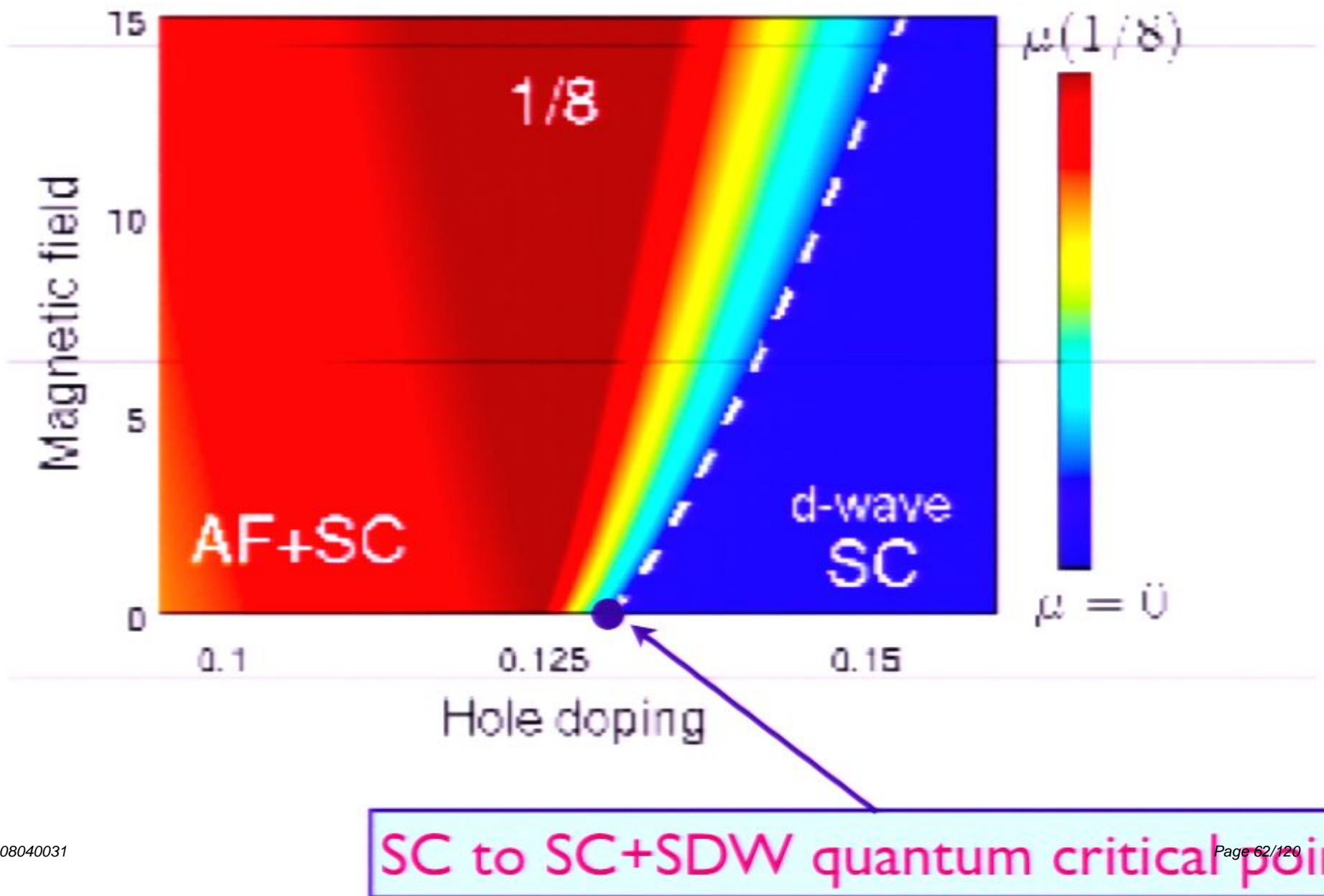
Tranquada *et al.*, Nature 04



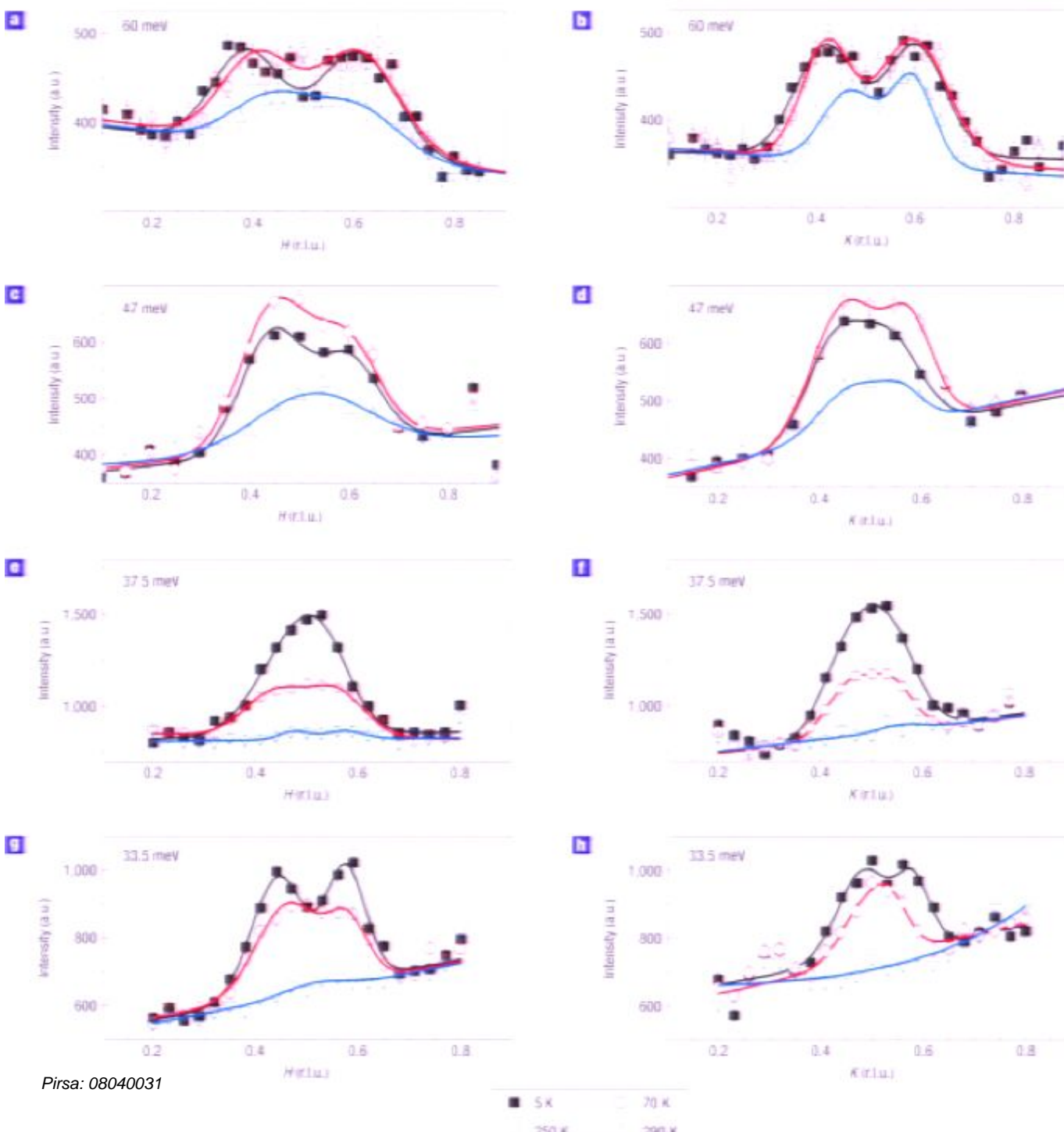
$T=0$



J. Chang et al. (PSI Mesot group), arXiv:0712.2181



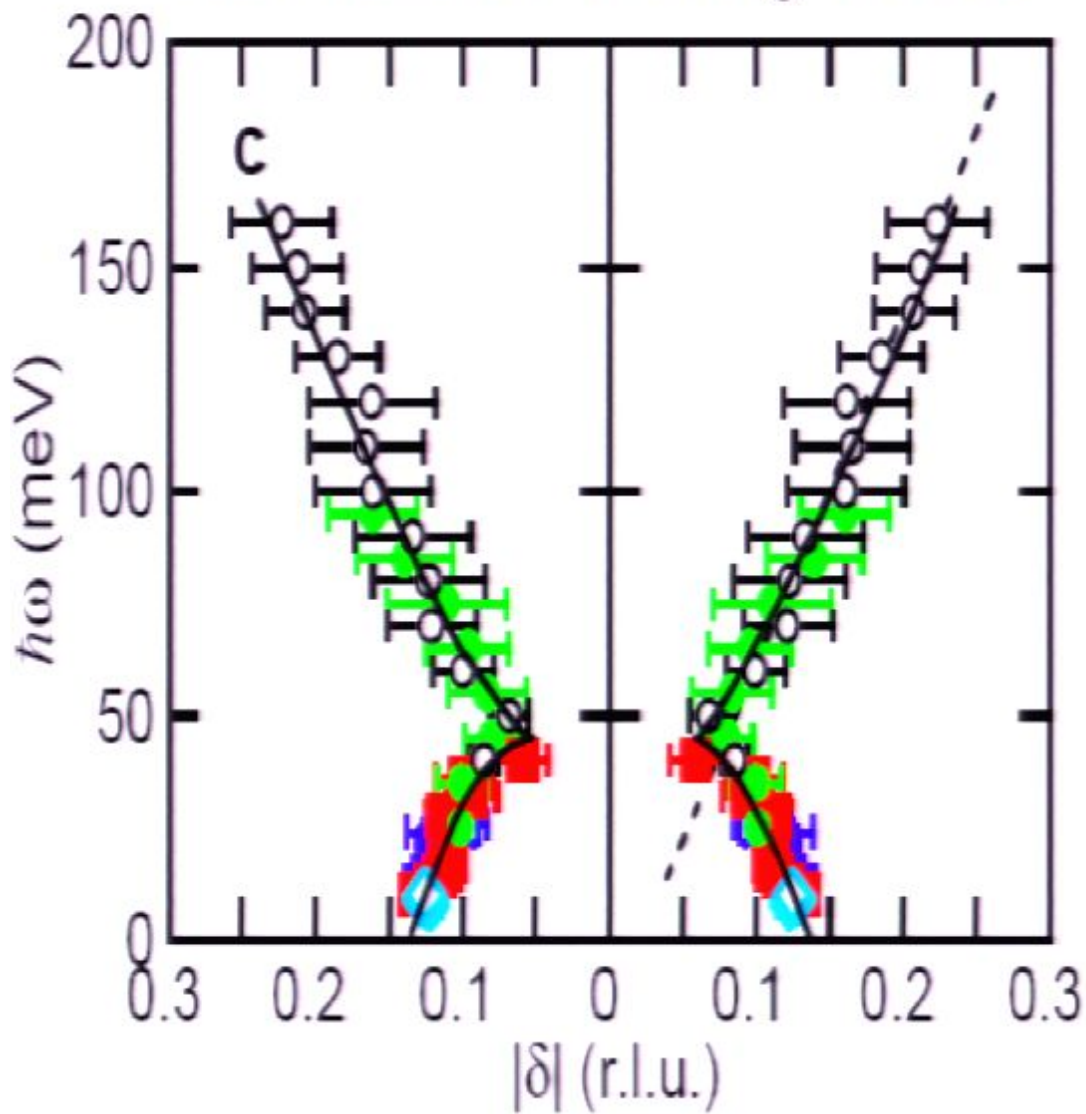
# Nematic order in YBCO



V. Hinkov, P. Bourges,  
S. Pailhès, Y. Sidis, A. Ivanov,  
C. D. Frost, T. G. Perring,  
C. T. Lin, D. P. Chen &  
B. Keimer *Nature Physics* **3**,  
780 - 785 (2007)

**a-h**, The energy transfer was fixed to 60 meV (a,b), 47 meV (c,d), 37.5 meV (e,f) and 33.5 meV (g,h). Panels a,c,e and g show scans along the *a* axis and panels b,d,f and h scans along the *b* axis. The lines are the results of fits to gaussian profiles. We show the raw triple-axis data; the only data processing applied is a subtraction of a constant at 250 and 290 K to account for the increased background from multiphonon scattering. Corrections for the Bose factor are small and were not applied to the data. The final wavevector was fixed to  $2.66 \text{ \AA}^{-1}$  for E37.5 meV and to  $4.5 \text{ \AA}^{-1}$  a Page 63/720e error bars indicate the statistical error.

## Neutron Scattering-LSCO

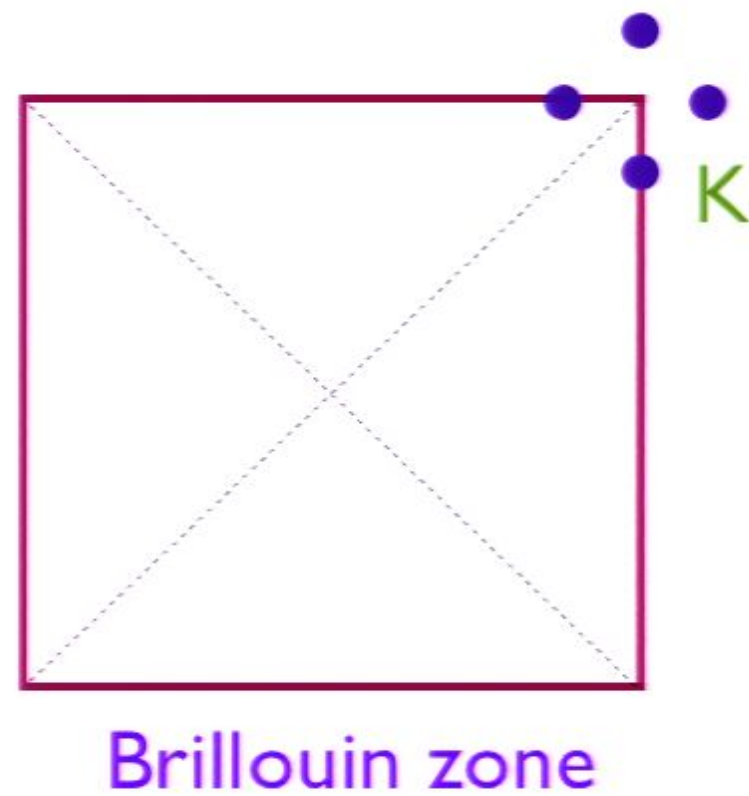


Vignolle *et al.*, Nature Phys. 07

Christensen *et al.*, PRL 04

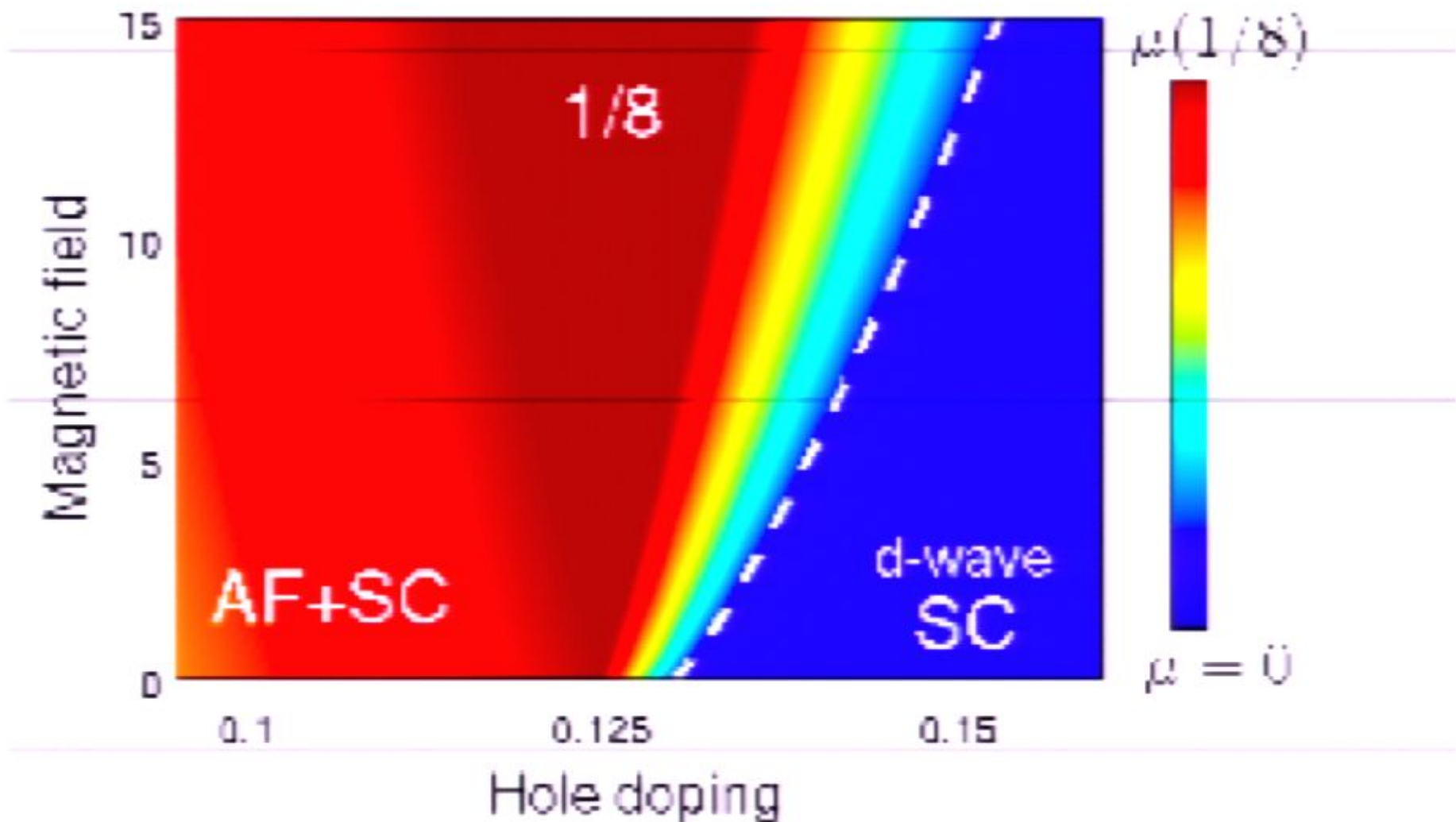
Hayden *et al.*, Nature 04

Tranquada *et al.*, Nature 04

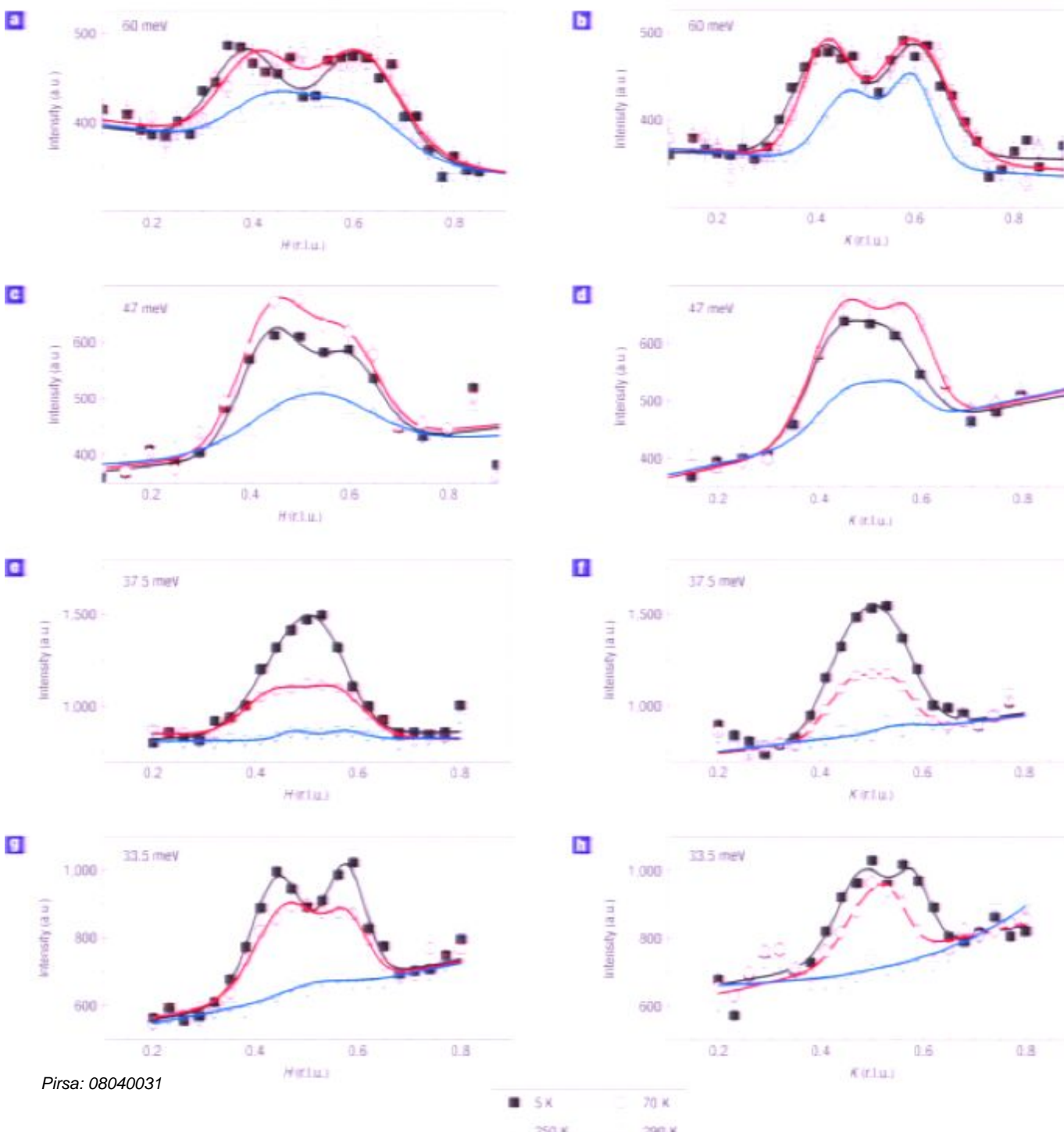


Brillouin zone

J. Chang et al. (PSI Mesot group), arXiv:0712.2181



# Nematic order in YBCO



V. Hinkov, P. Bourges,  
S. Pailhès, Y. Sidis, A. Ivanov,  
C. D. Frost, T. G. Perring,  
C. T. Lin, D. P. Chen &  
B. Keimer *Nature Physics* **3**,  
780 - 785 (2007)

**a-h**, The energy transfer was fixed to 60 meV (a,b), 47 meV (c,d), 37.5 meV (e,f) and 33.5 meV (g,h). Panels a,c,e and g show scans along the *a* axis and panels b,d,f and h scans along the *b* axis. The lines are the results of fits to gaussian profiles. We show the raw triple-axis data; the only data processing applied is a subtraction of a constant at 250 and 290 K to account for the increased background from multiphonon scattering. Corrections for the Bose factor are small and were not applied to the data. The final wavevector was fixed to  $2.66 \text{ \AA}^{-1}$  for E=37.5 meV and to  $4.5 \text{ \AA}^{-1}$  a. Page 66/120e error bars indicate the statistical error.

# Outline

## I. Theory of SC to SC+SDW transition

*Emergent  $O(4)$  symmetry*

## II. Nodal quasiparticles at the $O(4)$ critical point

*Unique selection of quasiparticle coupling to  
(composite) nematic order*

## III. Theory of the onset of nematic order in a d-wave superconductor

*Infinite anisotropy fixed point*

# Outline

## I. Theory of SC to SC+SDW transition

*Emergent  $O(4)$  symmetry*

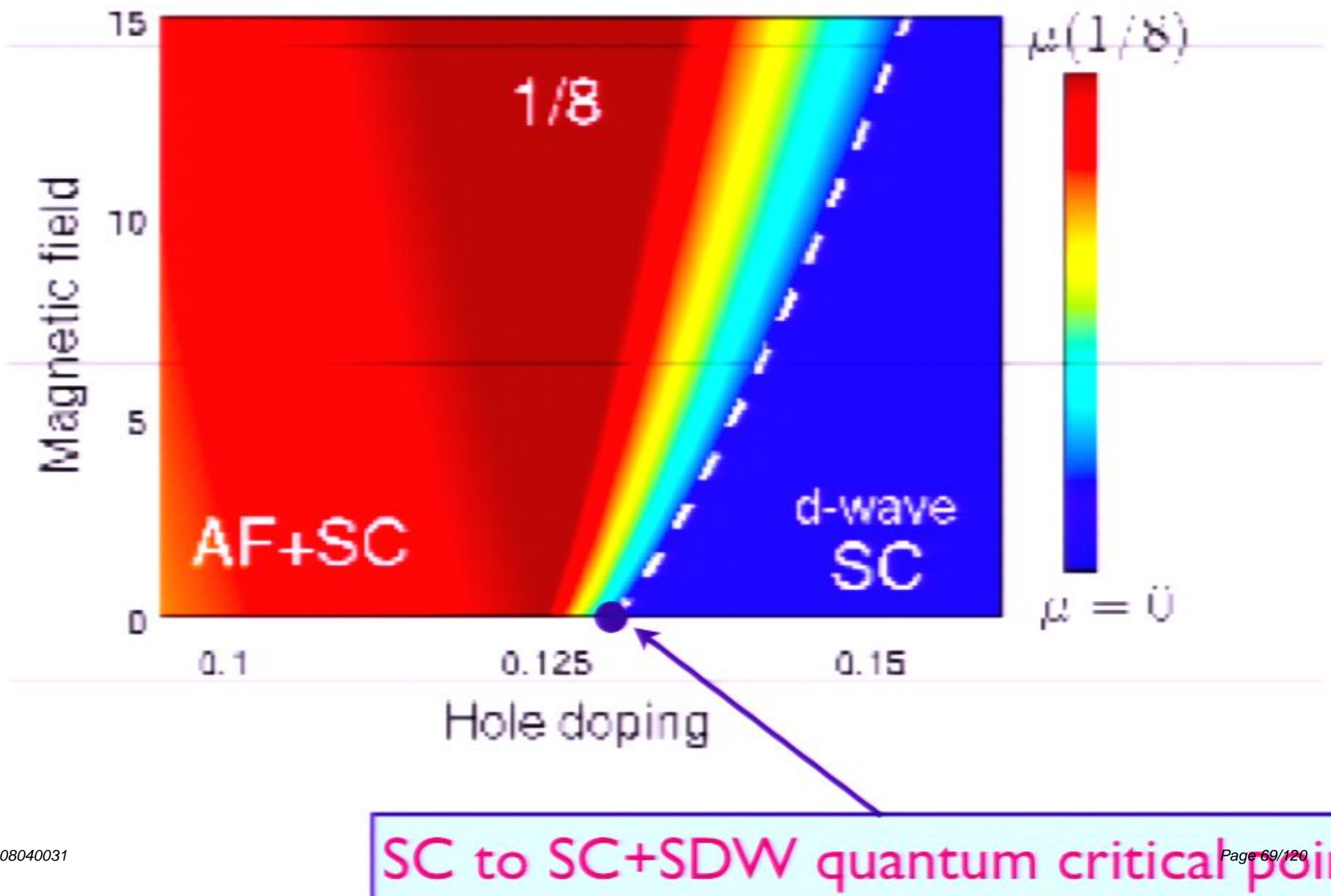
## II. Nodal quasiparticles at the $O(4)$ critical point

*Unique selection of quasiparticle coupling to  
(composite) nematic order*

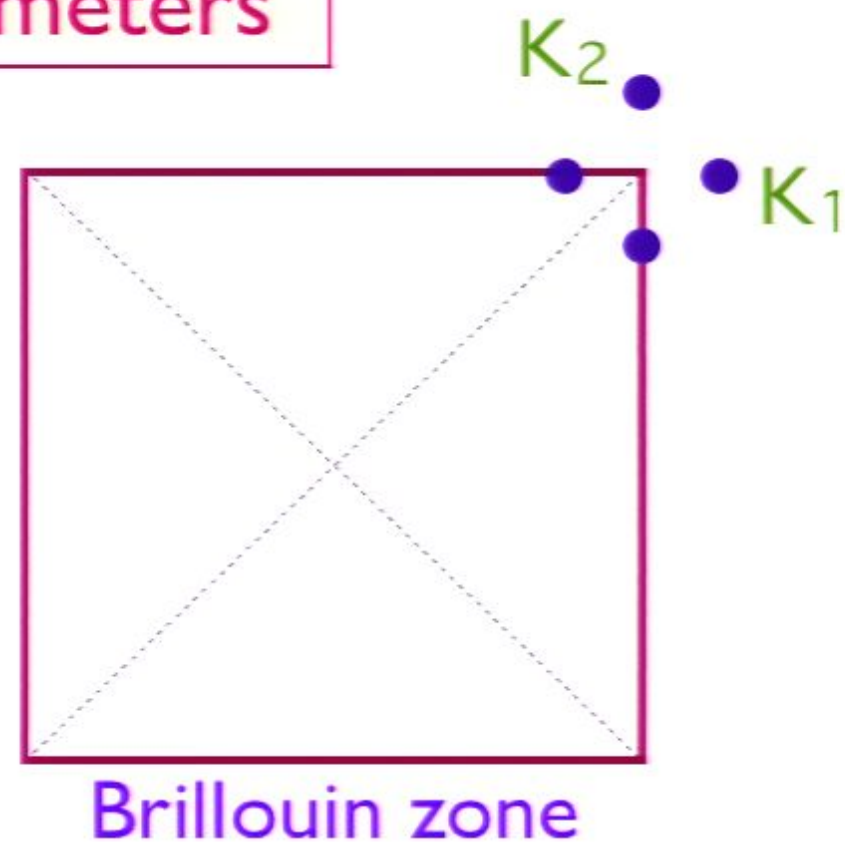
## III. Theory of the onset of nematic order in a d-wave superconductor

*Infinite anisotropy fixed point*

J. Chang et al. (PSI Mesot group), arXiv:0712.2181



## SDW order parameters

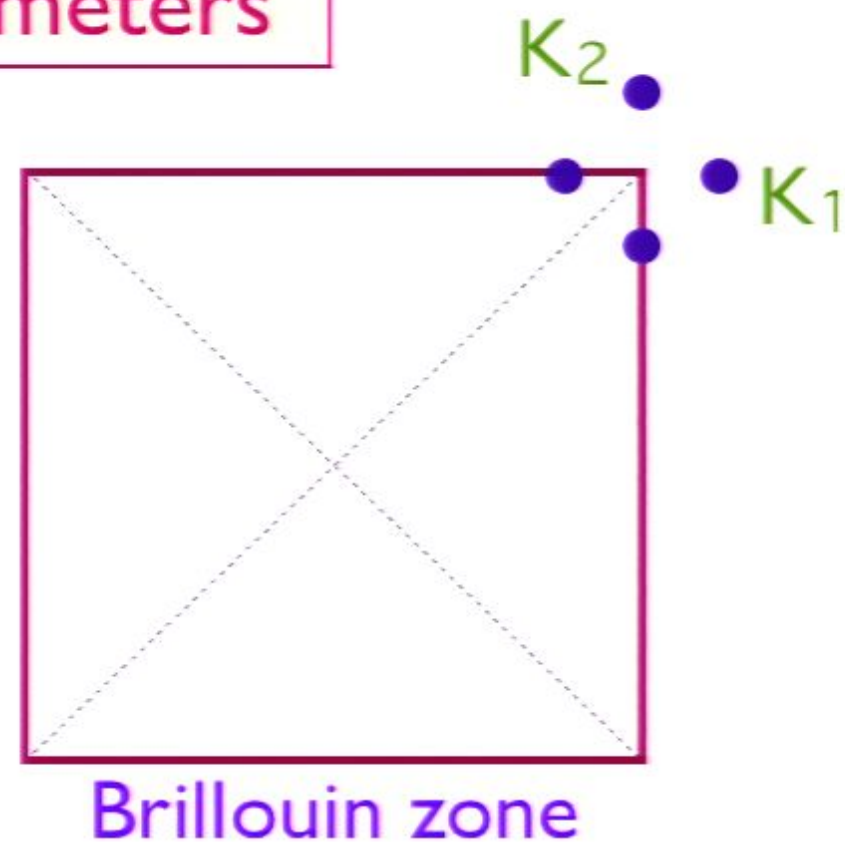


$$S_i(\mathbf{r}, \tau) = \text{Re} [e^{i\mathbf{K}_1 \cdot \mathbf{r}} \Phi_{1i}(\mathbf{r}, \tau) + e^{i\mathbf{K}_2 \cdot \mathbf{r}} \Phi_{2i}(\mathbf{r}, \tau)] .$$

$$\mathbf{K}_1 = \left( \frac{2\pi}{a} \right) \left( \frac{1}{2} - \vartheta, \frac{1}{2} \right) , \quad \mathbf{K}_2 = \left( \frac{2\pi}{a} \right) \left( \frac{1}{2}, \frac{1}{2} - \vartheta \right) ,$$



## SDW order parameters



$$S_i(\mathbf{r}, \tau) = \text{Re} [e^{i\mathbf{K}_1 \cdot \mathbf{r}} \Phi_{1i}(\mathbf{r}, \tau) + e^{i\mathbf{K}_2 \cdot \mathbf{r}} \Phi_{2i}(\mathbf{r}, \tau)] .$$

$$\mathbf{K}_1 = \left( \frac{2\pi}{a} \right) \left( \frac{1}{2} - \vartheta, \frac{1}{2} \right) , \quad \mathbf{K}_2 = \left( \frac{2\pi}{a} \right) \left( \frac{1}{2}, \frac{1}{2} - \vartheta \right) ,$$

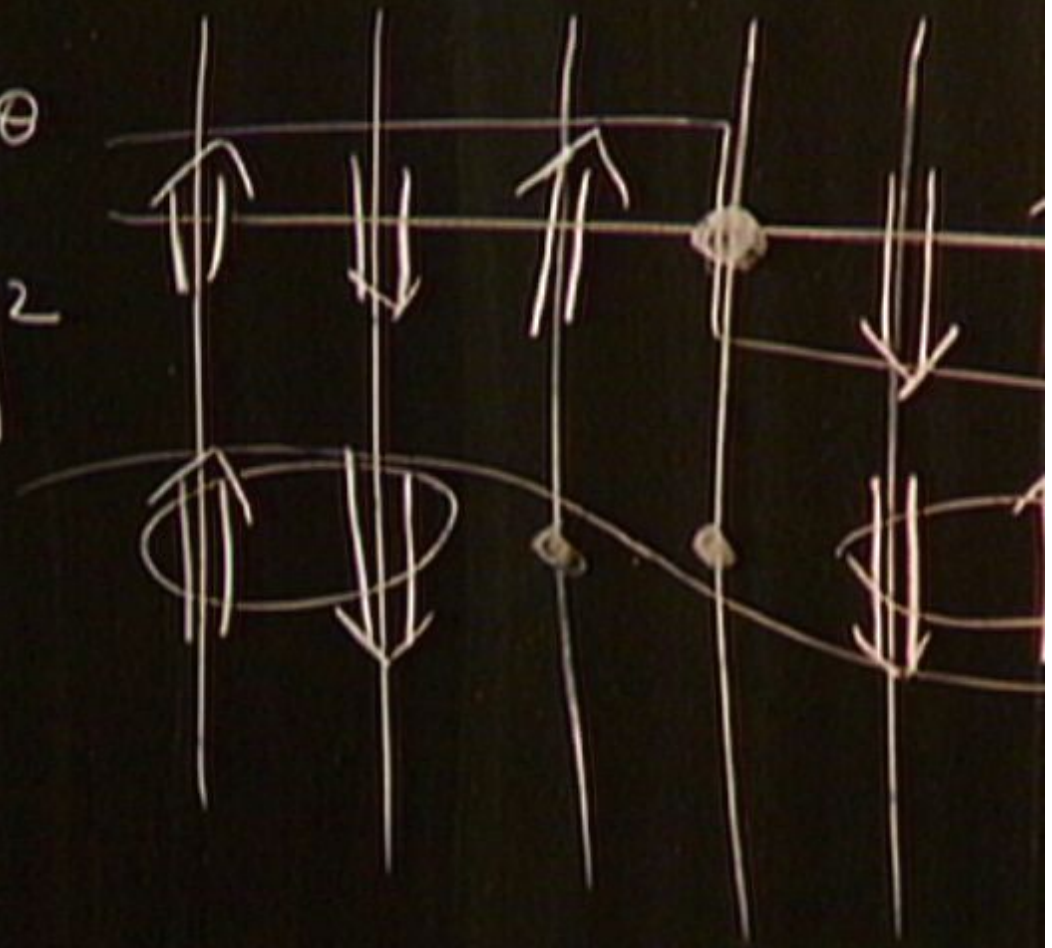
## SDW field theory

$$\begin{aligned}\mathcal{L}_\Phi = & |\partial_\tau \Phi_1|^2 + v_1^2 |\partial_x \Phi_1|^2 + v_2^2 |\partial_y \Phi_1|^2 \\ & + |\partial_\tau \Phi_2|^2 + v_2^2 |\partial_x \Phi_2|^2 + v_1^2 |\partial_y \Phi_2|^2 + r(|\Phi_1|^2 + |\Phi_2|^2) \\ & + \frac{u_1}{2} (|\Phi_1|^4 + |\Phi_2|^4) + \frac{u_2}{2} (|\Phi_1^2|^2 + |\Phi_2^2|^2) \\ & + w_1 |\Phi_1|^2 |\Phi_2|^2 + w_2 |\Phi_1 \cdot \Phi_2|^2 + w_3 |\Phi_1^* \cdot \Phi_2|^2\end{aligned}$$

Most general theory invariant under spin rotation, square lattice space group, and time-reversal symmetries

	$T_x$	$T_y$	$R$	$I$	$\mathcal{T}$
$\Phi_{1i}$	$-e^{-i\vartheta} \Phi_{1i}$	$-\Phi_{1i}$	$\Phi_{2i}$	$\Phi_{1i}^*$	$-\Phi_{1i}$
$\Phi_{2i}$	$-\Phi_{2i}$	$-e^{-i\vartheta} \Phi_{2i}$	$\Phi_{1i}^*$	$\Phi_{2i}^*$	$-\Phi_{2i}$

$$\Psi \sim e^{i\theta}$$
$$\partial_t \theta | \Psi |^2$$



## SDW field theory

$$\begin{aligned}\mathcal{L}_\Phi = & |\partial_\tau \Phi_1|^2 + v_1^2 |\partial_x \Phi_1|^2 + v_2^2 |\partial_y \Phi_1|^2 \\ & + |\partial_\tau \Phi_2|^2 + v_2^2 |\partial_x \Phi_2|^2 + v_1^2 |\partial_y \Phi_2|^2 + r(|\Phi_1|^2 + |\Phi_2|^2) \\ & + \frac{u_1}{2} (|\Phi_1|^4 + |\Phi_2|^4) + \frac{u_2}{2} (|\Phi_1^2|^2 + |\Phi_2^2|^2) \\ & + w_1 |\Phi_1|^2 |\Phi_2|^2 + w_2 |\Phi_1 \cdot \Phi_2|^2 + w_3 |\Phi_1^* \cdot \Phi_2|^2\end{aligned}$$

Symmetries:

$$U(1) \otimes U(1) \otimes Z_4 \otimes O(3)$$

x-translations

y-translations

lattice  
rotations

spin  
rotations

## SDW field theory

Stable fixed point in a 6-loop RG analysis:

$$w_1^* = u_1^* - u_2^*, \quad w_2^* = w_3^* = u_2^*, \quad v_1^* = v_2^*$$

$O(4) \otimes O(3)$  invariant theory for  $\varphi_{ai}$ , with  $a = 1 \dots 4$  an  $O(4)$  index, and  $i = 1 \dots 3$  an  $O(3)$  index, and

$$\Phi_{1i} = \varphi_{1i} + i\varphi_{2i}, \quad \Phi_{2i} = \varphi_{3i} + i\varphi_{4i}.$$

M. De Prato, A. Pelissetto, and E. Vicari  
Phys. Rev. B **74**, 144507 (2006).

## SDW field theory

$$\begin{aligned}\mathcal{L}_\Phi = & |\partial_\tau \Phi_1|^2 + v_1^2 |\partial_x \Phi_1|^2 + v_2^2 |\partial_y \Phi_1|^2 \\ & + |\partial_\tau \Phi_2|^2 + v_2^2 |\partial_x \Phi_2|^2 + v_1^2 |\partial_y \Phi_2|^2 + r(|\Phi_1|^2 + |\Phi_2|^2) \\ & + \frac{u_1}{2} (|\Phi_1|^4 + |\Phi_2|^4) + \frac{u_2}{2} (|\Phi_1^2|^2 + |\Phi_2^2|^2) \\ & + w_1 |\Phi_1|^2 |\Phi_2|^2 + w_2 |\Phi_1 \cdot \Phi_2|^2 + w_3 |\Phi_1^* \cdot \Phi_2|^2\end{aligned}$$

Symmetries:

$$U(1) \otimes U(1) \otimes Z_4 \otimes O(3)$$

x-translations

y-translations

lattice rotations

spin rotations

## SDW field theory

Stable fixed point in a 6-loop RG analysis:

$$w_1^* = u_1^* - u_2^*, \quad w_2^* = w_3^* = u_2^*, \quad v_1^* = v_2^*$$

$O(4) \otimes O(3)$  invariant theory for  $\varphi_{ai}$ , with  $a = 1 \dots 4$  an  $O(4)$  index, and  $i = 1 \dots 3$  an  $O(3)$  index, and

$$\Phi_{1i} = \varphi_{1i} + i\varphi_{2i}, \quad \Phi_{2i} = \varphi_{3i} + i\varphi_{4i}.$$

M. De Prato, A. Pelissetto, and E. Vicari  
Phys. Rev. B **74**, 144507 (2006).

## SDW field theory

Symmetries:

$$U(1) \otimes U(1) \otimes Z_4 \otimes O(3)$$

x-translations

y-translations

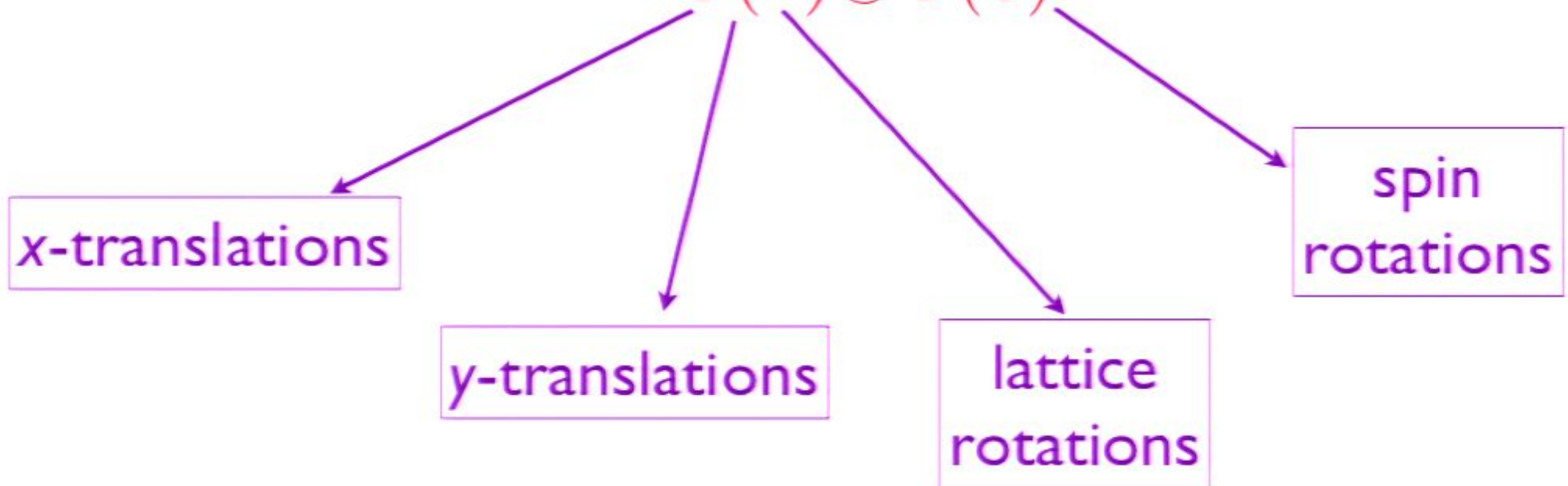
lattice  
rotations

spin  
rotations

# SDW field theory

Symmetries:

$$O(4) \otimes O(3)$$



## Properties of $O(4) \otimes O(3)$ fixed point:

The following 9 order parameters have divergent fluctuations at the spin-density wave ordering transition with the same exponent  $\bar{\gamma}$ :

- The real ‘nematic’ order parameter,  $\phi \equiv \sum_i (|\Phi_{1i}|^2 - |\Phi_{2i}|^2)$  which measures breaking of  $Z_4$  symmetry
- Charge density waves at  $2\mathbf{K}_1$  and  $2\mathbf{K}_2$ :  $\sum_i \Phi_{1i}^2$  and  $\sum_i \Phi_{2i}^2$
- Charge density waves at  $\mathbf{K}_1 \pm \mathbf{K}_2$ :  $\sum_i \Phi_{1i}\Phi_{2i}$  and  $\sum_i \Phi_{1i}^*\Phi_{2i}$

At the quantum critical point, the susceptibilities of these orders *all* diverge as  $\chi \sim T^{-\bar{\gamma}}$ , with

$$\bar{\gamma} = \begin{cases} 0.90(36) & \text{MZM, 6 loops} \\ 0.80(54) & d = 3 \overline{\text{MS}}, 5 \text{ loops} \end{cases}$$

# Outline

## I. Theory of SC to SC+SDW transition

*Emergent  $O(4)$  symmetry*

## II. Nodal quasiparticles at the $O(4)$ critical point

*Unique selection of quasiparticle coupling to  
(composite) nematic order*

## III. Theory of the onset of nematic order in a d-wave superconductor

*Infinite anisotropy fixed point*

# Outline

## I. Theory of SC to SC+SDW transition

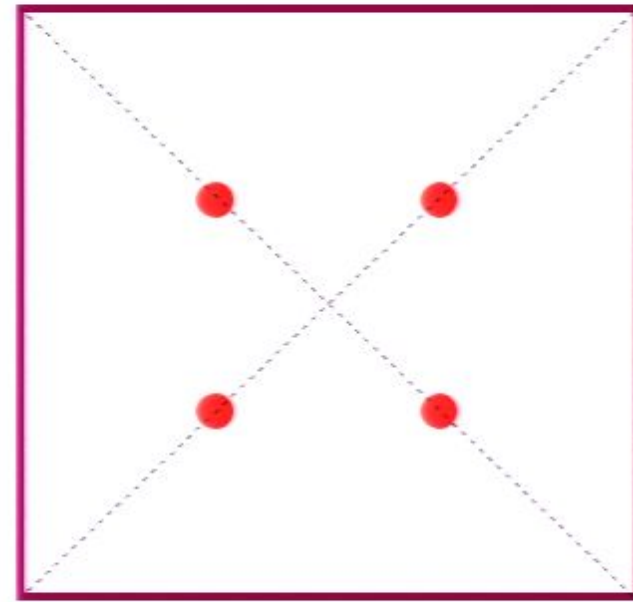
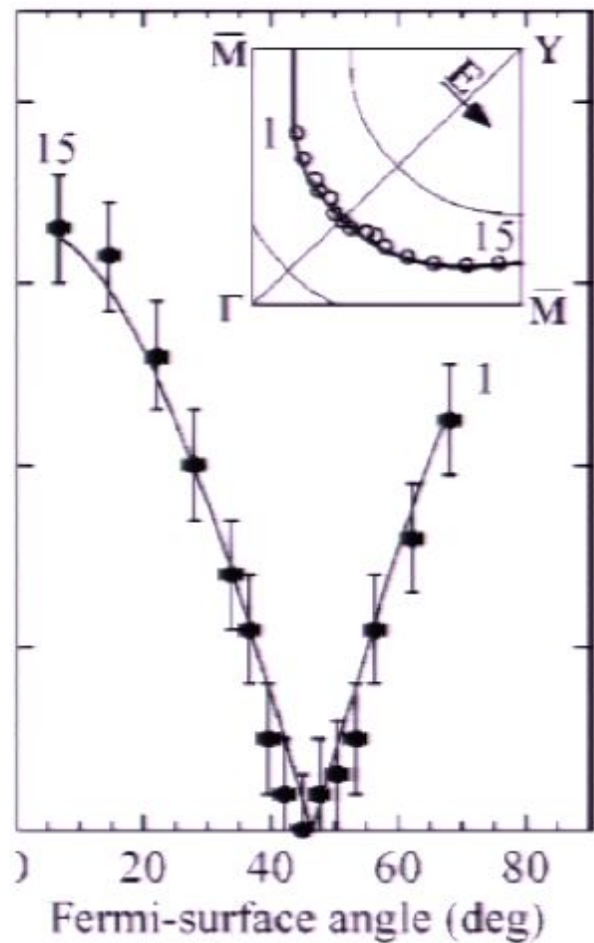
*Emergent  $O(4)$  symmetry*

## II. Nodal quasiparticles at the $O(4)$ critical point

*Unique selection of quasiparticle coupling to  
(composite) nematic order*

## III. Theory of the onset of nematic order in a d-wave superconductor

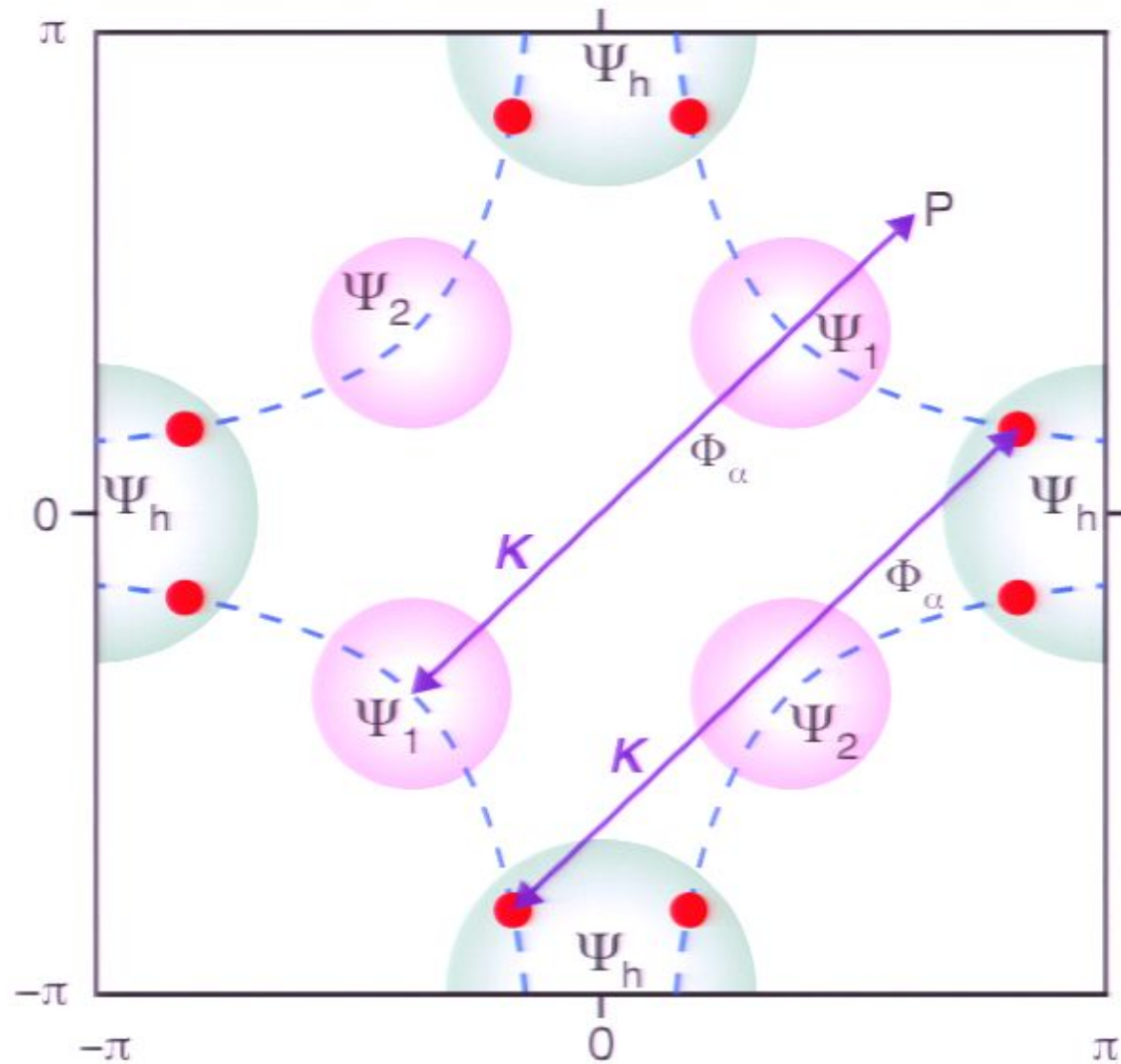
*Infinite anisotropy fixed point*



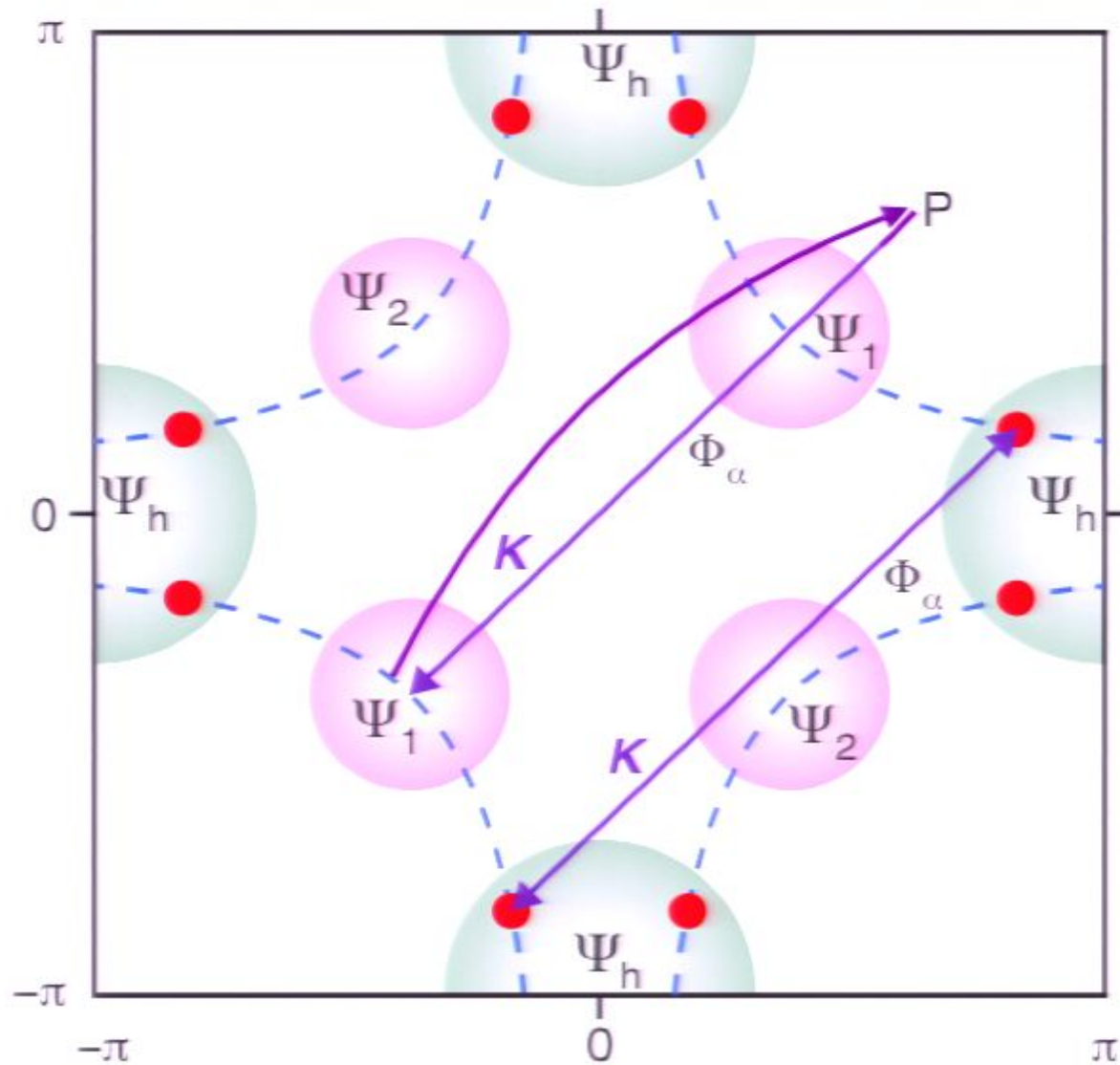
Brillouin zone

$$\begin{aligned} \mathcal{L}_\Psi = & \Psi_1^\dagger \left( \partial_\tau - i \frac{v_F}{\sqrt{2}} (\partial_x + \partial_y) \tau^z - i \frac{v_\Delta}{\sqrt{2}} (-\partial_x + \partial_y) \tau^x \right) \Psi_1 \\ & + \Psi_2^\dagger \left( \partial_\tau - i \frac{v_F}{\sqrt{2}} (-\partial_x + \partial_y) \tau^z - i \frac{v_\Delta}{\sqrt{2}} (\partial_x + \partial_y) \tau^x \right) \Psi_2. \end{aligned}$$

# Coupling of quasiparticles to SDW order



# Coupling of quasiparticles to SDW order



## Coupling of quasiparticles to SDW order

Higher - order couplings allowed by symmetry:

$$\mathcal{L}_1 = \lambda_1 (|\Phi_1|^2 + |\Phi_2|^2) (\Psi_1^\dagger \tau^z \Psi_1 + \Psi_2^\dagger \tau^z \Psi_2)$$

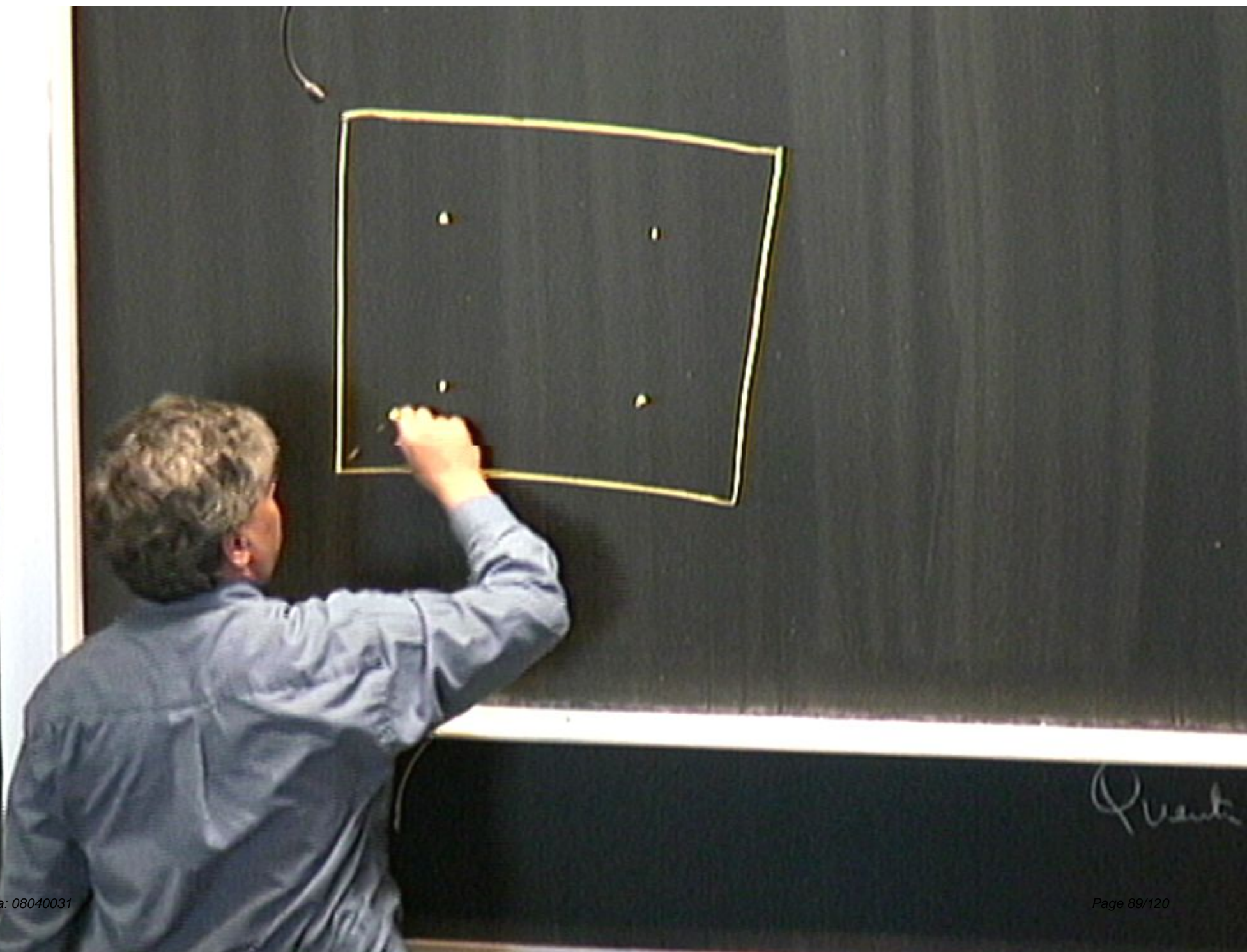
Energy-energy coupling

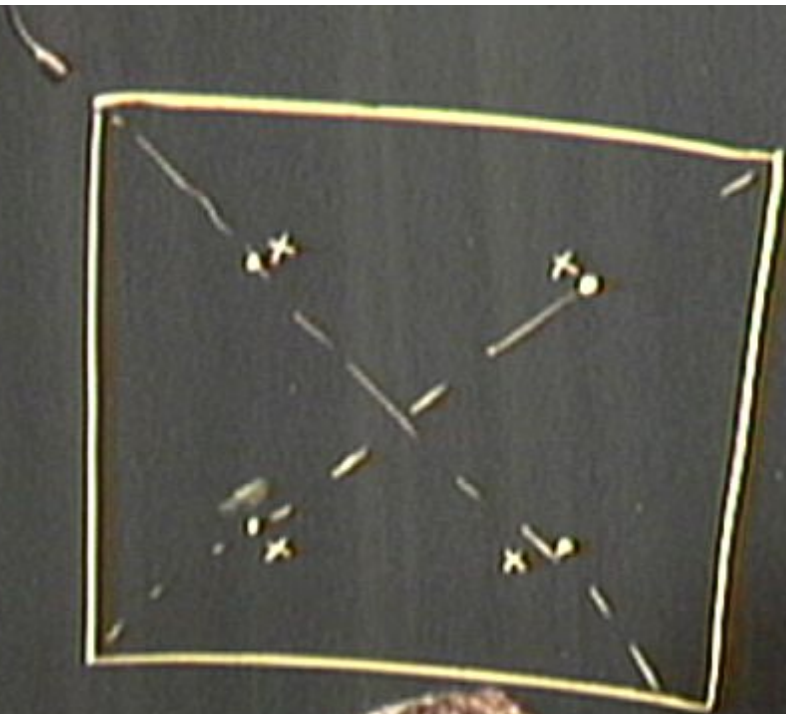
## Coupling of quasiparticles to SDW order

Higher - order couplings allowed by symmetry:

$$\mathcal{L}_2 = \lambda_2 (|\Phi_1|^2 - |\Phi_2|^2) (\Psi_1^\dagger \tau^x \Psi_1 + \Psi_2^\dagger \tau^x \Psi_2)$$

Nematic coupling





Quantum cut

## Coupling of quasiparticles to SDW order

Higher - order couplings allowed by symmetry:

$$\mathcal{L}_2 = \lambda_2 (|\Phi_1|^2 - |\Phi_2|^2) (\Psi_1^\dagger \tau^x \Psi_1 + \Psi_2^\dagger \tau^x \Psi_2)$$

Nematic coupling

## Coupling of quasiparticles to SDW order

Higher - order couplings allowed by symmetry:

$$\begin{aligned}\mathcal{L}_3 = \epsilon_{ijk} & \left[ \right. \\ & \left( \Phi_{1j}^* \Phi_{1k} + \Phi_{2j}^* \Phi_{2k} \right) \left( -\lambda_3 \Psi_2^\dagger \tau^x \sigma^i \Psi_2 + \lambda'_3 \Psi_1^\dagger \tau^z \sigma^i \Psi_1 \right) \\ & \left. + \left( \Phi_{1j}^* \Phi_{1k} - \Phi_{2j}^* \Phi_{2k} \right) \left( \lambda_3 \Psi_1^\dagger \tau^x \sigma^i \Psi_1 - \lambda'_3 \Psi_2^\dagger \tau^z \sigma^i \Psi_2 \right) \right].\end{aligned}$$

Spiral spin order coupling

## Coupling of quasiparticles to SDW order

Scaling dimensions of these couplings:

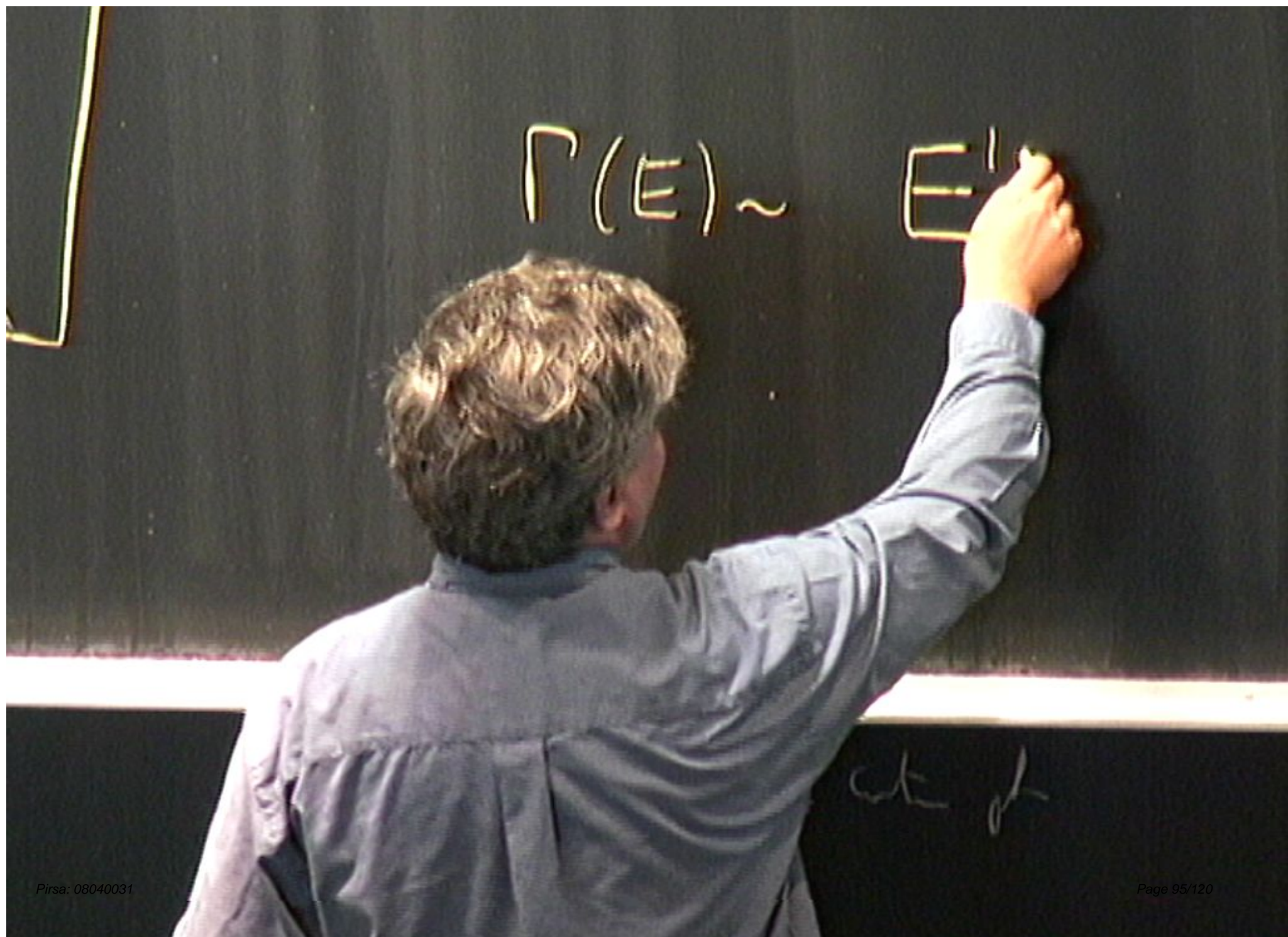
$$\dim[\lambda_1] = \frac{1}{\nu} - 2 = -0.9(2)$$

$$\dim[\lambda_2] = \frac{(\bar{\gamma} - 1)}{2} = \begin{cases} -0.05(18) & \text{MZM, 6 loops} \\ -0.10(27) & d = 3 \overline{\text{MS}}, 5 \text{ loops} \end{cases}$$

$$\dim[\lambda_3, \lambda'_3] = \begin{cases} -0.84(8) & \text{MZM, 6 loops} \\ -0.76(8) & d = 3 \overline{\text{MS}}, 5 \text{ loops} \end{cases}$$



$$\Gamma(E) \sim E^{\alpha}$$



$$\Gamma(E) \sim E^{1+0.05}$$

Quantum field

## Coupling of quasiparticles to SDW order

Scaling dimensions of these couplings:

$$\dim[\lambda_1] = \frac{1}{\nu} - 2 = -0.9(2)$$

$$\dim[\lambda_2] = \frac{(\bar{\gamma} - 1)}{2} = \begin{cases} -0.05(18) & \text{MZM, 6 loops} \\ -0.10(27) & d = 3 \overline{\text{MS}}, 5 \text{ loops} \end{cases}$$

$$\dim[\lambda_3, \lambda'_3] = \begin{cases} -0.84(8) & \text{MZM, 6 loops} \\ -0.76(8) & d = 3 \overline{\text{MS}}, 5 \text{ loops} \end{cases}$$

## Coupling of quasiparticles to SDW order

Scaling dimensions of these couplings:

$$\dim[\lambda_1] = \frac{1}{\nu} - 2 = -0.9(2)$$

$$\dim[\lambda_2] = \frac{(\bar{\gamma} - 1)}{2} = \begin{cases} -0.05(18) & \text{MZM, 6 loops} \\ -0.10(27) & d = 3 \overline{\text{MS}}, 5 \text{ loops} \end{cases}$$

$$\dim[\lambda_3, \lambda'_3] = \begin{cases} -0.84(8) & \text{MZM, 6 loops} \\ -0.76(8) & d = 3 \overline{\text{MS}}, 5 \text{ loops} \end{cases}$$

# Coupling of quasiparticles to SDW order

Coupling of nematic order is nearly marginal:

Quantum-critical features appear in fermion spectrum via coupling to nematic fluctuations of spin density wave order.

# Coupling of quasiparticles to SDW order

Coupling of nematic order is nearly marginal:

Quantum-critical features appear in fermion spectrum via coupling to nematic fluctuations of spin density wave order.

# Outline

## I. Theory of SC to SC+SDW transition

*Emergent  $O(4)$  symmetry*

## II. Nodal quasiparticles at the $O(4)$ critical point

*Unique selection of quasiparticle coupling to  
(composite) nematic order*

## III. Theory of the onset of nematic order in a d-wave superconductor

*Infinite anisotropy fixed point*

# Outline

## I. Theory of SC to SC+SDW transition

*Emergent  $O(4)$  symmetry*

## II. Nodal quasiparticles at the $O(4)$ critical point

*Unique selection of quasiparticle coupling to  
(composite) nematic order*

## III. Theory of the onset of nematic order in a d-wave superconductor

*Infinite anisotropy fixed point*

Ignore SDW orders  $\Phi_{1,2i}$  and focus directly on nematic order  $\phi = \sum_i (|\Phi_{1i}|^2 - |\Phi_{2i}|^2)$

$$S_\phi^0 = \int d^2x d\tau \left[ \frac{1}{2}(\partial_\tau \phi)^2 + \frac{c^2}{2}(\nabla \phi)^2 + \frac{r}{2}\phi^2 + \frac{u_0}{24}\phi^4 \right]$$

### Ising theory for nematic ordering

$$\begin{aligned} S_\Psi &= \int \frac{d^2k}{(2\pi)^2} T \sum_{\omega_n} \Psi_{1a}^\dagger (-i\omega_n + v_F k_x \tau^z + v_\Delta k_y \tau^x) \Psi_{1a} \\ &+ \int \frac{d^2k}{(2\pi)^2} T \sum_{\omega_n} \Psi_{2a}^\dagger (-i\omega_n + v_F k_y \tau^z + v_\Delta k_x \tau^x) \Psi_{2a}. \end{aligned}$$

### Free nodal quasiparticles

Ignore SDW orders  $\Phi_{1,2i}$  and focus directly on nematic order  $\phi = \sum_i (|\Phi_{1i}|^2 - |\Phi_{2i}|^2)$

$$S_{\Psi\phi} = \int d^2x d\tau \left[ \lambda_0 \phi \left( \Psi_{1a}^\dagger \tau^x \Psi_{1a} + \Psi_{2a}^\dagger \tau^x \Psi_{2a} \right) \right],$$

**Yukawa coupling is now permitted  
and is strongly relevant**

**RG analysis close to 3 dimensions  
yields runaway flow to strong coupling**

## Expansion in number of fermion spin components $N_f$

The nematic action is dominated by the non-analytic fermion loop contribution

$$S_\phi = \frac{N_f}{2} \int \frac{d\omega}{2\pi} \int \frac{d^2k}{4\pi^2} |\phi(k, \omega)|^2 G_\phi^{-1}(k, \omega) K^{-1}(k^2/\Lambda^2)$$

where  $G_\phi$  is given by a fermion loop integral,  $K$  is a smooth ultraviolet cutoff function, which suppresses fluctuations above the momentum scale  $\Lambda$ .

$$G_\phi^{-1}(k, \omega) = r + \frac{\lambda_0^2}{8v_F v_\Delta} \left[ \frac{\omega^2 + v_F^2 k_x^2}{\sqrt{\omega^2 + v_F^2 k_x^2 + v_\Delta^2 k_y^2}} + (x \leftrightarrow y) \right]$$

Similar results apply to terms to all orders in  $\phi$

## Renormalization group analysis

The  $1/N_f$  expansion has only one coupling constant at criticality:  $v_\Delta/v_F$ .

The RG has the structure:

$$\text{dynamic critical exponent : } z = 1 + \frac{1}{N_f} F_1(v_\Delta/v_F)$$

$$\text{fermion anomalous dimension : } \eta_f = \frac{1}{N_f} F_2(v_\Delta/v_F)$$

$$\text{RG flow equation : } \frac{d(v_\Delta/v_F)}{d\ell} = \frac{1}{N_f} F_3(v_\Delta/v_F)$$

where we have computed the functions  $F_{1,2,3}(v_\Delta/v_F)$ .

## Renormalization group analysis

The RG flow is to  $v_\Delta/v_F \rightarrow 0$  with

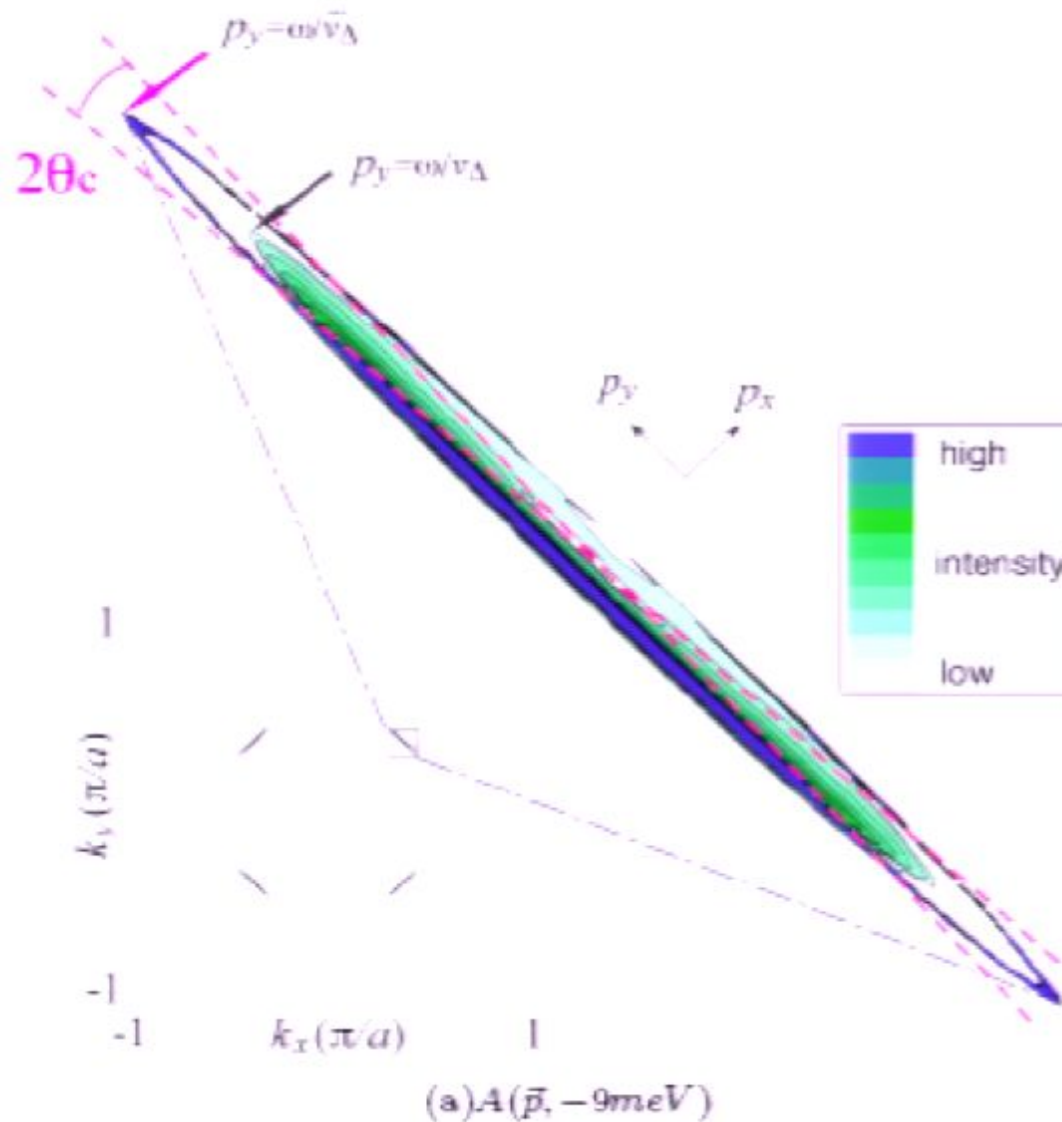
$$\frac{d(v_\Delta/v_F)}{d\ell} = -\frac{4}{\pi^2 N_f} (v_\Delta/v_F)^2 \ln \left( \frac{0.46987}{(v_\Delta/v_F)} \right)$$

This implies that at the critical point, as  $T \rightarrow 0$  we have the asymptotic result

$$\frac{v_\Delta}{v_F} = \frac{\pi^2 N_f}{4} \frac{1}{\ln \left( \frac{\Lambda}{T} \right) \ln \left[ \frac{0.1904}{N_f} \ln \left( \frac{\Lambda}{T} \right) \right]},$$

and a more precise result is obtained by numerically integrating the RG equation.

# Fermion spectral functions



# Conclusions

$v_\Delta/v_F$

$v_\Delta/v_F$

$v_\Delta/v_F$

# Conclusions

I.Theories for damping of nodal quasiparticles in LSCO

2 SFRY's  
functions

$$v_\Delta/v_F$$

$$v_\Delta/v_F$$

$$v_\Delta/v_F$$

# Conclusions

1. Theories for damping of nodal quasiparticles in LSCO
2. SDW theory yields (nearly) quantum critical spectral functions with arbitrary values of  $v_\Delta/v_F$

$$v_\Delta/v_F$$

$$v_\Delta/v_F$$

## Conclusions

1. Theories for damping of nodal quasiparticles in LSCO
2. SDW theory yields (nearly) quantum critical spectral functions with arbitrary values of  $v_\Delta/v_F$
3. Nematic theory has a fixed point with  $v_\Delta/v_F = 0$

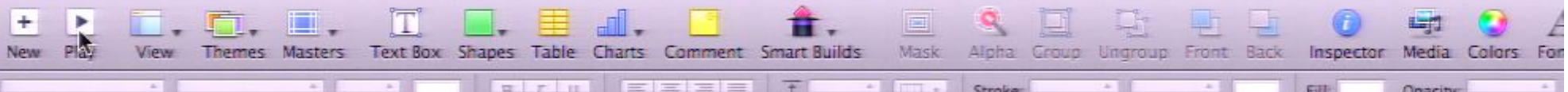
$$v_\Delta/v_F$$

## Conclusions

1. Theories for damping of nodal quasiparticles in LSCO
2. SDW theory yields (nearly) quantum critical spectral functions with arbitrary values of  $v_\Delta/v_F$
3. Nematic theory has a fixed point with  $v_\Delta/v_F = 0$  which is approached logarithmically. The theory is expressed as an expansion in  $v_\Delta/v_F$



## perimeter2



# Conclusions

1. Theories for damping of nodal quasiparticles in LSCO
2. SDW theory yields (nearly) quantum critical spectral functions with arbitrary values of  $v_\Delta/v_F$
3. Nematic theory has a fixed point with  $v_\Delta/v_F = 0$  which is approached logarithmically. The theory is expressed as an expansion in  $v_\Delta/v_F$
4. Theories yield “Fermi arc” spectra.

## perimeter2



## Conclusions

1. Theories for damping of nodal quasiparticles in LSCO
2. SDW theory yields (nearly) quantum critical spectral functions with arbitrary values of  $v_\Delta/v_F$
3. Nematic theory has a fixed point with  $v_\Delta/v_F = 0$  which is approached logarithmically. The theory is expressed as an expansion in  $v_\Delta/v_F$
4. Theories yield “Fermi arc” spectra.

## perimeter2



## Conclusions

1. Theories for damping of nodal quasiparticles in LSCO
2. SDW theory yields (nearly) quantum critical spectral functions with arbitrary values of  $v_\Delta/v_F$
3. Nematic theory has a fixed point with  $v_\Delta/v_F = 0$  which is approached logarithmically. The theory is expressed as an expansion in  $v_\Delta/v_F$
4. Theories yield “Fermi arc” spectra.

## perimeter2



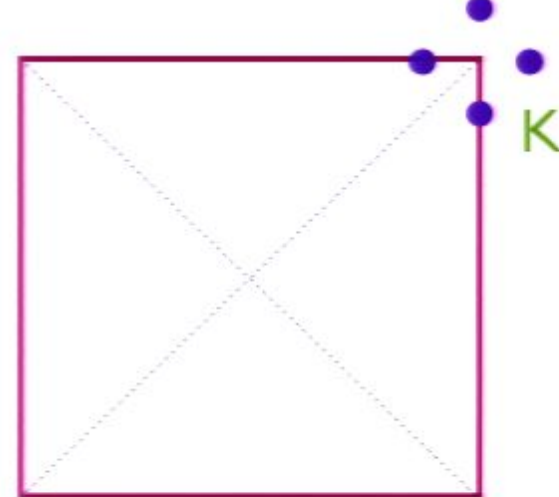
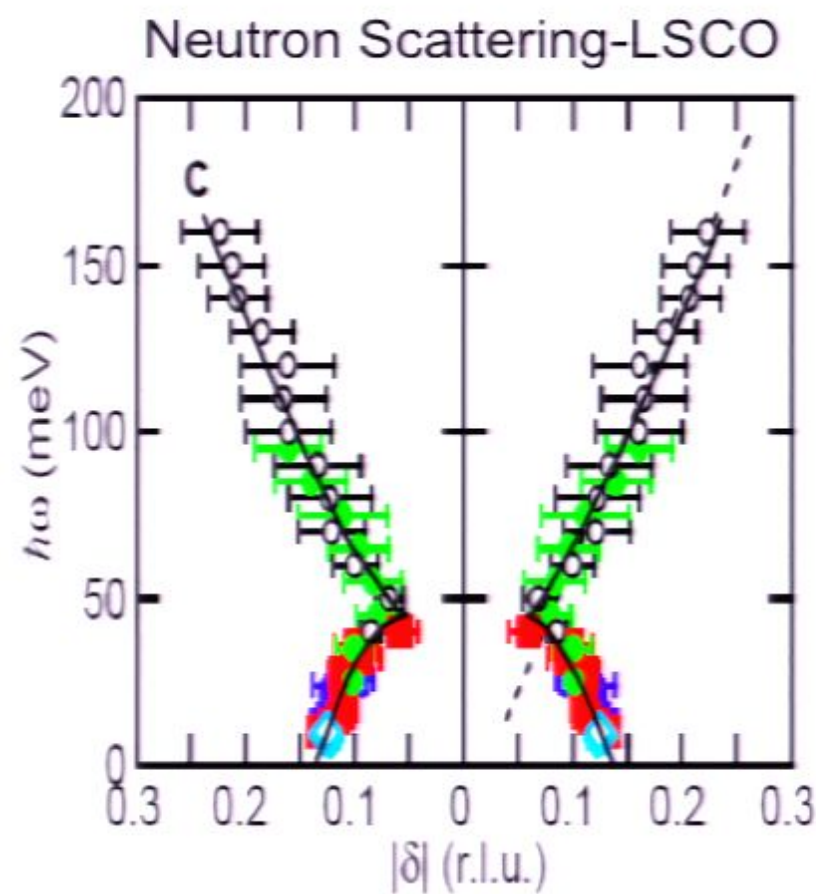
- Slides
- 1
  - 2
  - 3
  - 4
  - 5
  - 6
  - 7
  - 8
  - 9
  - 10
  - 11
- Conclusions
1. Theories for damping of nodal quasiparticles in LSCO
  2. SDW theory yields (nearly) quantum critical spectral functions with arbitrary values of  $v_\Delta/v_F$
  3. Nematic theory has a fixed point with  $v_\Delta/v_F = 0$  which is approached logarithmically. The theory is expressed as an expansion in  $v_\Delta/v_F$
  4. Theories yield “Fermi arc” spectra.



perimeter2

Slides

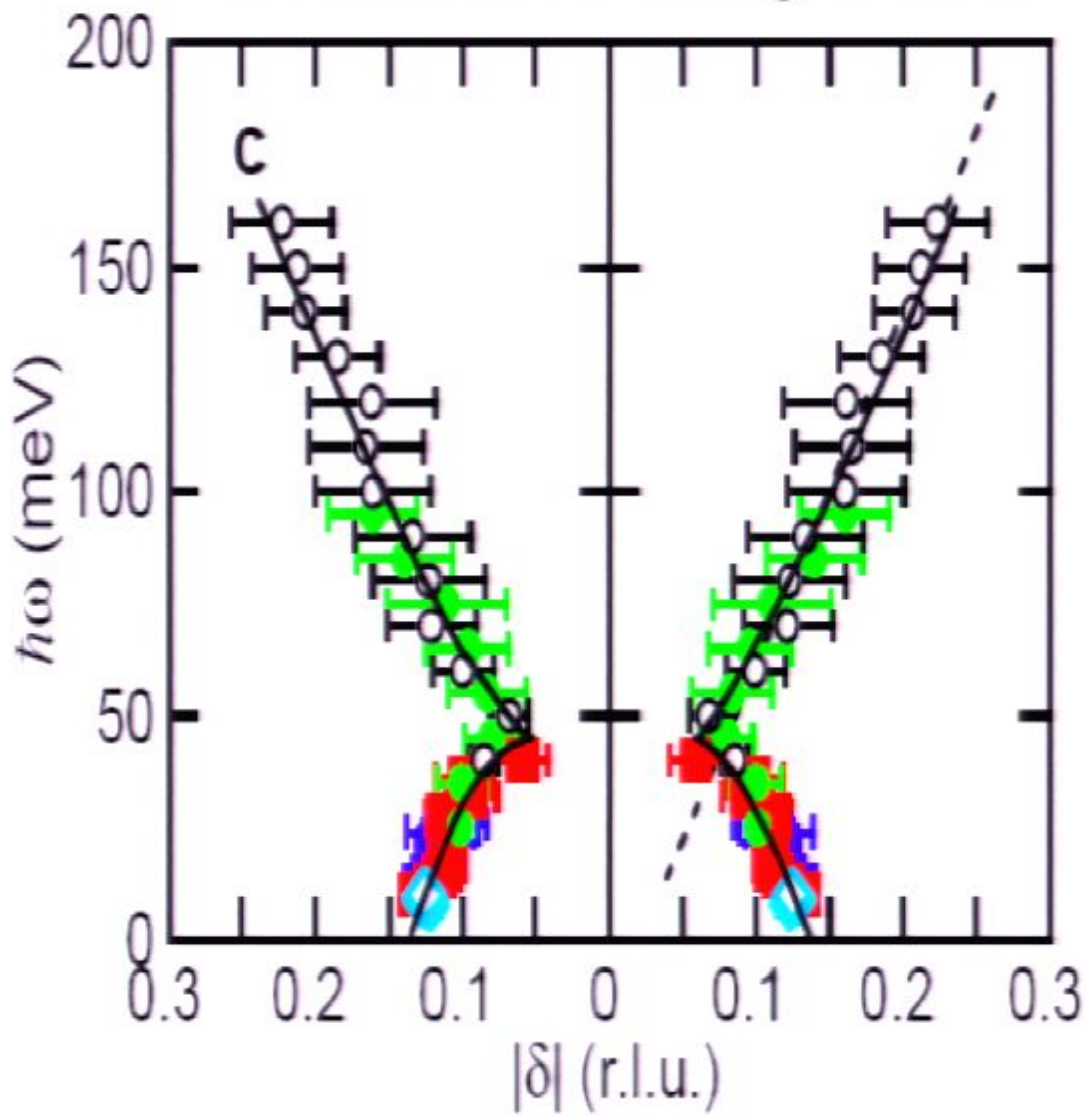
- 1
- 2
- 3
- 4
- 5
- 6
- 7
- 8
- 9
- 10
- 11



Brillouin zone

- Vignolle *et al.*, Nature Phys. 07  
Christensen *et al.*, PRL 04  
Hayden *et al.*, Nature 04  
Tranquada *et al.*, Nature 04

## Neutron Scattering-LSCO

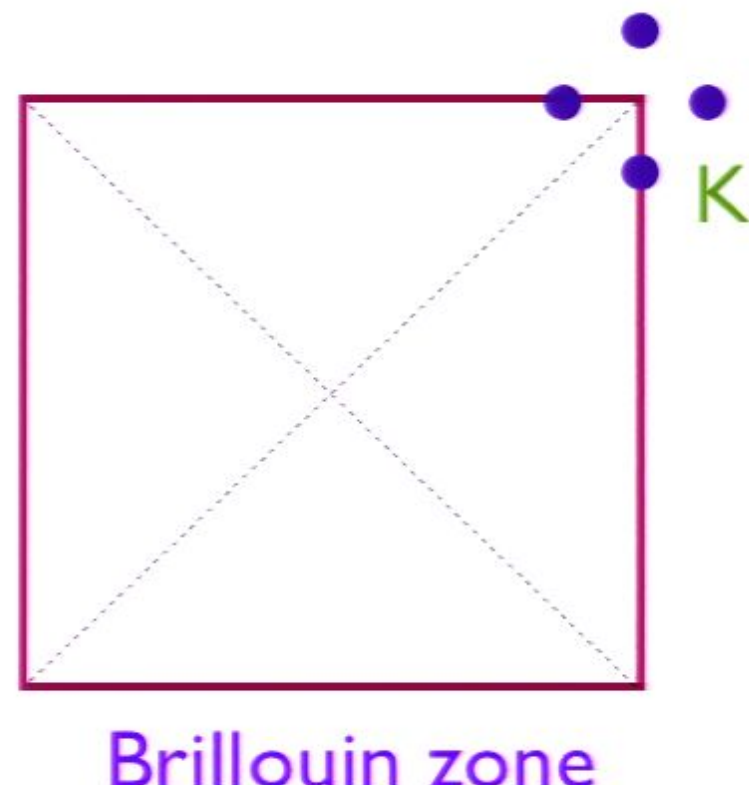


Vignolle *et al.*, Nature Phys. 07

Christensen *et al.*, PRL 04

Hayden *et al.*, Nature 04

Tranquada *et al.*, Nature 04



Brillouin zone